Industry Canada CRC

# ANALYSIS OF HIGH-LATITUDE HF PROPAGATION CHARACTERISTICS AND THEIR IMPACT FOR DATA COMMUNICATIONS

*by*

T.J. Willink

CRC REPORT NO. 97-001

April 1997
Ottawa



The work described in this document was sponsored by the Department of National Defence under Task 5BD14.

Canada

# ANALYSIS OF HIGH-LATITUDE HF PROPAGATION CHARACTERISTICS AND THEIR IMPACT FOR DATA COMMUNICATIONS

*by*

**T.J. Willink**



The work described in this document was sponsored by the Department of National Defence under Task 5BD14.

**COMMUNICATION RESEARCH CENTRE, INDUSTRY CANADA**
CRC REPORT NO. 97-001

Canada

April 1997
Ottawa

# ABSTRACT

The Doppler And Multipath SOunding Network (DAMSON) is a system developed by the Defence Research Agency, UK, and the Communications Research Centre to measure the propagation characteristics of high frequency (HF) radio channels. The system is installed in northern Scandinavia, providing a unique opportunity to study the properties of high-latitude ionospheric HF links.

In this report, the DAMSON system is outlined and the geography of the transmitters and receivers is described. The DAMSON signals were transmitted on ten pre-assigned frequencies from 2 to 22 MHz, with a minute-long transmission every ten minutes on each frequency. The SNR, multipath spread, number of modes, Doppler spread and Doppler shift were extracted from data recorded between April and October 1995 on each of four high-latitude HF links. A detailed analysis of these propagation parameters has been undertaken in this study.

The statistics of each propagation parameter have been examined, including diurnal variation and differences by season in daylight and darkness. In this report, the characteristics of some of the DAMSON frequencies are presented in detail to provide a comprehensive overview of the properties of these high latitude HF links. Where appropriate, the predictions obtained from a high-latitude model are presented for comparison with the observed data.

Data communication over channels at these latitudes can be difficult, and low data rate robust waveforms are required. The DAMSON data has been analysed to determine the range of conditions that must be considered when designing such a waveform. The main findings of this analysis are presented in this report.

# RÉSUMÉ

Le système DAMSON (**D**oppler **A**nd **M**ultipath **SO**unding **N**etwork) a été développé par la Defence Research Agency (DRA) au Royaume-Uni, et le Centre de Recherche sur les Communications dans le but de mesurer les caractéristiques de propagation des ondes radio à hautes fréquences (HF). Le système, situé au nord de la Scandinavie, fournit une occasion unique d'étudier les propriétés des liens ionosphériques HF à haute latitude.

Dans ce rapport, le système DAMSON est présenté, et la topologie des transmetteurs et des récepteurs est décrite. Les signaux DAMSON étaient transmis sur 10 fréquences pré-assignées de 2 à 22 MHz, chaque fréquence étant utilisée pendant une minutes toutes les dix minutes. Le rapport signal sur bruit, l'étalement temporel multi-trajet, le nombre de modes, l'étalement Doppler et le décalage Doppler ont été extrait des données enregistrées entre avril et octobre 1995, sur chacun des 4 liens HF à haute latitude. Une analyse détaillée de ces paramètres de propagation a été entreprise pour cette étude.

Les statistiques de chacun des paramètres de propagation ont été examinées, incluant les variations quotidiennes et les différences saisonnières pendant le jour et la nuit. Dans ce rapport, les caractéristiques de certaines fréquences DAMSON sont présentées en détail pour donner une vue complète des caractéristiques de ces liens HF à haute latitude. Des prédictions obtenues d'un modèle à haute latitude sont présentées, lorsque approprié, pour effectuer la comparaison avec les données recueuillies.

La transmission de données sur des canaux à ces latitudes peut s'avérer difficile; des formes d'onde robustes à bas débit sont requises. Les données DAMSON ont été analysées pour déterminer la plage de conditions à considérer lors du design de ces formes d'ondes. Les découvertes principales de cette analyse sont présentées dans ce rapport.

# EXECUTIVE SUMMARY

The Doppler And Multipath SOunding Network (DAMSON) was designed to measure the propagation parameters of high-latitude high frequency (HF) links, using 3 kHz channels over a range of frequencies.

Throughout most of 1995, the system was installed in northern Scandinavia, with transmit sites at Harstad, Norway and Isfjord on Svalbard. The signals were received at two receivers, located at Kiruna, Sweden and Tuentangen, Norway. The links originating at Isfjord were trans-auroral, while the Harstad-Tuentangen link was mainly sub-auroral. The Harstad-Kiruna link is short and approximately parallel to the southerly edge of the auroral oval. The transmitter and receiver sites were inside or just south of the auroral oval, depending on the time of day and the level of geomagnetic activity.

The DAMSON signals were transmitted at about 250 W, and were cycled through ten frequencies from 2 to 22 MHz every ten minutes. The received data was processed to extract the propagation parameters. The parameters considered in this analysis were the number of modes, the overall multipath spread, the Doppler spread and Doppler shift on the two strongest modes and the overall Doppler spread. In addition, the signal-to-noise ratio (SNR) was estimated.

The extracted propagation parameters have been analysed for each frequency on each of the four links. Preliminary studies indicated differences between the characteristics in the spring and late summer, as would be expected, hence the data sets were divided by season when appropriate. Diurnal variations indicate significant differences between daylight and darkness conditions, which is again expected. The detailed analyses were therefore performed on data in the time periods 08:00 - 14:00 and 20:00 - 02:00, all in local time.

The multipath spread, defined as the time difference between the start of the first received mode and the end of the last detected mode, was considered alongside the predictions obtained from the ICEPAC program for frequencies up to the predicted MUF. It was found that the prediction program provided a reasonable representation, in general, of the measured multipath spread characteristics and of the number of propagating modes. However, significant propagation was observed above the predicted MUF, much of which has been attributed to scattering off irregularities in the auroral oval or off the southerly edge of the auroral zone. On the three north-south links, i.e. excluding Harstad-Kiruna, propagation above the MUF was predominantly single-moded. On the west-east Harstad-Kiruna link, above the MUF propagation was multi-moded, and the modes were often elongated, i.e. they were very dispersed in time. The overall multipath spread was very large, particularly up to 6 MHz or so above the predicted MUF.

The SNR was estimated using a different part of the DAMSON signal than that used to extract multipath and Doppler parameters, hence no direct relationships could be determined. In addition, SNR characteristics will be affected, in part, by the transmit and receive antennas, hence the results of this analysis must be applied with caution to other systems. However, the determination of overall trends in signal power is important for communications purposes. Another significant factor is the relative power in different propagation modes. This has been studied by calculating the percentage of total signal power that is received in the strongest mode. When many modes were supported, this value tended to be 40-60%, however means of 70-90% were common when two-moded propagation was dominant.

The Doppler spreads measured on all of the links were quite dependent on the time of day. In general,

more severe conditions were observed at night, with highly variable estimates during dawn and dusk periods. The Harstad-Kiruna link exhibited the largest Doppler spreads, with 90th percentiles exceeding 50 Hz, the system's maximum capability, at some frequencies above the MUF. On the Harstad-Tuentangen link, which was assumed to be mainly sub-auroral from geographic considerations, mean Doppler spreads were measured to be similar to those seen on the trans-auroral Isfjord-Tuentangen link. Doppler spreads in excess of 30 Hz were observed on all the links from time to time. The large Doppler spreads and extremely elongated modes seen on the Harstad-Kiruna link above the MUF are indicative of off-great-circle propagation, with scattering from irregularities along the southerly edge of the auroral oval.

Small mean Doppler shifts were measured on all the links, increasing with frequency and negative on all except the most northerly link, Isfjord-Kiruna. On all the links, large Doppler shifts were seen from time to time, typically between dusk and dawn.

Data communications over HF at high-latitudes must be able to handle some of the severe conditions observed in this study. Even though the prediction program ICEPAC determines that propagation is limited above MUFs in the range 6-14 MHz on these links, propagation is observed to be reliable at higher frequencies. To minimise interference, it may be necessary to use the frequencies above the predicted MUF, despite their tendency to have more challenging propagation characteristics. For example, it is to be expected that an automatic channel selection procedure would choose these frequencies for use when the lower frequencies become congested.

In the design of a robust HF waveform for use at high-latitudes, multipath spreads of up to 10 ms and Doppler spreads up to 40 to 50 Hz must be considered. Doppler shift is unlikely to be an important factor. The SNR capabilities will clearly depend on the platform on which the waveform will be utilised.

# CONTENTS

# 1.0 INTRODUCTION

The transmission of high frequency (HF) signals in beyond-line-of-sight (BLOS) communication systems relies on the ionosphere for propagation. The quality of the received signal depends strongly on the characteristics of the ionospheric medium. Time dispersion of the signal results in fading at the receiver. Time-dependent changes in the ionospheric layers cause Doppler spread and shift in the signal. In addition, multiple hops may occur, and different layers of the ionosphere may cause multiple modes with different characteristics. For a thorough exposition of the properties of HF propagation, see Davies [1]. All of these effects present challenges to the system designer, who must attempt to exploit or mitigate the effects as much as possible.

At high latitudes, the propagation characteristics can be very harsh and variable. The ionosphere in the auroral zone and polar cap regions is highly disturbed, and the turbulence can introduce severe Doppler fading and increased time spread on each propagation mode. The rapid motion of irregularities may result in large Doppler shifts being seen at the receiver. For a discussion of the causes of these effects, see for example [2] and [3].

Little has been published on the statistical properties of high-latitude ionospheric HF links. In 1964, Gerson [4] concluded that HF propagation at high latitudes was too severe to consider using HF as a communication medium at all, and a submarine cable should be considered. Shepherd and Lomax [5] presented results quantifying the Doppler spread and shift characteristics of two long-haul (4000-5000 km) links. The median Doppler spreads were 3 Hz on the trans-auroral link, compared to 0.3 Hz on the mid-latitude link.

The **D**oppler **A**nd **M**ultipath **SO**unding **N**etwork (DAMSON) was conceived in 1992 as a system to measure the propagation parameters of high-frequency (HF) ionospheric links. It has been established in Norway and Sweden since 1994, and data has been collected also on links between the UK and Ottawa. Initial results were published in [6], [7], [8] and [9].

## 1.1 THE DAMSON NETWORK

Although some special campaigns have enabled DAMSON signals to be received at other sites [7], [10], the experiment is well established in Scandinavia, where it is monitored by staff of the Norwegian Defence Research Establishment (FFI), the Space Physics Institute at Uppsala University (IRFU) and the Swedish Defence Research Establishment (FOA).

Each transmitter site is equipped with a personal computer (PC) housing a DSP32C digital signal processing card and a global positioning system (GPS) card. A rubidium standard is also used to ensure frequency accuracy in the Racal 3751 drive unit. The power output to the antenna at each site is approximately 250 W. The transmitter at Isfjord on Svalbard (78.06 N, 13.63 E) has a rhombic antenna directed due south, while the one at Harstad, Norway (68.48 N, 16.30 E) uses a horizontal wideband dipole, directed at 191° east of north. The transmitters can be remotely controlled via telephone modem, and are also equipped with an automatic restart feature.

GPS cards and DSP32Cs are also used in PCs at the receiver sites, where Racal 3711 receiver units are fed from a sloping Vee antenna pointing due north at Tuentangen, Norway (59.94 N, 11.09 E), and a sloping dipole tuned to 2.8 MHz at Kiruna, Sweden (67.84 N, 20.40 E).

The location of the four sites is shown in figure 1.1, where the predicted auroral oval is shown for $Q = 1$ at local geomagnetic midnight, using the method presented in [11]. The auroral oval prediction is shown in figure 1.2 for $Q = 6$ at the local geomagnetic noon. $Q$ is a local geomagnetic index which is not readily available for specific sites. The planetary index $K_p$ is a three hourly index of geomagnetic activity ranging from 0-very quiet to 9-extremely disturbed. Tables of $K_p$ are available on the internet, for example at the

Space Environment Center homepage [12]. The following empirical equations were derived by Dandekar [13] for mapping the $K_p$ index to the local $Q$ index for improving auroral oval prediction

$$\begin{aligned} Q &= 0.964K_p - 0.3 \qquad for \qquad K_p \leq 2+ \\ Q &= 2.04K_p - 2.7 \qquad for \qquad K_p > 2+ . \end{aligned} \tag{1}$$

Jodalen [14] indicated that this mapping is superior to previous relationships, particularly at lower values of $K_p$. Thus, figure 1.1 corresponds to a $K_p$ value of approximately 1+, and figure 1.2 to $K_p = 4+$. The variation in $K_p$ throughout 1995 is shown in figure 1.3. Note that, overall, 80 % of observations register little disturbance ($K_p < 3+$).

From this modelling of the auroral oval, it can be concluded that the Isfjord-Kiruna link has reflection points in the auroral oval and polar cap regions. Multiple-hop paths on the Isfjord-Tuentangen link may have reflection points inside the polar cap, in the auroral zone and below the auroral zone, depending on the time of day and the level of geomagnetic activity. The Harstad-Kiruna link is closely aligned with the southern edge of the auroral zone at night for low geomagnetic activity, and is slightly below the auroral zone during the day, unless the $Q$ index is high, in which case the link will likely be within the auroral region. The Harstad-Tuentangen link is predominantly sub-auroral, except at nighttime during high levels of geomagnetic activity.

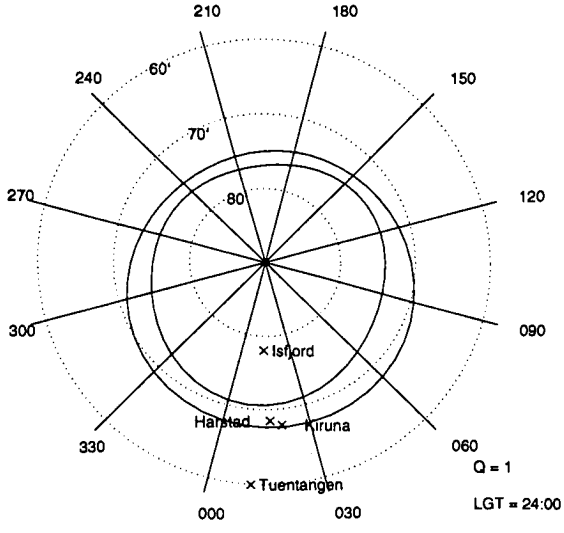


Figure 1.1: Predicted auroral oval for $Q = 1$ at local geomagnetic midnight

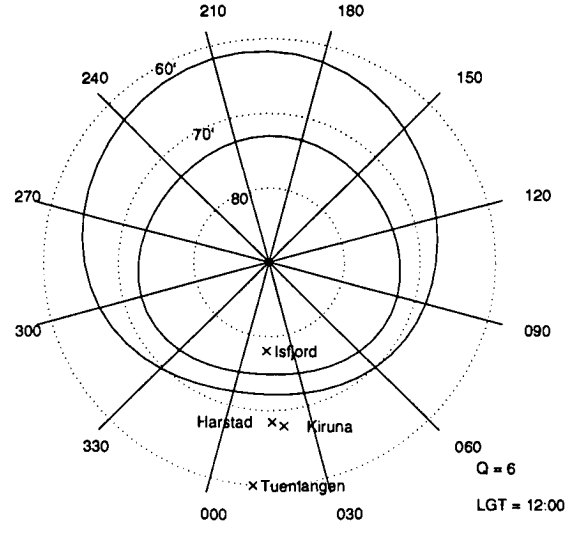


Figure 1.2: Predicted auroral oval for $Q = 6$ at local geomagnetic noon

## 1.2 DAMSON OPERATION

The DAMSON signal is a composite of several waveform formats, which is repeated every minute on each of ten preassigned frequencies from 2 to 22 MHz in a 3 kHz channel, cycling through the frequencies every ten minutes. At the receivers, initial processing is performed on a digital signal processing board, and the

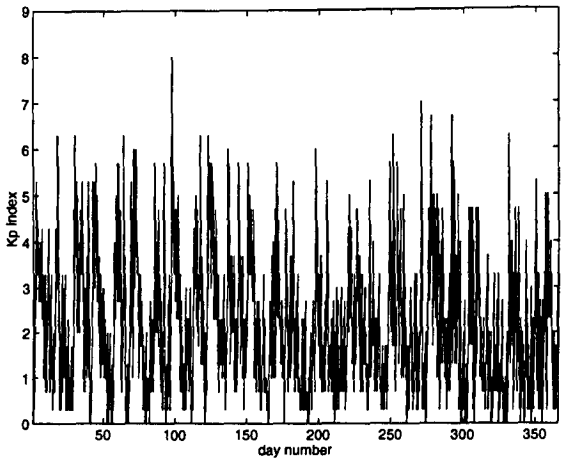


Figure 1.3: Variation in $K_p$ during 1995

output is saved to hard disc. Periodically, the hard disc is copied to a digital audio tape (DAT) backup. The data from the DATs is analysed in a procedure known as "tagging", which separates out the data sets when the propagation parameters are extractable and saves those parameters to file. These parameter data files are used for subsequent propagation analysis.

The various aspects of the DAMSON system and operation are described in more detail in the following sections.

### 1.2.1 DAMSON signals

The core of the DAMSON signal is the delay-Doppler (DD) waveform. This consists of six sections, each of which comprise 128 Barker pulse compression sequences [15] of length 13 symbols, repeated at 12.5 ms intervals. These sequences have the property that, when correlated in burst mode, the peak correlation is 13 and the sidelobes are at one or zero. The correlation can thus be used as an approximate channel response estimate. A time-of-flight (TOF) waveform, transmitted prior to the delay-Doppler waveform, uses 64 repetitions of the length-13 Barker sequence at intervals of 40 ms. There are two continuous wave (CW) signals, one before and one after the delay-Doppler waveform, each lasting 4.3 s. A noise measurement period, when no signal is transmitted, lasts 2.8 s.

### 1.2.2 Signal processing

For both the TOF and DD sections of the DAMSON signal, the received signal is correlated with a Barker-13 sequence. The correlation is modified by a filter which reduces the sidelobes associated with amplitude and group delay distortions in the single sideband (SSB) filtering in the transmitter and receiver. The correlation yields sequential complex channel impulse responses. During the DD phase, the impulse responses are fast-Fourier transformed at each sampling point to give the scattering function [16, chap. 7], and the six successive scattering functions are averaged noncoherently to improve the statistical properties. Each 128-sequence section of the DD-waveform yields an integration time of 1.6 s. The frequency resolution is 0.62 Hz, and the total Doppler range is $\pm$ 40 Hz. In the TOF waveform, the channel impulse responses

are combined noncoherently and the result is used to determine the time of transmission. Because of the relatively small amount of integration in this waveform, the TOF waveform is not always distinguishable in poor SNR conditions, although the DD may be successful.

The CW is used to give an indication of ionospheric support, and its relatively long integration time and narrow bandwidth makes it a useful source for SNR estimates. However, it is unable to distinguish multiple propagation modes.

### 1.2.3 Data extraction

The main source of propagation parameters is the DD waveform, which is processed to give a snap-shot of the scattering function, as discussed in section 1.2.2. From this, the number of modes can be determined and modal characteristics can be extracted. The characteristics which are used in this report are the modal power, Doppler bandwidths that hold 80 % of the total mode power (Doppler spread), median Doppler frequency (Doppler shift) and the time difference between the start of the earliest mode and the end of the latest mode (multipath spread).

The parameter extraction routine, written at the UK Defence Research Agency, performs several numerical algorithms on the calculated scattering function. The first step is to determine time and frequency extremities for each mode which define the limits of the power based on the background noise level. Statistical analysis of the power spectrum within each box then provides the time and frequency bandwidths, power, etc. These values are shown diagrammatically in figure 1.4, which shows the scattering function of a hypothetical example of bi-modal propagation. 'DS $n$' denotes the Doppler spread (80 % bandwidth) of the $n$th mode, 'shift $n$' is the median power point on the $n$th mode and 'P $n$' indicates the modal power. The SNR is also calculated, but in the data sets being considered in this report, the measurement is made using the CW portion of the transmitted signal.

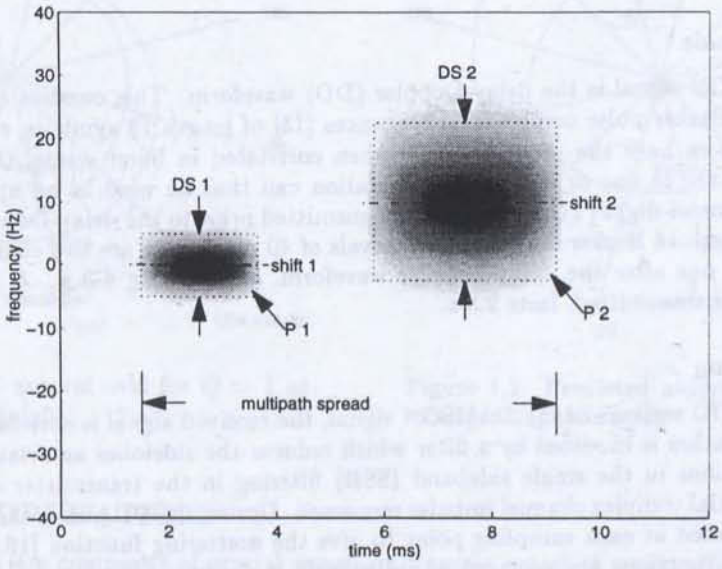


Figure 1.4: Example of DAMSON parameter extraction

The data extraction is a very manually-intensive process, in which an operator must view graphical displays of the signals every minute and determine whether the automatic analysis is satisfactory ('GOOD'), could be improved with more sophisticated processing ('DIFFICULT') or unextractable ('BAD'), for example if there is no propagation or interference is too severe. A manual analysis routine has been written at CRC which will enable many of the 'DIFFICULT' cases to be corrected to 'GOOD', but it has not yet been incorporated into the main automatic analysis routine, and only a small amount of data has been processed using it.

The data extracted by the above procedure is written to binary files which are available for subsequent processing. They have been used extensively for case studies on interesting links for times coinciding with specific geomagnetic phenomena, for example [8], [17]. Preliminary studies have also been performed examining the time-stability of the parameters [18]. Ongoing work uses the DAMSON data for playback simulators and to assess the benefits of frequency steering at HF.

## 1.3 DATA COMMUNICATIONS AT HF

High frequency (HF) data communications have been experiencing a resurgence in recent years with the increasing availability of fast, low-cost digital signal processing products. An inexpensive alternative to satellite communications, HF communications are no longer limited to a few hundred bits per second (bps). In relatively good conditions, fixed frequency serial-tone modems such as those employing phase-skift keying (PSK) can achieve 2400 to 3600 bps [19], [20]. Higher rates, up to 6400 or 9600 bps, have been achieved using QAM serial tone waveforms and orthogonal antennas [21]. New parallel tone modems, such as the Australian trellis-coded modulation parallel-tone system [22], have been seen to be quite resistant to common forms of interference at HF.

One of the most difficult problems facing the HF system designer is that of addressing the differing nature of the communications channels. While high data rates are possible on benign channels, links with severe propagation characteristics require waveforms that are more robust to the effects of Doppler spread and multipath spread. In many applications such as manpacks and airborne communications, the transmitter power is low and the antenna characteristics are poor, and a robust waveform may be required to communicate at low SNR on an otherwise quiescent channel.

The need for reliable, low SNR communications has resulted in a number of proposals for robust waveforms. Some of these have been developed under the auspices of the NATO High Frequency Communications System Group (HFCSG) which has been tasked with developing a suite of waveforms. The data rate of the required robust waveform was set at 40-80 bps, and the Mil-Std-188-110A 75 bps mode [23] is a strong candidate. Lower data rate waveforms have also been designed for short tactical and emergency messages and for systems in which throughput is less important than reliability. Furman [24] proposes a series of PSK waveforms with data rates down to 5 bps based on the Mil-Std-188-110A 75 bps mode. These waveforms operate in SNRs down to -19 dB on an additive white Gaussian noise (AWGN) channel.

HF communication at high latitudes is particularly difficult. The Doppler spread tends to be more severe on trans-auroral links than at mid-latitudes, and the propagation paramaters vary quite rapidly [18]. In order to design waveforms to operate in this environment, it is necessary to assess the ranges of propagation parameters that any candidate waveform must be able to handle.

The location of the DAMSON transmitters during 1995, i.e. northern Scandinavia, has provided an excellent opportunity to make these assessments. Data is available on four links, ranging from upper-mid-latitude to trans-auroral, during several months from April to October. This report presents an analysis of this available data, and addresses the specific requirements of a robust waveform for operation in these conditions.

## 1.4 OUTLINE

Analysis of the DAMSON data is the major focus of this report, and it is presented for each of the four links separately in sections 2.0 to 5.0. In each of these sections, the following parameters are considered:

a. **predicted performance** - the program ICEPAC (**I**onospheric **C**ommunications **E**nhanced **P**rofile **A**nalysis and **C**ircuit prediction program [25]), which is an advancement on IONCAP (**ION**ospheric **C**ommunications **A**nalysis and **P**rediction program [26]) containing a high-latitude model, is used to determine the expected lowest usable frequency (LUF) and maximum usable frequency (MUF) at all times of day.

b. **multipath spread** - diurnal variation in multipath spread is considered in light of the most likely modes of propagation predicted by ICEPAC. The mean and percentiles of the distribution at each frequency is presented. The multipath spread is taken to be the difference in arrival time between the slowest edge of the last propagating mode to arrive, and the fastest edge of the first, as shown in figure 1.4.

c. **SNR** - the diurnal variation in SNR is shown for various frequencies, and the mean and percentiles are evaluated for each of the DAMSON frequencies. The distribution of the signal power is also considered, in which the ratio of the power in the strongest mode to the overall signal power is calculated. The SNR is measured using the CW portion of the DAMSON signal which occurs after the DD waveform.

d. **Doppler spread** - again, the diurnal variation of the Doppler spread is presented for a range of frequencies. Where there are generally two or more modes of propagation, the Doppler spreads on each of the strongest two modes are considered separately. The Doppler spread is taken as the 80 % power bandwidth, i.e.

$$DS = f_{90} - f_{10}$$

where $f_{10}$ and $f_{90}$ are the lower and upper percentiles of the power spectrum. For the overall Doppler spread, the power spectra of all the modes are combined, and the 80 % power bandwidth is determined as above.

e. **Doppler shift** - in addition to the diurnal variations of Doppler shift on the two strongest modes, if applicable, the means and percentiles are calculated across the frequency band to determine if any trends are evident. The Doppler shift is taken as the median of the power spectrum of the respective mode.

f. **parameter interaction** - to assess whether the propagation parameters show any correlation, the joint distributions of Doppler spread on two modes, Doppler spread and multipath spread, and Doppler shift and multipath spread are calculated for a range of frequencies.

# 2.0 HARSTAD-TUENTANGEN

The Harstad-Tuentangen link is 981 km long, with an azimuth of 197°. The data points available are from 28 days during July, August and September 1995. Of these, 14 days were in July, 11 days were in August and three were in September. A total of 15,891 data points were extracted for SNR analysis, and 16,510 for Doppler and multipath analysis. The distribution of points across the frequency band is shown in table 2.1.

| frequency (MHz) | SNR | Doppler & multipath |
|---|---|---|
| 2.8 | 486 | 437 |
| 4.0 | 1940 | 1916 |
| 4.7 | 2391 | 2285 |
| 6.8 | 2434 | 2405 |
| 9.0 | 2215 | 2240 |
| 11.2 | 2175 | 2179 |
| 14.4 | 1800 | 1932 |
| 17.5 | 1166 | 1384 |
| 19.1 | 786 | 1091 |
| 21.9 | 498 | 641 |
| total | 15891 | 16510 |

Table 2.1: Number of data points on Harstad-Tuentangen link for SNR and Doppler/multipath analysis

According to the auroral oval prediction [11], the mid-point of this path falls within the auroral oval for geomagnetic index $Q \geq 4$ (roughly equivalent to $K_p \geq 3+$, [13]) at local geomagnetic midnight. At $Q = 6$ ($K_p = 4+$), the mid-point is within the auroral oval from approximately 22:00 to 04:00 local time (LT). From the $K_p$ values on the days when data is available, it is seen that, during the day (08:00 to 14:00 LT), $K_p \geq 3+$ for about 12 % of the time, and $K_p$ never exceeded 4. At night (20:00 - 02:00 LT), again $K_p \geq 3+$ approximately 12 % of the time, and $K_p \geq 4+$ for 5 % of the time. Thus, this path can be considered sub-auroral for the purposes of this analysis.

The prediction program ICEPAC has been used to extract the LUF and MUF for this path, which are shown in figure 2.1, using a smoothed sunspot number of 16 for August, 1995. From figure 2.1, it is seen that the frequency 4.0 MHz is in the predicted LUF/MUF window at all times of day. 11.2 MHz is above the predicted MUF, but propagation is still supported reliably, as seen in table 2.1. These frequencies will thus be considered throughout the following sections which present the analysis of multipath, SNR, Doppler spread and Doppler shift on this path.

## 2.1 MULTIPATH SPREAD

The prediction program ICEPAC has been used to determine the expected modes of propagation throughout the day. These are shown in figure 2.2, where the time of day is in universal time (UT). E modes are marked with 'o', F1 and F2 modes are indicated with '×' and '+', respectively, and sporadic-E (Es) modes are marked '*'. The 1E and 2E modes, which are expected during daylight hours, are somewhat obscured in the plots by the less reliable one and two-hop Es modes. F2 mode propagation dominates during the night, with 3F1 modes possible during the dawn and dusk transition times. Note that the delays indicate the predicted

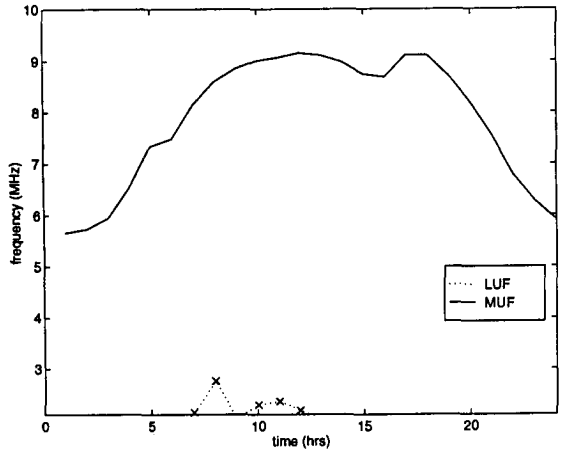


Figure 2.1: Predicted LUF/MUF for August 1995

time-of-flight, not the delay spread of the mode. The multipath spread can be predicted from the range of delays obtained from ICEPAC.

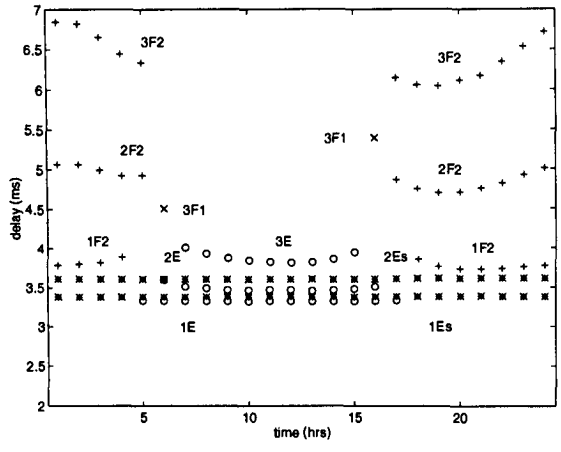


Figure 2.2: Predicted propagating modes at 4.0 MHz for August, 1995

The diurnal variation in the observed multipath spread is shown in figure 2.3 for 4.0 MHz. The adjacent plot, figure 2.4, shows the variation in the number of modes detected. In each plot, the points represent one or more occurrences of the given value at that time of day (in local time, LT) and the solid line indicates the mean at each measurement interval, averaged over all the days in the data set. Clearly, the observations are quite similar to the prediction, with small multipath spread during the period 08:00 - 15:00 LT corresponding to predominantly single mode propagation. At night, the number of detected modes increases significantly,

with a mean around two, and four seen fairly often. The multipath spread is also larger, with means in excess of 3 ms, compared to under 1 ms during daylight. Note that this is not the time of flight, which is shown in figure 2.2, but rather the time spread of the signal power. Thus, at night multipath spreads of more than 4 ms are not uncommon, which corresponds to the predicted propagation modes of 1F2, 2F2 and 3F2.

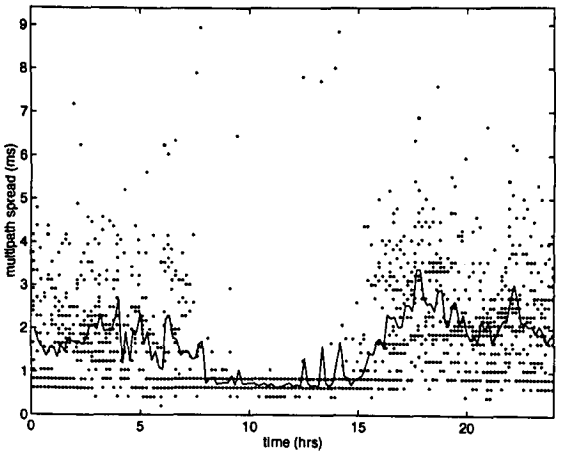


Figure 2.3: Diurnal variation in multipath spread at 4.0 MHz

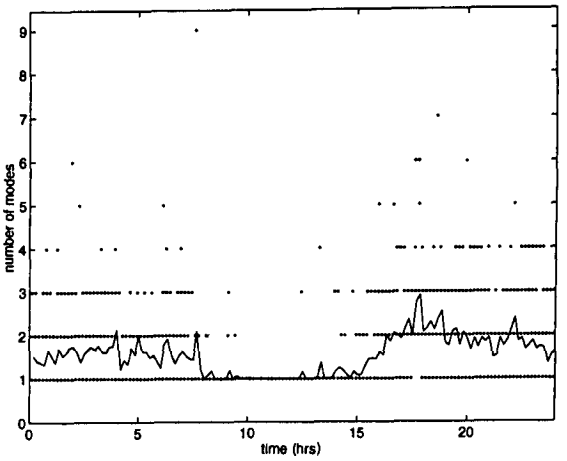


Figure 2.4: Diurnal variation in number of modes at 4.0 MHz

As the frequency approaches the MUF, the predicted behaviour changes significantly. Figures 2.5 and 2.6 show the predicted propagation modes at 4.7 MHz and 6.8 MHz, respectively. Figure 2.1 showed the predicted MUF is above 4.7 MHz at all times of day. In the plot of predicted modes, it is seen that multiple hop propagation is expected to cease when the frequency is closest to the MUF. The predicted MUF exceeds 6.8 MHz for about 18 hours, from 04:00 to 22:00, UT. During daylight at 4.7 MHz, 1E, 2F1 and 3F2 mode propagations are predicted, whereas at 6.8 MHz, 1F1 propagation is possible during the same period.

The observed multipath spread is shown in figures 2.7 and 2.8 for 4.7 MHz and 6.8 MHz, and the corresponding diurnal variations in the number of detected propagation modes are shown in figures 2.9 and 2.10. At 4.7 MHz, there are peaks in the average multipath spread observed at dawn and dusk, with corresponding increases in the number of propagating modes detected. Four or five modes are quite frequently detected at these times, with multipath spreads in excess of 5 ms, which indicates multihop propagation is supported by the F2 layer. At 6.8 MHz, there is significantly less diurnal variation, with mean multipath spreads between 1 and 2 ms at all times of day, and 3 propagation modes detected infrequently. There are scattered instances of large multipath spreads, up to 9 ms, but these are too isolated to have much effect on the mean values.

Above the MUF, there is generally less variation in the multipath spread, except around dusk. Figure 2.11 shows the diurnal variation in multipath spread at 11.2 MHz, and figure 2.12 shows the variation in the number of propagating modes detected at the same frequency. During the day, a single propagating mode is uniformly detected, with a corresponding multipath spread close to the lower limits of the DAMSON measurement system. During darkness, additional modes are detected, occasionally three or more, but the mean multipath spread only shows significant variation in the dusk region, where several instances of 9 ms

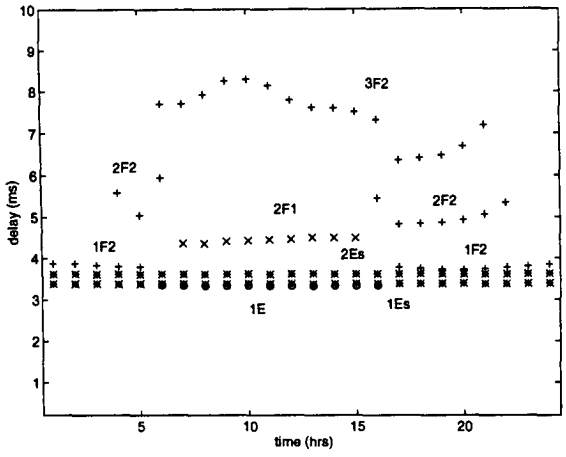


Figure 2.5: Predicted propagating modes at 4.7 MHz for August, 1995

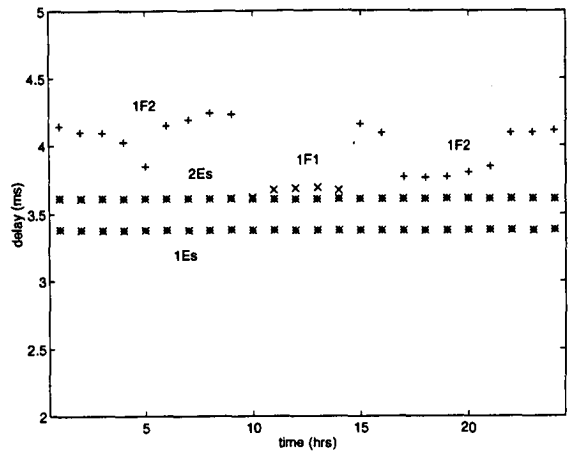


Figure 2.6: Predicted propagating modes at 6.8 MHz for August, 1995

multipath spread are seen. These modes are unexpected, according to the prediction program ICEPAC, which indicates only sporadic-E and possibly F1 layer propagation. They suggest some off-great-circle propagation, perhaps reflecting from the edge of the auroral oval, which is typically just south of the transmitter during the night period.

Figures 2.13 and 2.14 show the mean multipath spread across the frequency band during the day (08:00 - 14:00 LT) and night (20:00 - 02:00 LT). The 80th, 90th and 95th percentiles are also shown. During the day, the multipath spread peaks just below the MUF, and is consistently low above the predicted MUF, where a single propagating mode is most commonly observed. At night, the multipath spread decreases with frequency. The mean multipath spreads around 1 ms at night are again indicative of single mode propagation, although the time dispersoin is generally greater than during the daytime.

The distributions of the number of modes detected at 4.0 MHz, 6.8 MHz, 11.2 MHz and 17.5 MHz are shown in figures 2.15 and 2.16 for the periods 08:00 - 14:00 LT and 20:00 - 02:00 LT, respectively. At all frequencies except 6.8 MHz, single mode propagation is dominant during the day, with more modes being detected at night. At 6.8 MHz, there are more observations with two or modes detected during the day than at night.

## 2.2 SNR

The SNR measurements, taken from the CW portion of the DAMSON waveform, show diurnal cycles. These are obscured to some extent by the large standard deviation in the measurements due to the underlying fading process and the short measurement interval (4.3 s.).

The diurnal variations at 4.0 MHz and 11.2 MHz are shown in figures 2.17 and 2.18. At 4.0 MHz, i.e. below the MUF, the mean SNR is highest during the night. The situation is reversed above the MUF, although the difference is less marked.

The distributions of the SNR measurements during the day and night periods are shown in figures 2.19 and 2.20. They clearly show the higher SNR, with less variability, seen at 11.2 MHz during the period 08:00

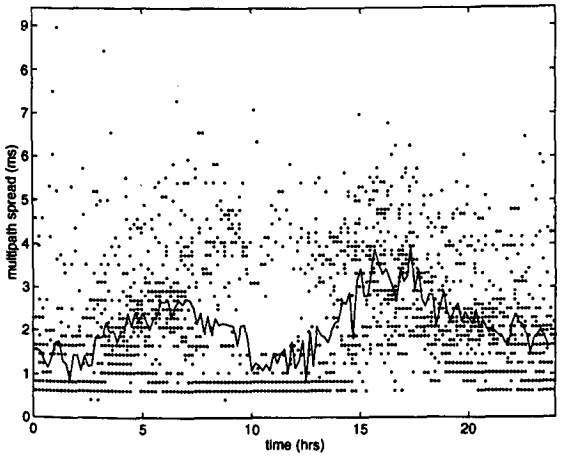


Figure 2.7: Diurnal variation in multipath spread at 4.7 MHz

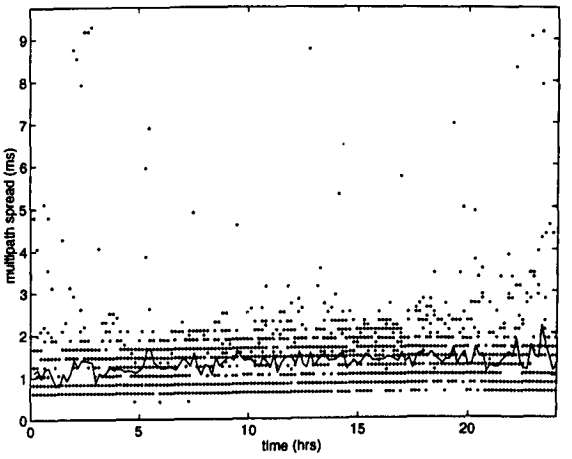


Figure 2.8: Diurnal variation in multipath spread at 6.8 MHz

- 14:00 compared to 4.0 MHz. At night, the distributions are quite similar.

The mean and percentiles of the SNR during the day (08:00 - 14:00) and night (20:00 - 02:00) are shown in figures 2.21 and 2.22. Figure 2.21 shows a clear peak in the SNR distribution just above the predicted MUF, with a mean of almost 20 dB at 9.0 MHz, compared to -12 dB at 2.8 MHz. Above 9.0 MHz, the mean SNR decreases with frequency, however the distribution broadens such that the 90th and 95th percentiles vary little, and the 5th and 10th percentiles decrease more rapidly.

At night, there is less variation in the mean SNR, although the distributions are again broader at higher frequencies. There is a small peak in the mean SNR at around 4.7 MHz, which is close to the predicted MUF in this time range.

### 2.2.1 Distribution of signal power

It was seen in section 2.1 that there are a significant number of secondary modes only during the nighttime, and only below the MUF. The distribution of the percentage of power that is in the strongest mode during this time at 4.0 MHz is shown in figure 2.23. About 50 % of the measurements show that the strongest mode contains at least 80 % of the total power, while 20 % have 90 % or more of the total power.

## 2.3 DOPPLER SPREAD

Overall, the Doppler spread on this path is fairly small, as would be expected for a sub-auroral path in reasonably quiescent geomagnetic conditions. Across all the frequencies, the mean Doppler spread does not exceed 2 Hz. Note that only the overall Doppler spread is considered in this section, as there were insufficient multiple mode occurrences during the periods of interest to generate satisfactory statistical conclusions regarding relative Doppler spreads.

Figures 2.24 and 2.25 show the diurnal variation in the overall Doppler spread at 4.0 MHz and 11.2 MHz, respectively. The sharp peaks in figure 2.24 are due to single observations with very large Doppler spreads, which may be true observations or artifacts. Below the MUF, there is more variation at night, but the mean

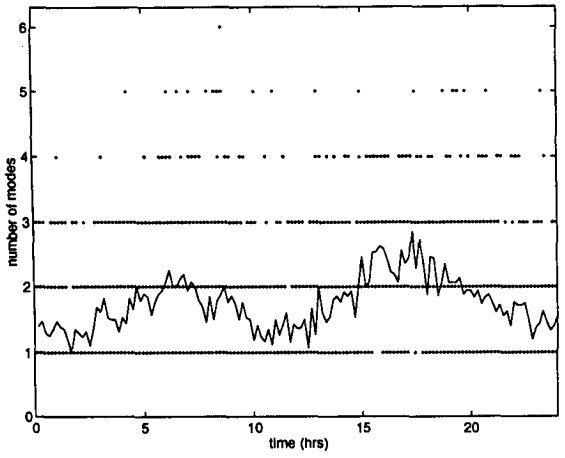


Figure 2.9: Diurnal variation in number of modes at 4.7 MHz

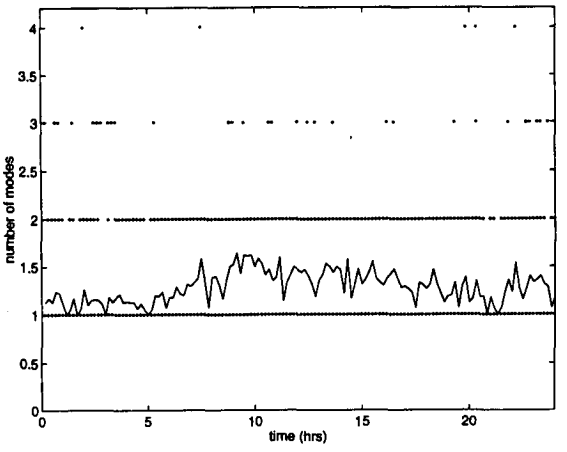


Figure 2.10: Diurnal variation in number of modes at 6.8 MHz

varies very little. Above the predicted MUF, it is seen that there is significantly more variation at night, and the mean tends to be a factor of almost two higher than during the day.

The mean and percentiles of the overall Doppler spread distributions are shown in figures 2.26 and 2.27 for the time periods 08:00 - 14:00 LT and 20:00 - 02:00 LT, respectively. At both times of day, the mean Doppler spread increases with frequency above the predicted MUF. Below the MUF, however, the mean decreases with frequency during the day, and tends to increase with frequency during the night. Overall, the distributions are broader and the means are higher at night.

## 2.4 DOPPLER SHIFT

In general, the Doppler shift observed on this path is very small. Only the shift seen on the strongest mode is considered, as secondary modes were not seen often enough to make valid statistical comments.

Figures 2.28 and 2.29 show the diurnal variations of measured Doppler shift at the two frequencies under main consideration, 4.0 MHz and 11.2 MHz. With very few exceptions, the Doppler shifts seen at 4.0 MHz were within $\pm 1$ Hz. The main deviations from this were just before local midnight. At 11.2 MHz, there is more significant variation at dusk and during darkness, mostly in a positive direction. Overall, most observations showed a slight trend towards negative Doppler shifts.

The means and percentiles of the distributions are shown in figure 2.30 for the hours 08:00 - 14:00 LT, and figure 2.31 for 20:00 - 02:00 LT. In both figures, it is seen that Doppler shifts tend to be very small, with 90 % within $\pm 3$ Hz at most frequencies. At both times of day, there is a clear trend for increasingly negative mean Doppler shifts with frequency, although below the predicted MUF the distributions have a positive bias, particularly during the daytime. These shifts indicate reflection from layers that are moving away from the great-circle direction, which corresponds to the direction of rotation of the auroral oval with respect to the transmitter and receiver.

## 2.5 PARAMETER INTERACTION

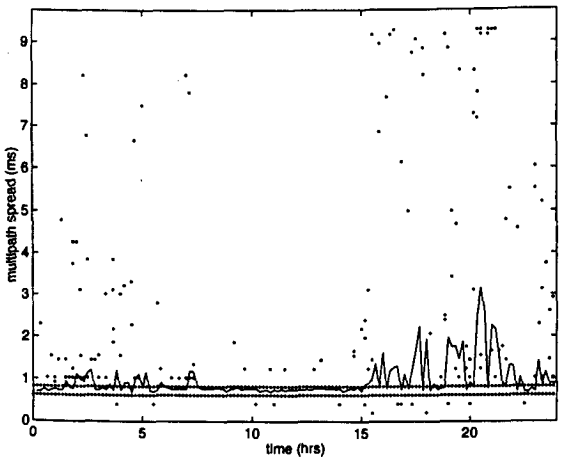


Figure 2.11: Diurnal variation in multipath spread at 11.2 MHz

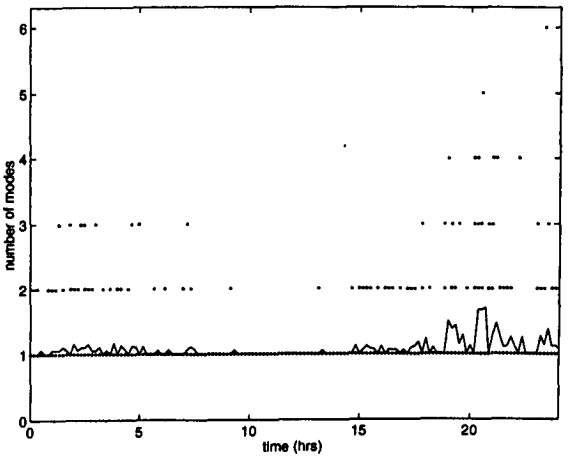


Figure 2.12: Diurnal variation in number of modes at 11.2 MHz

For robust data communication over high-latitude ionospheric HF links, not only must each propagation characteristic be considered, but any relationship between the parameters may also affect the performance of the modem.

### 2.5.1 Doppler spread on two modes

The only time range when there are sufficient data points with two or more propagation modes detected is at night below the MUF. The joint distribution of the Doppler spreads on the strongest and second strongest modes is shown in figure 2.32 for 20:00 - 02:00 at 4.0 MHz. In general, the Doppler spreads on the two modes are similar, however there is some elongation along both axes, which indicates that one mode may have a large Doppler spread while the other is small. It was seen in section 2.2.1 that the strongest mode tends to contain a significant proportion of the total signal power. However, figure 2.32 suggests that when the Doppler spread on one of the modes is large, the two modes have similar powers, hence either can be selected as the strongest. The correlation coefficient does not provide any useful information, as the resolution limitations of the measurements override any underlying correlation.

### 2.5.2 Doppler spread and multipath spread interaction

There is no particular relationship between Doppler spread and multipath spread. The joint distributions of the two parameters tend to be impulse-like when there is a single mode, and elongated along the multipath axis at night below the MUF, when the multipath spread shows some variability (section 2.1).

### 2.5.3 Doppler shift and multipath spread interaction

There is little variability in the Doppler shifts measured on this path, hence there is no specific relationship between Doppler shift and multipath spread.

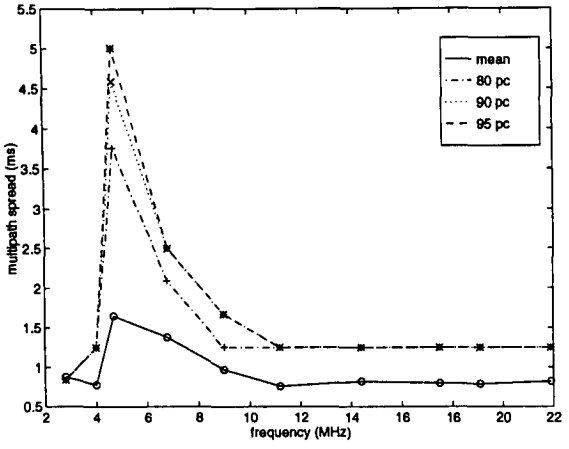


Figure 2.13: Percentiles of the multipath spread distributions for 08:00 to 14:00

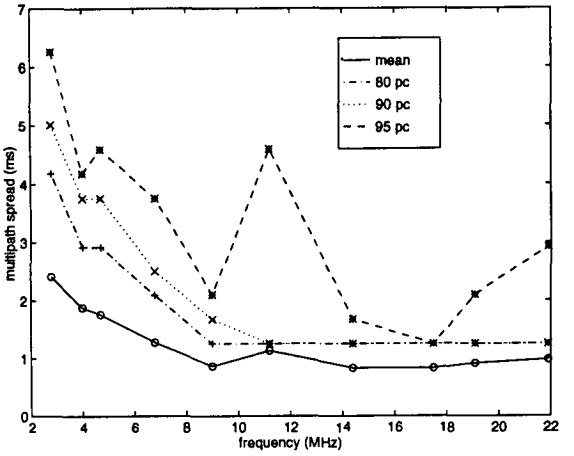


Figure 2.14: Percentiles of the multipath spread distributions for 20:00 to 02:00

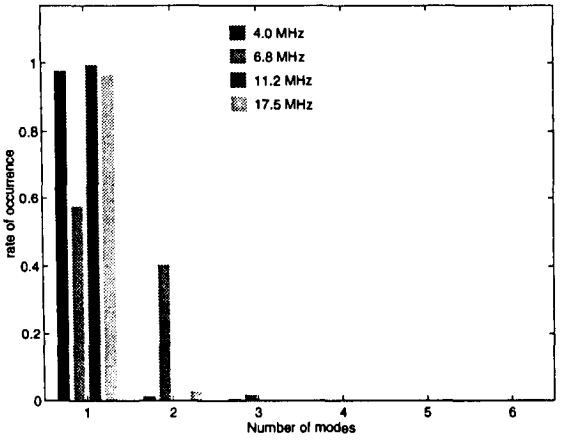


Figure 2.15: Distributions of number of propagating modes for 08:00 to 14:00

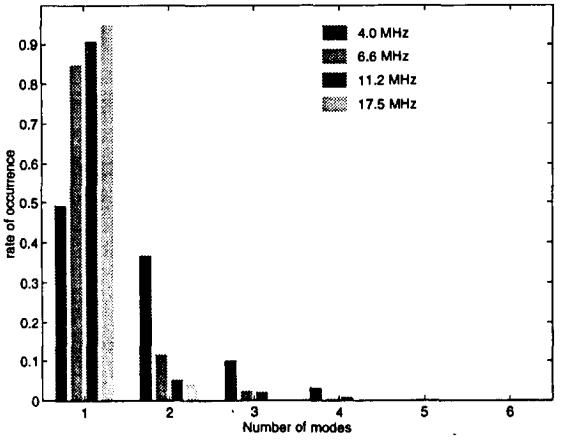


Figure 2.16: Distributions of number of propagating modes for 20:00 to 02:00

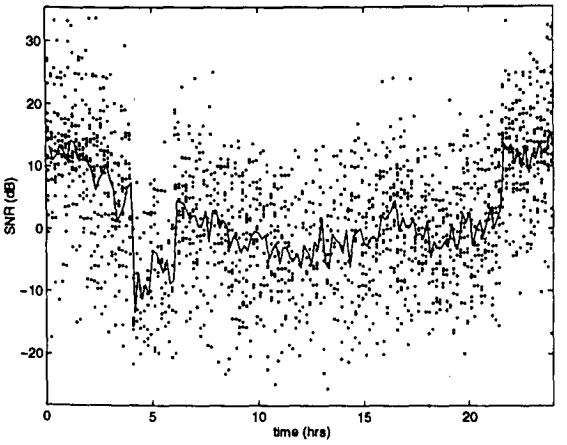


Figure 2.17: Diurnal variation in SNR at 4.0 MHz

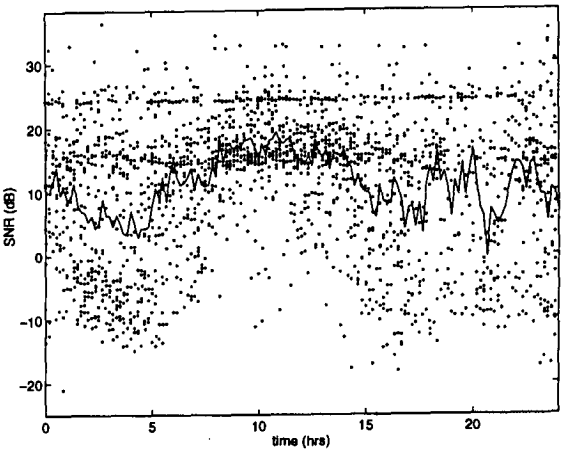


Figure 2.18: Diurnal variation in SNR at 11.2 MHz

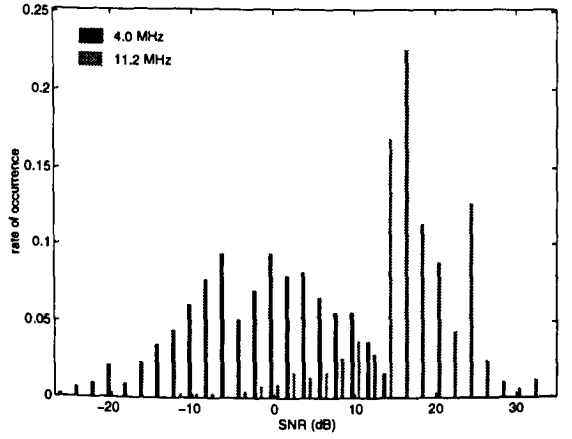


Figure 2.19: Distribution of SNR at 4.0 MHz and 11.2 MHz, 08:00 - 14:00

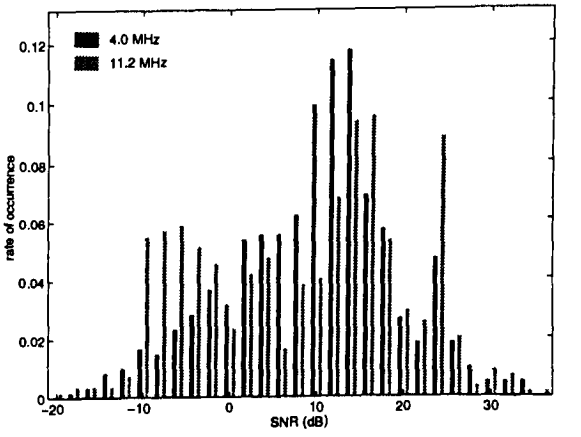


Figure 2.20: Distribution of SNR at 4.0 MHz and 11.2 MHz, 20:00 - 02:00

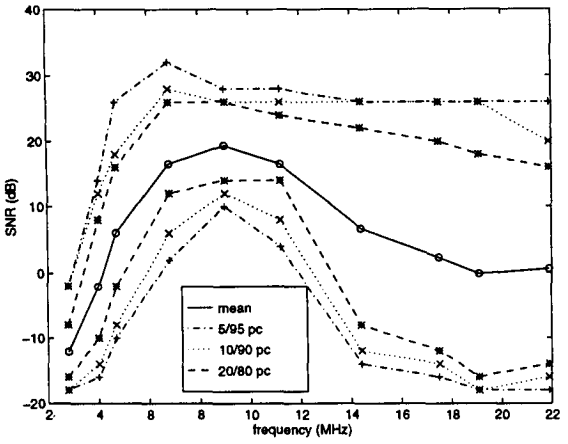


Figure 2.21: Percentiles of the SNR distributions for 08:00 to 14:00

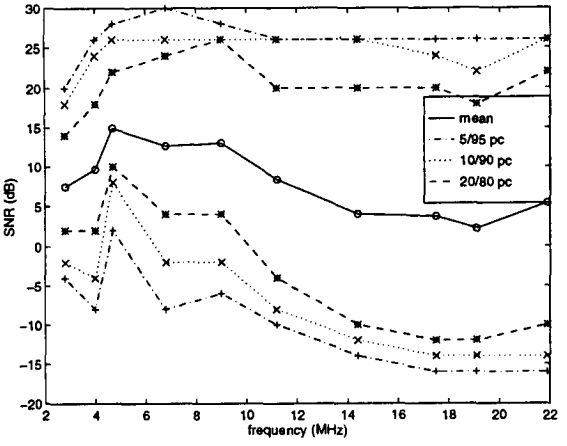


Figure 2.22: Percentiles of the SNR distributions for 20:00 to 02:00

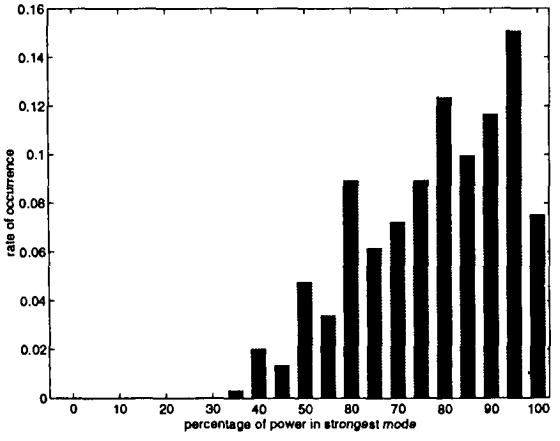


Figure 2.23: Distribution of percentage power in strongest mode at 4.0 MHz for 20:00 - 02:00 LT

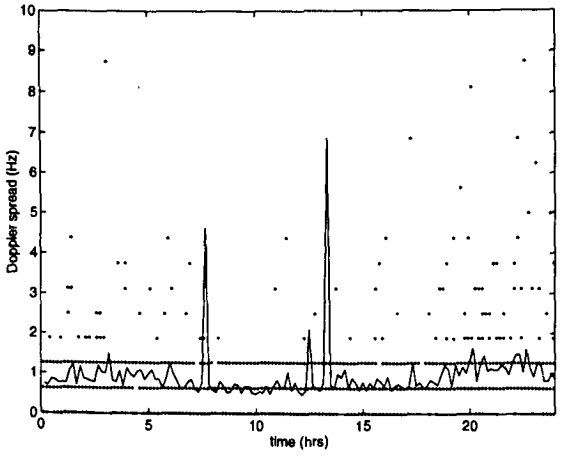


Figure 2.24: Diurnal variation in overall Doppler spread at 4.0 MHz

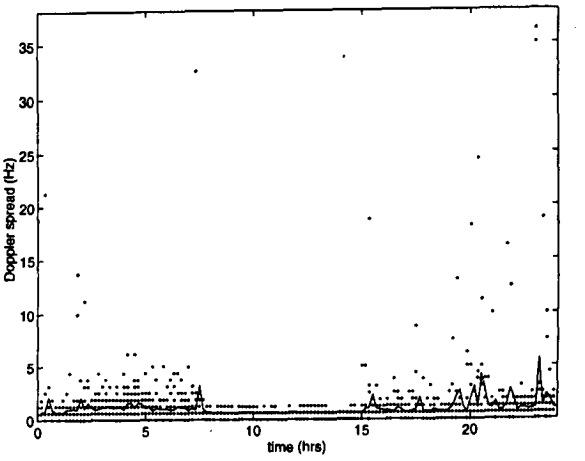


Figure 2.25: Diurnal variation in overall Doppler spread at 11.2 MHz

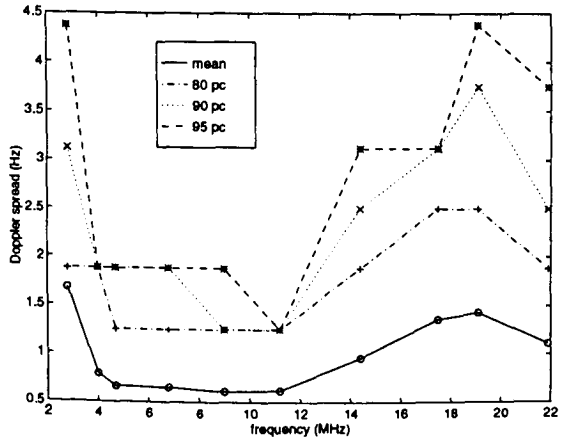


Figure 2.26: Percentiles of the overall Doppler spread distributions for 08:00 to 14:00

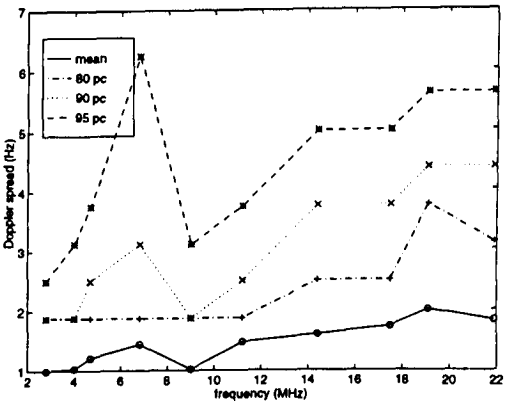


Figure 2.27: Percentiles of the overall Doppler spread distributions for 20:00 to 02:00

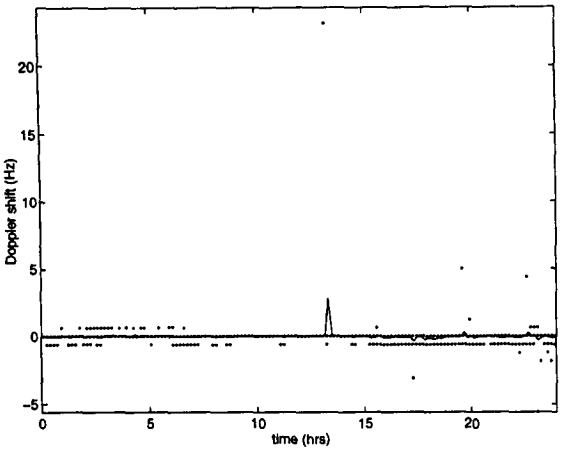


Figure 2.28: Diurnal variation in Doppler shift on strongest mode at 4.0 MHz

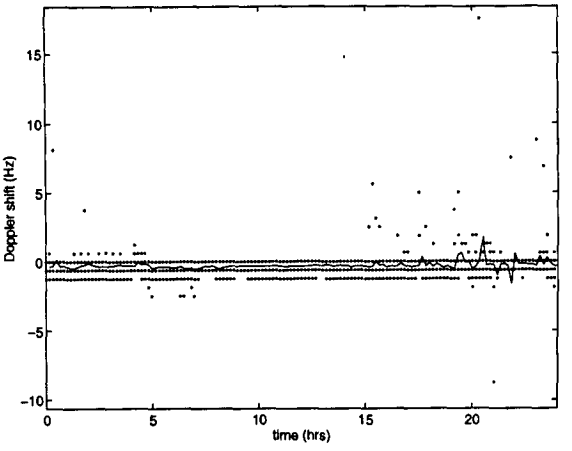


Figure 2.29: Diurnal variation in Doppler shift on strongest mode at 11.2 MHz

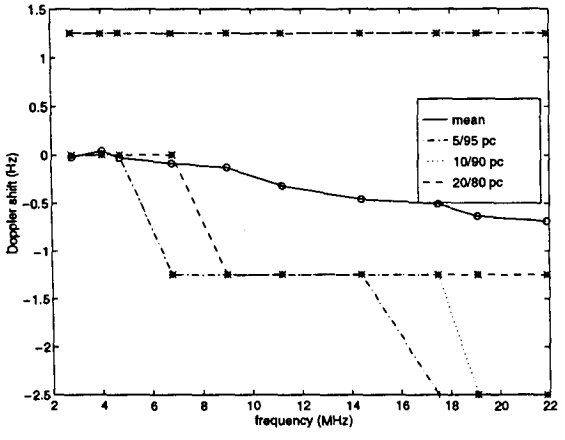


Figure 2.30: Percentiles of the Doppler shift distributions on strongest mode for 08:00 to 14:00

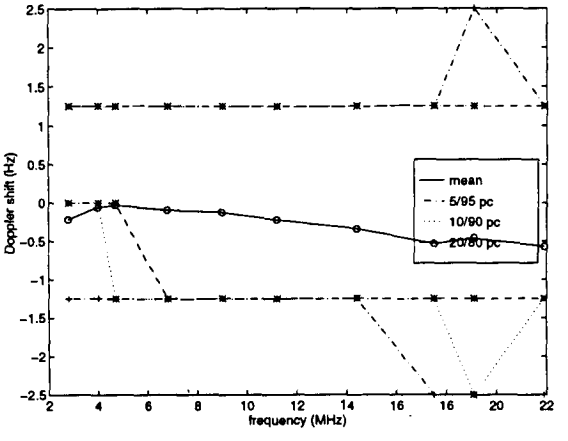


Figure 2.31: Percentiles of the Doppler shift distributions on strongest mode for 20:00 to 02:00

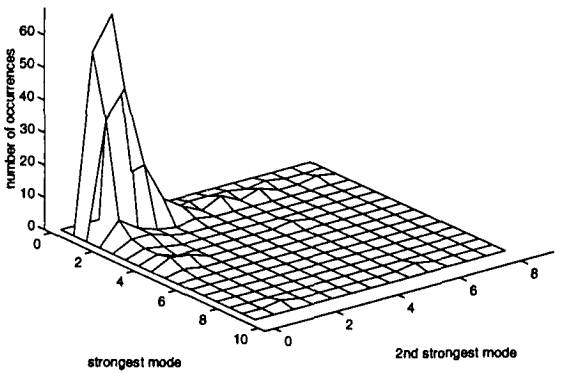


Figure 2.32: Joint distribution of Doppler spread on strongest and second strongest modes, 20:00 - 02:00, 4.0 MHz

## 2.6 SUMMARY

This link is predominatly sub-auroral, and demonstrates relatively benign characteristics. The multipath spread results in the predicted LUF/MUF window support the propagation mode predictions from ICEPAC to a large extent. Above the MUF, there is still significant propagation, which tends to be predominantly single mode. Below the MUF, there are many more observations with 2 or more propagating modes, with a resulting increase in the multipath spread. During the day, the mean SNR is higher near the top of the LUF/MUF window, but the distribution with frequency is more uniform at night.

The Doppler spreads are generally fairly small, with means consistently below 2 Hz, but increasing above the MUF. The resolution limitations of the system preclude accurate estimates in this region. Similarly, the Doppler shifts are small, with 5th and 95th percentiles in the range -2.5 to 2.5 Hz. The magnitudes of the Doppler shifts increase, i.e. become more negative, with increasing frequency at all times of day. This provides a basis for the suggestion that propagation above the MUF is occurring via reflection from the edge of the auroral zone, which is off-great-circle for this link.

# 3.0 HARSTAD-KIRUNA

The Harstad-Kiruna link is 184 km long, at an azimuth of 111°. The data set for this path includes measurements from seven days in May, eight days in August, seven days in September and 12 days in October, all from 1995. There are a total of 19,374 data points used for Doppler and multipath analysis, and 19,577 for SNR. Some significant differences in the parameter statistics have been observed between the May and August-October data sets, hence the two times of year have been analysed separately in this section. The data points are divided among the frequencies and times of year as shown in table 3.1.

| frequency | SNR | | Doppler & multipath | |
|---|---|---|---|---|
| (MHz) | May | Aug-Oct | May | Aug-Oct |
| 2.8 | 1300 | 2148 | 1291 | 2133 |
| 4.0 | 1398 | 2248 | 1397 | 2236 |
| 4.7 | 1390 | 2298 | 1370 | 2275 |
| 6.8 | 920 | 2098 | 906 | 2033 |
| 9.0 | 370 | 1195 | 337 | 1129 |
| 11.2 | 548 | 1640 | 544 | 1498 |
| 14.4 | 181 | 440 | 229 | 367 |
| 17.5 | 18 | 84 | 45 | 140 |
| 19.1 | 185 | 283 | 223 | 335 |
| 21.9 | 494 | 339 | 429 | 457 |
| total | 6804 | 12773 | 6771 | 12603 |

Table 3.1: Number of data points on Harstad-Kiruna link for SNR and Doppler/multipath analysis

The prediction program ICEPAC has been used to determine the MUF for great-circle propagation between Harstad and Kiruna. The predicted MUF is shown in figure 3.1; the LUF is below 2 MHz for all times of day for both months. Note that only three of the DAMSON frequencies fall below the predicted MUF for part or all of the time for which data has been collected. However, as seen in table 3.1, considerable propagation was seen at frequencies above the predicted MUF.

In the following sections, the main findings of the analysis of multipath spread, SNR, Doppler spread and Doppler shift will be presented and discussed. Brief consideration is also given to the interaction of the observed parameters.

## 3.1 MULTIPATH SPREAD

ICEPAC can be used to predict the modes supporting propagation throughout the day; plots showing these predictions for May and September, 1995, have been generated for comparison with the measured parameters. In the plots, E modes are marked with 'o', sporadic-E modes are marked '*', and F1 and F2 modes are indicated with '×' and '+', respectively. The time scales are in hours, universal time (UT).

The predicted propagation modes for 4.0 MHz are shown in figures 3.2 and 3.3. The multipath spread is greatest at night, when this frequency is close to the MUF. More modes are predicted during the nighttime in May, as the predicted MUF is below 4.0 MHz in September from 20:00 to 05:00 LT. The effect of the shorter daylight hours is also quite marked in September compared to May, as the F1 layer supports propagation only during daylight. In both months, it is common to see two or three supporting modes during the day,

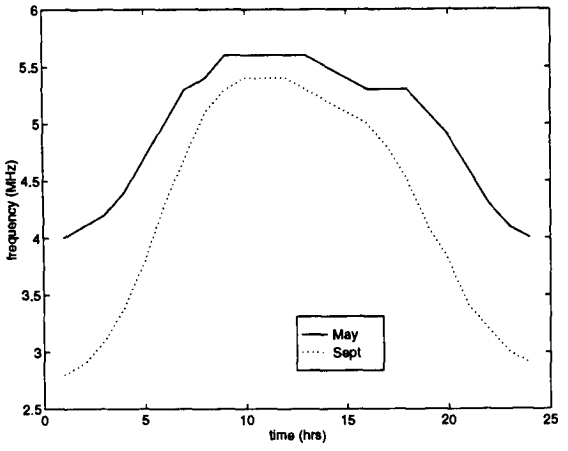


Figure 3.1: Predicted maximum usable frequency for May and September, 1995

according to the prediction program.

The diurnal variation in the multipath spread measured by the DAMSON system at 4.0 MHz is shown in figures 3.4 and 3.5 for the May and August-October time periods, respectively.

While the majority of the estimates fall within the predicted range, there are a few points which occur at the maximum of the DAMSON time range (approximately 12 ms). It is believed that these points are due to off-great-circle scatter. While there are some observations which correspond to propagation along, or close to, the great circle path most likely via the Es layer, these are predominantly at night. At these times, the Es layer is effectively shielding the F2 layer. The observed data is fairly closely representative of the predicted performance, with more severe and variable multipath spread at night. During the day, shorter multipath spreads are seen, probably single and multiple hops reflected from the F1 layer.

The corresponding plots showing the number of propagating modes detected is shown in figures 3.6 and 3.7. During both time periods, there are fewer modes detected during the local geomagnetic mid-day period, 06:00-14:00 local time (LT), and more during the darkness hours. In particular, there is a peak in the number of modes detected at dawn in May, which coincides with a peak seen in the multipath spread, figure 3.4, and with the predicted transition from F2 to F1 mode propagation. There is a slight decrease in the number of modes seen around the local geomagnetic midnight period, 22:00 to 24:00 LT, particularly during the August-October period. This corresponds to the time when this frequency is very close to the predicted MUF. The average number of modes observed is greater during the August-October period than in May, with three modes being detected frequently during the hours of darkness.

The observed propagation characteristics are similar at the two lowest DAMSON frequencies, particularly during the day when they are both below the MUF. A significant change is noted between the predicted propagation as the frequency increases from 4.0 MHz to 4.7 MHz. As the frequency increases, it is predicted that multiple modes are supported only during daylight hours, although propagation via the sporadic-E layer is possible at any time.

The main difference in the observed propagation characteristics compared to 4.0 MHz is the increased variability in the estimated multipath spread. In May, figure 3.8, this variability is primarily seen during daylight hours, whereas in the August-October period, figure 3.9, there is greater variability during the hours

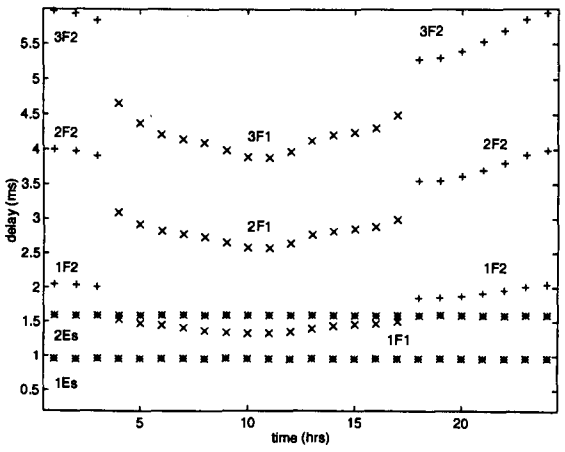


Figure 3.2: Predicted propagating modes at 4.0 MHz for May, 1995

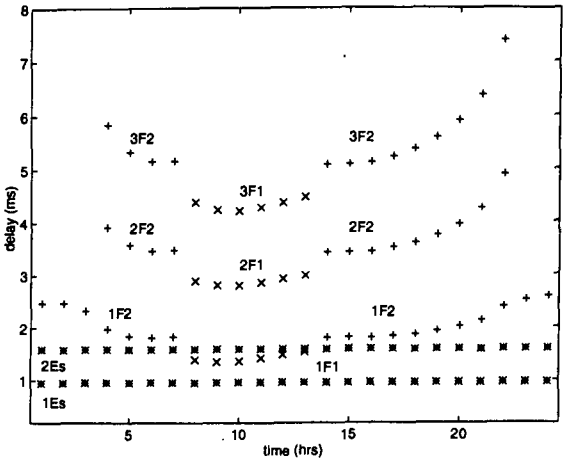


Figure 3.3: Predicted propagating modes at 4.0 MHz for September, 1995

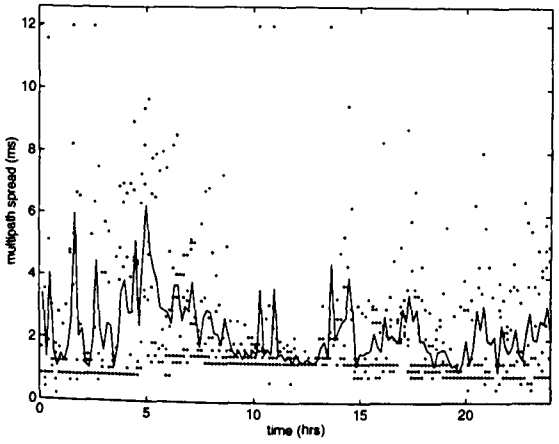


Figure 3.4: Diurnal variation in multipath spread at 4.0 MHz for May, 1995

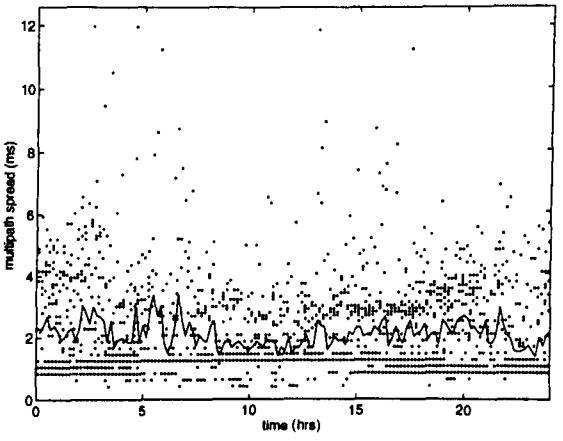


Figure 3.5: Diurnal variation in multipath spread at 4.0 MHz for August-October, 1995

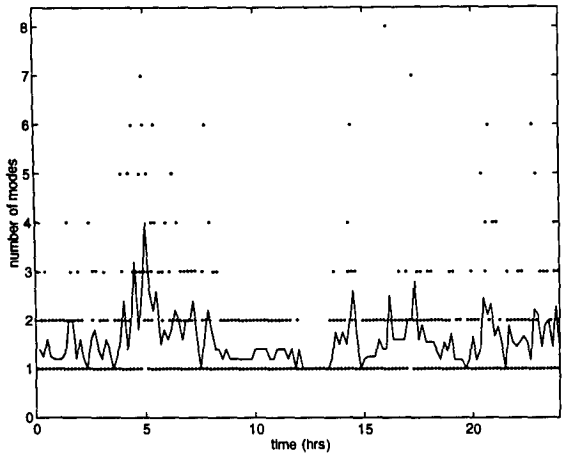


Figure 3.6: Diurnal variation in number of modes at 4.0 MHz for May, 1995

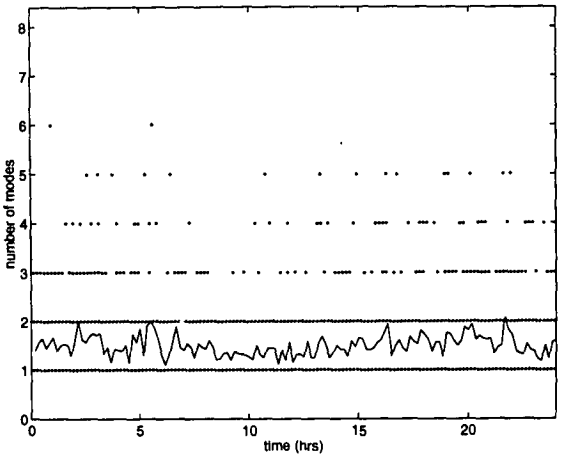


Figure 3.7: Diurnal variation in number of modes at 4.0 MHz for August-October, 1995

of darkness, with a corresponding increase in the mean value. These observations are believed to be due to off-great-circle scatter, possibly from the edge of the auroral region. The number of propagating modes detected during these time periods closely reflects the multipath spread observations.

At frequencies of 6.8 MHz and higher, i.e. above the MUF, ICEPAC predicts that 1F2 is the most probable propagating mode although it is not reliable. Sporadic-E is again possible throughout the 24 hours. The MUF is below 6 MHz for all times of day in May and September, but support for propagation does exist, at least up to 11.2 MHz with some reliability, as shown in table 3.1.

The variation actually seen in the total multipath spread is substantial on this path for frequencies above the predicted MUF. A condition that is commonly seen is very elongated modes, which are not easily separated either automatically or manually. The early (or left) side elongation is believed to be due to either E-mode or ground-wave propagation. The propagation time for each is very similar, and a direction finding system would be required to distinguish the angles of arrival. From the physical geography of the path, it is to be expected that the groundwave component would be negligible, as the coastal mountains prevent line-of-sight propagation.

The multipath spread is also elongated to the right, or late, side. The receiving antenna at Kiruna is omnidirectional, and can therefore receive substantial signal power from the off-great-circle direction. As both the transmitter and receiver sites are close to the auroral zone, it is suspected that there is considerable power received from scatter off moving irregularities.

The diurnal variations in the observed multipath spreads are shown in figures 3.10 to 3.11 for May and August-October at 11.2 MHz. This is fairly typical of the variations seen at 6.8 MHz and 9.0 MHz. It is noted that the overall means exceed 6 ms at 9.0 MHz and 11.2 MHz in the August-October period, but are somewhat lower in May. The number of modes detected is consistently higher in the August-October period than in May, with observations of six or more modes occurring quite frequently, especially during daylight, in the August-October period, and very rarely during May.

In each of the diurnal variations for the August-October period, there is a band of large multipath spreads which appears during the day. At 6.8 MHz, this band is in the range 6 to 10 ms, at 9.0 MHz it is 8 to 12 ms,

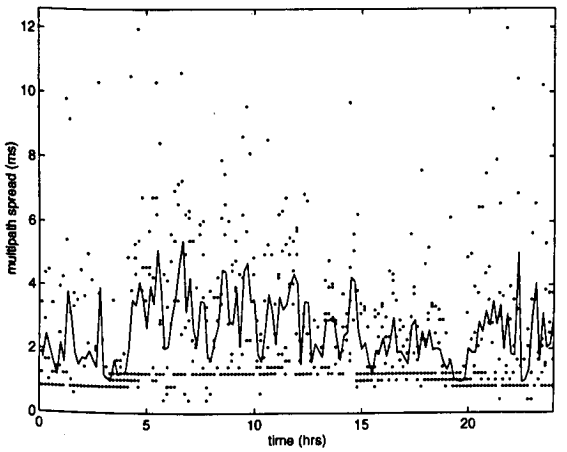


Figure 3.8: Diurnal variation in multipath spread at 4.7 MHz for May, 1995

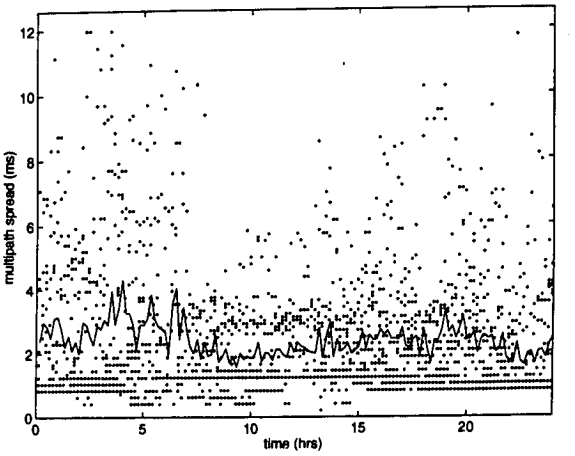


Figure 3.9: Diurnal variation in multipath spread at 4.7 MHz for August-October, 1995

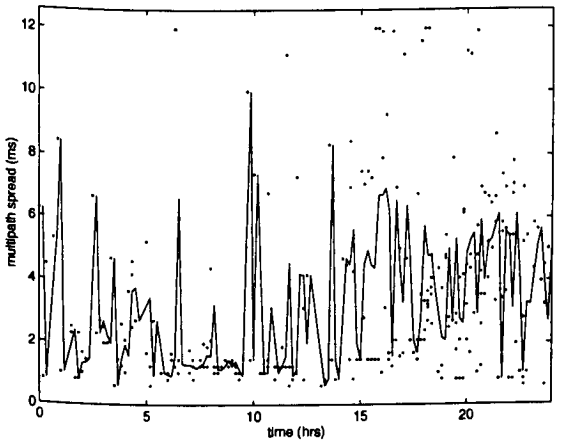


Figure 3.10: Diurnal variation in multipath spread at 11.2 MHz for May, 1995

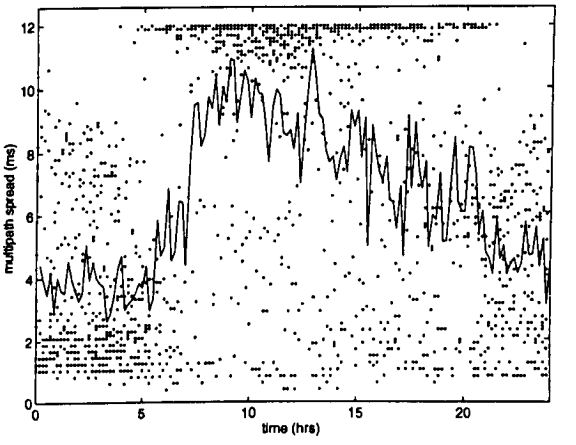


Figure 3.11: Diurnal variation in multipath spread at 11.2 MHz for August-October, 1995

and at 11.2 MHz the band appears at the limits of the measurement system, in the range 10 ms to in excess of 12 ms. These bands are accompanied only by a small increase in the number of modes, which indicate that these are instances of the very elongated modes which were discussed earlier. A similar effect is noted at 6.8 MHz in the May data set, but not at higher frequencies although there is considerable variation in the multipath spread estimates there. These bands are highlighted in figures 3.12 and 3.13, which show the cumulative distributions of multipath spread averaged over all times of day at 6.8 MHz, 9.0 MHz and 11.2 MHz.

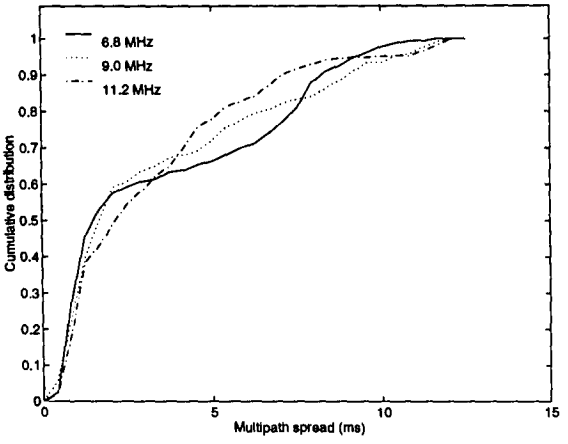


Figure 3.12: Cumulative distribution of multipath spreads above the MUF for May, 1995

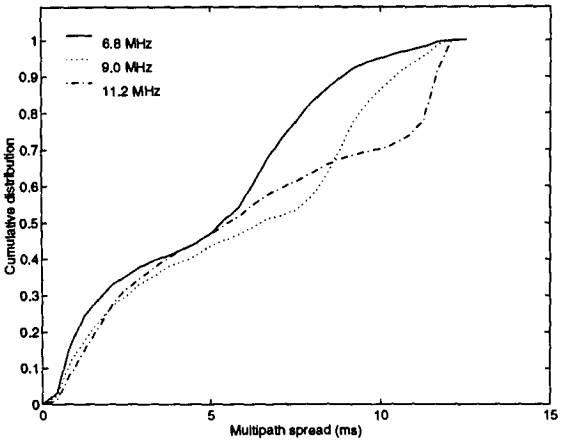


Figure 3.13: Cumulative distribution of multipath spreads above the MUF for August-October, 1995

The distribution of multipath spreads across the frequency band is shown in figures 3.14 and 3.15 for May and August-October, respectively. These values have been obtained by averaging over all data points, at all times of day. Note that the distribution at each frequency has been normalised by the number of estimates extracted from the received signals. The distribution in the May data set is fairly uniform across the frequency band. The distribution of the number of modes detected is similar (figure 3.16), but smoother. In the August-October period, there is a marked change in the distribution in the mid-band frequencies, 6 to 12 MHz, as discussed above. In this range, there are many more occurrences of large multipath spreads. There is a small corresponding increase in the number of modes detected, as seen in figure 3.17.

The mean values of the multipath are shown in figures 3.18 and 3.19 for daytime and nighttime, respectively. The 80th, 90th and 95th percentiles are also shown. Note that the 95th percentile point for 2.8 MHz in May exceeded 12 ms, which is the limitation of the analysis. It is shown at a default value of 15 ms. Note also that there are insufficient data points to generate a distribution at 17.5 MHz during daylight hours. The hours used for daytime were 08:00 to 14:00 LT, which corresponds to the six hour period centred on 13:00, local geomagnetic time. The nighttime period was taken as 20:00 to 02:00 LT. These time periods were chosen as they include only daylight or darkness hours, respectively.

The figures show the increase in multipath spread seen at night across the frequency band. In the higher frequencies during the day, it is noted that the distribution is quite compact near the mean value, with only a few outliers causing a significant gap between the 90th and 95th percentiles.

The daylight and darkness percentiles of multipath spread for the August-October period are shown in figures 3.20 and 3.21. During the day, there is a significant difference from the May data in the mid-range

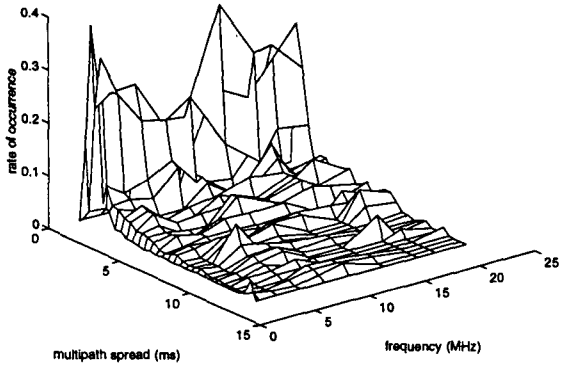


Figure 3.14: Distribution of multipath spreads for May, 1995

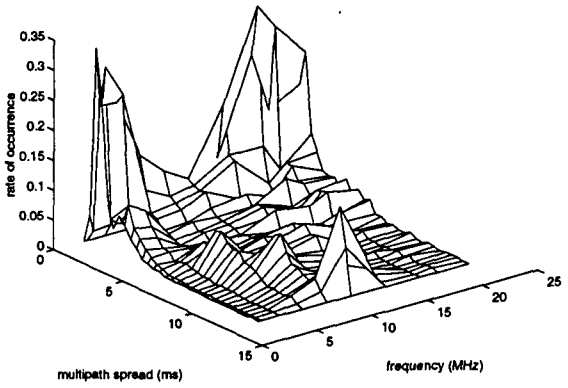


Figure 3.15: Distribution of multipath spreads for August-October, 1995

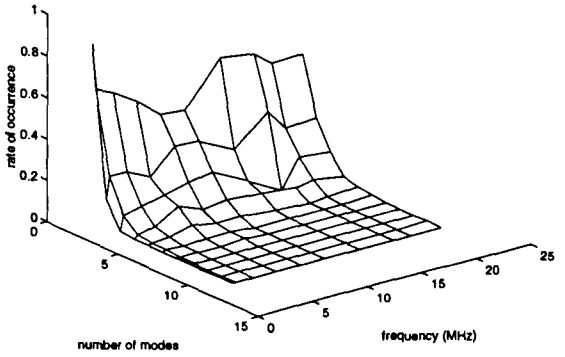


Figure 3.16: Distribution of number of modes for May, 1995

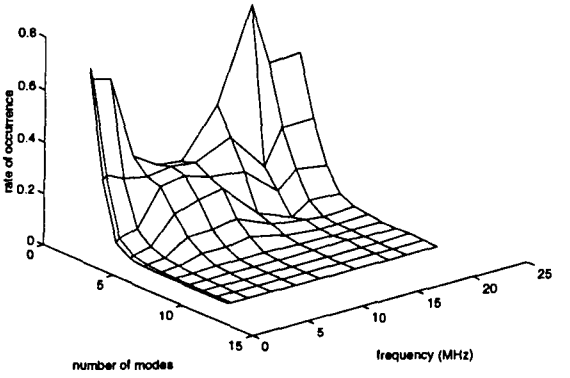


Figure 3.17: Distribution of number of modes for August-October, 1995

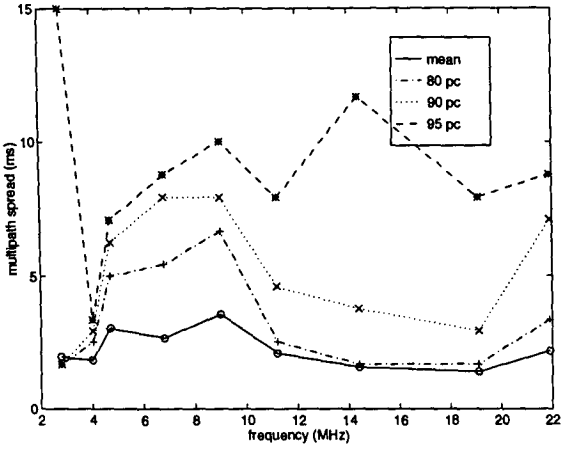


Figure 3.18: Percentiles of the multipath spread distributions for 08:00 to 14:00 May, 1995

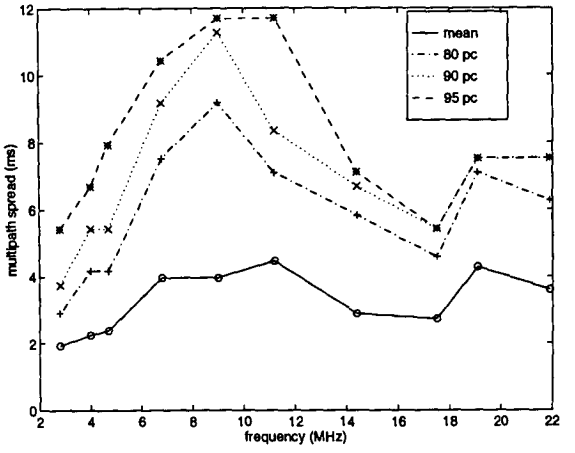


Figure 3.19: Percentiles of the multipath spread distributions for 20:00 to 02:00 May, 1995

of frequencies, where the multipath spread is very high during the August-October period. This has been attributed to off-great-circle scatter. At night, the multipath spreads seen during both times of year are similar.

## 3.2 SNR

The variation in the estimated SNR varies, on average, throughout the day. However, the values also change significantly from one measurement interval to the next, ten minutes later. This is likely due, in part, to the short measurement period and the channel fading. A large part of this effect is also believed to be due to the rapid movements of the ionosphere in this region.

The diurnal variations in SNR are shown in figures 3.22 and 3.23 for 4.0 MHz in May and August-October. At both times of year, the daytime SNR tends to be about 10 dB higher than at night. The band seen at approximately 24 dB is believed to be due to the measurement system.

Figures 3.24 and 3.25 show the dirunal variation for 11.2 MHz, above the predicted MUF. There is less variation than was seen at 4.0 MHz, and the SNR is 10-20 dB lower than at frequencies below the predicted MUF. As the lower end of the measurement range is limited by the system, there is less variation in these data sets than at the lower frequency.

The mean SNR obtained at each frequency is shown in figures 3.26 and 3.27 for the daylight hours (08:00 to 14:00 LT) and darkness hours (20:00 to 02:00 LT) in May. The 5th, 10th, 20th, 80th, 90th and 95th percentiles are also shown. Corresponding plots for the August-October period are shown in figures 3.28 and 3.29. Figure 3.1 shows that the predicted MUF on this path does not exceed 6 MHz at any time of day. Evidence of this can be seen from the SNR distributions, where the means decrease steadily above 4.7 MHz. The mean daytime SNR at 2.8 MHz is lower than that at 4.0 MHz and 4.7 MHz in May, which is not predicted, as the LUF is below 2 MHz. In the August-October period, there is also a lower SNR at this frequency during the daytime (figure 3.28), although the difference compared to 4.0 MHz is not as great as in May.

There is little difference in the overall statistics of the SNR seen during the May and August-October

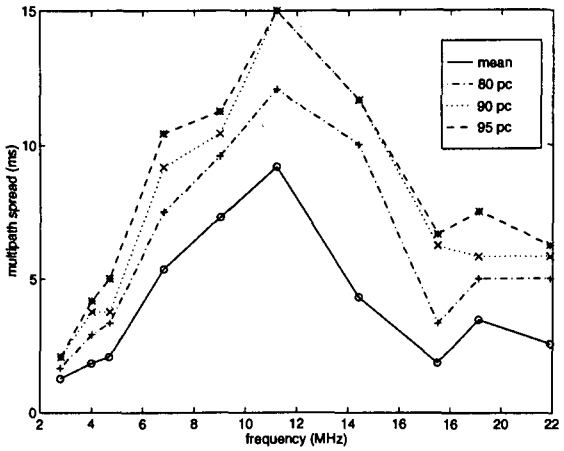


Figure 3.20: Percentiles of the multipath spread distributions for 08:00 to 14:00 August-October, 1995

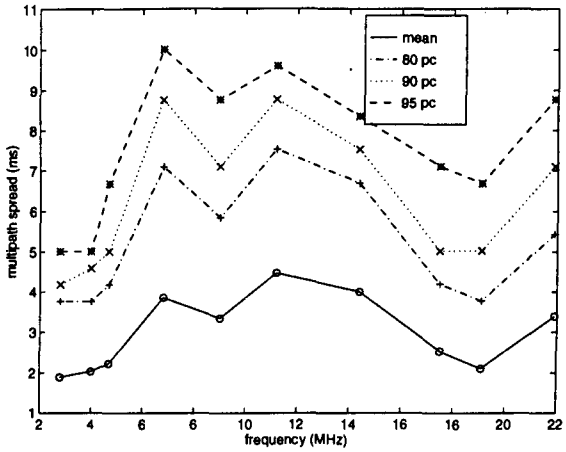


Figure 3.21: Percentiles of the multipath spread distributions for 20:00 to 02:00 August-October, 1995

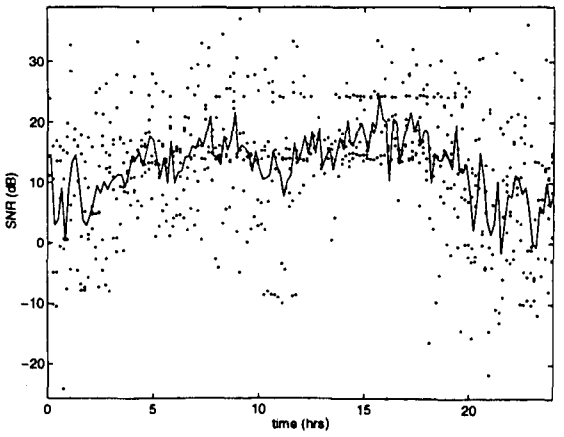


Figure 3.22: Diurnal variation in SNR at 4.0 MHz, May 1995

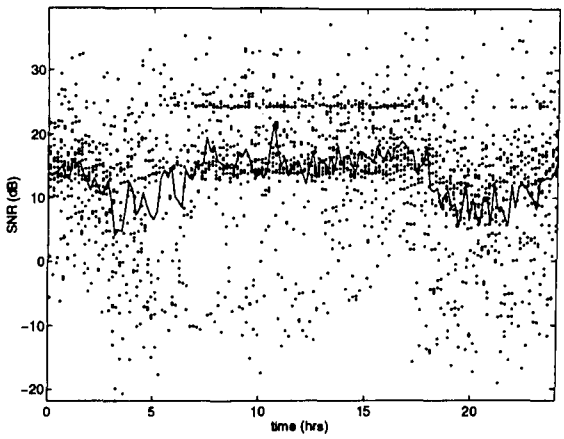


Figure 3.23: Diurnal variation in SNR at 4.0 MHz, August-October 1995

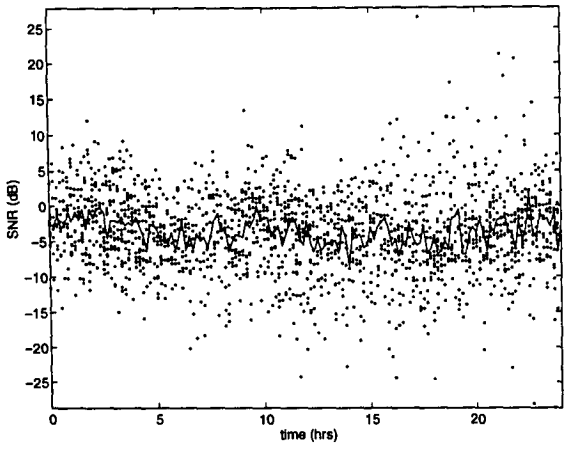


Figure 3.24: Diurnal variation in SNR at 11.2 MHz, May 1995

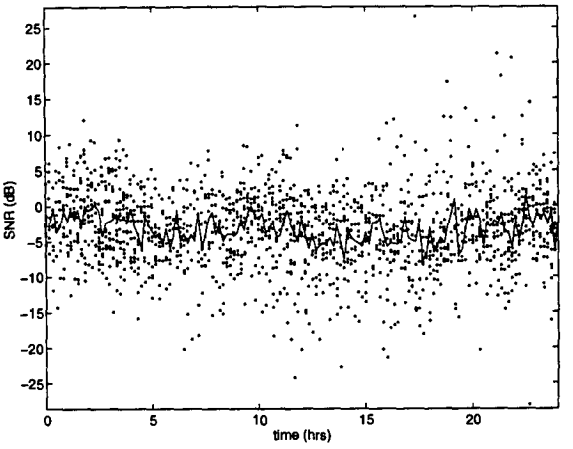


Figure 3.25: Diurnal variation in SNR at 11.2 MHz, August-October 1995

periods. The daytime mean SNRs are higher, on average, than during darkness at frequencies below 6 MHz, i.e. below the MUF. However, the SNRs above the MUF tend to be higher during the nighttime, which may indicate more scatter propagation.

### 3.2.1 Distribution of signal power

Figures 3.30 and 3.31 show the distribution of the percentage of power in the strongest mode at 4.0 MHz, for 08:00-14:00 LT and 20:00-02:00 LT in May and August-October, respectively. The distributions are similar for 2.8 MHz and 4.7 MHz, which were seen in section 3.2 also to have similar SNR characteristics. There are only slight differences between daytime and nighttime distributions at frequencies below the predicted MUF. The main difference is that the mean percentage is slightly greater during the nighttime in the August-October period. In May, the mean is smaller at night.

Looking at the number of modes observed, figures 3.32 and 3.33, it is seen that there are more cases where three or more modes are detected at night. This is more pronounced in May than August-October, which explains, at least partially, the reduction in mean percentage power in the strongest mode noted above.

For frequencies above the MUF, the distributions are typified by those shown in figures 3.34 and 3.36, for 11.2 MHz. The May distributions are similar at 4.0 MHz and 11.2 MHz, except there is a lower mean above the predicted MUF, especially at night. This corresponds to an increase in the number of modes detected (figure 3.35). In August-October, there is a marked difference in the distributions at 4.0 MHz and 11.2 MHz. Above the predicted MUF, a much greater proportion of measurements indicate the strongest mode contains 50-70 % of the total signal power. The median values are 90 % at 4.0 MHz and 70 % at 11.2 MHz during the daytime. At 11.2 MHz, the distribution is shifted at night such that the power in the strongest mode is higher. This corresponds to a decrease in the number of observations with three or more modes, compared to daytime at the same frequency.

## 3.3 DOPPLER SPREAD

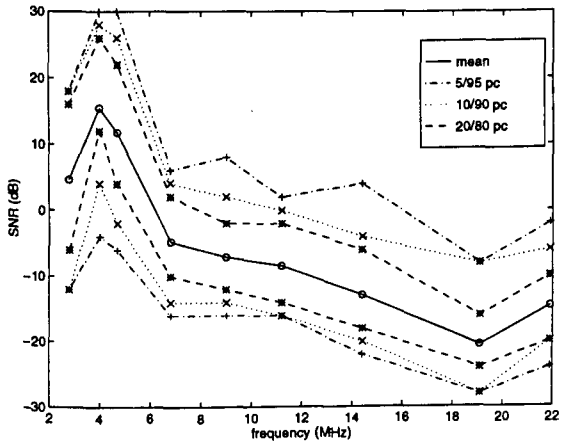


Figure 3.26: Percentiles of the SNR distributions for 08:00 to 14:00 May, 1995

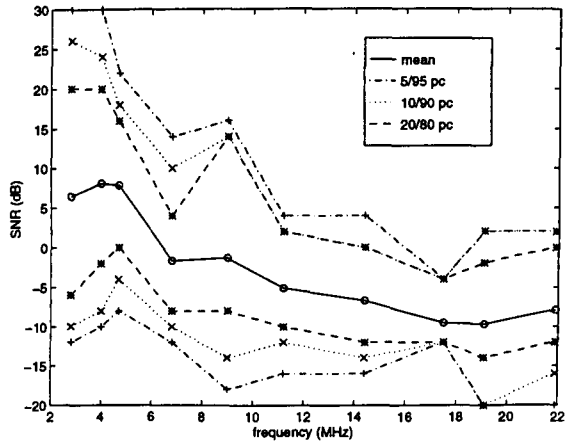


Figure 3.27: Percentiles of the SNR distributions for 20:00 to 02:00 May, 1995

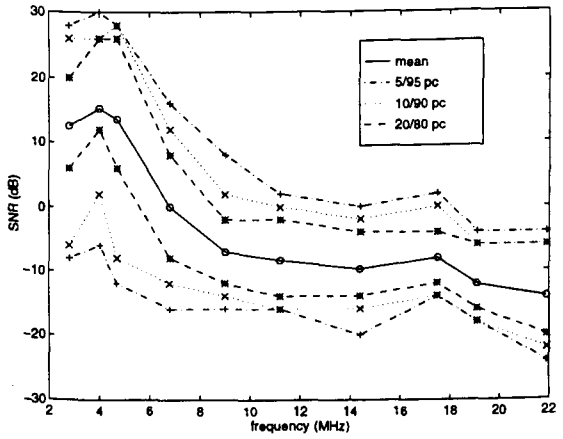


Figure 3.28: Percentiles of the SNR distributions for 08:00 to 14:00 August-October, 1995

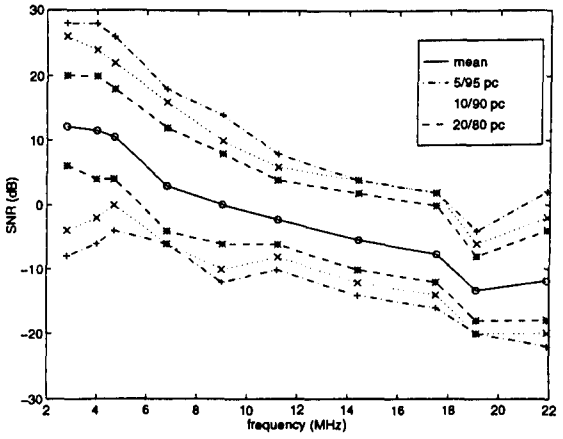


Figure 3.29: Percentiles of the SNR distributions for 20:00 to 02:00 August-October, 1995

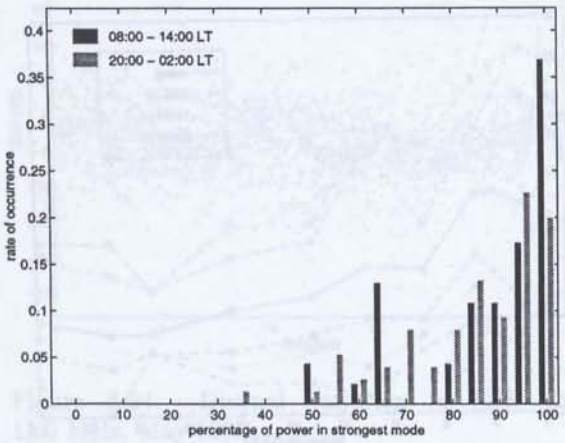


Figure 3.30: Distribution of percentage of power in strongest mode at 4.0 MHz, day and night, May, 1995

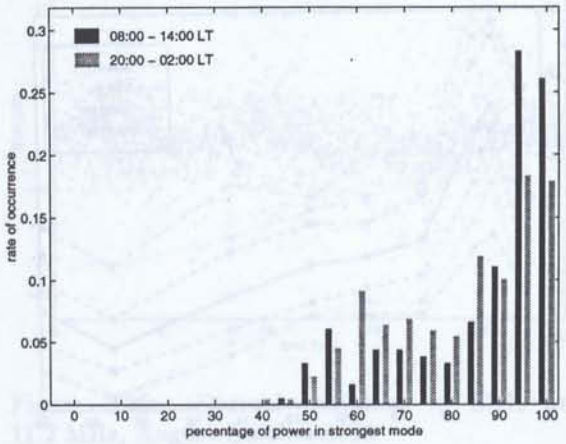


Figure 3.31: Distribution of percentage of power in strongest mode at 4.0 MHz, day and night, August-October, 1995

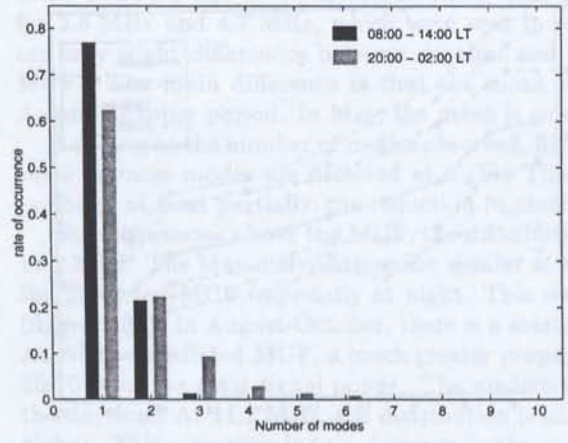


Figure 3.32: Distribution of number of modes at 4.0 MHz, day and night, May, 1995

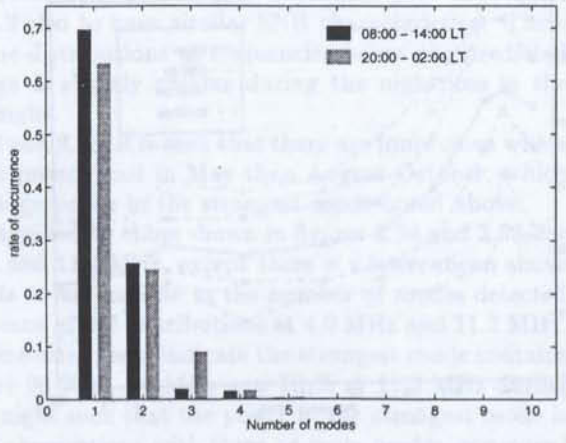


Figure 3.33: Distribution of number of modes at 4.0 MHz, day and night, August-October, 1995

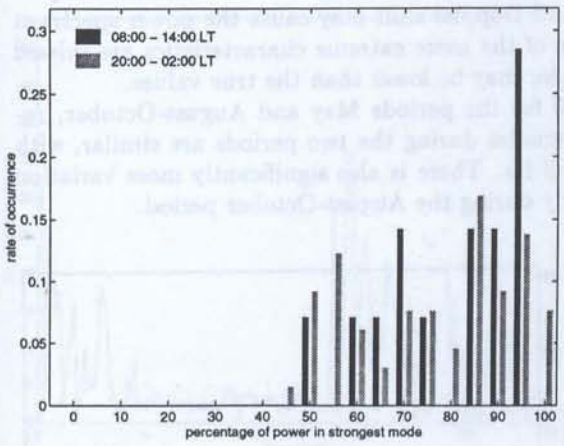


Figure 3.34: Distribution of percentage of power in strongest mode at 11.2 MHz, day and night, May, 1995

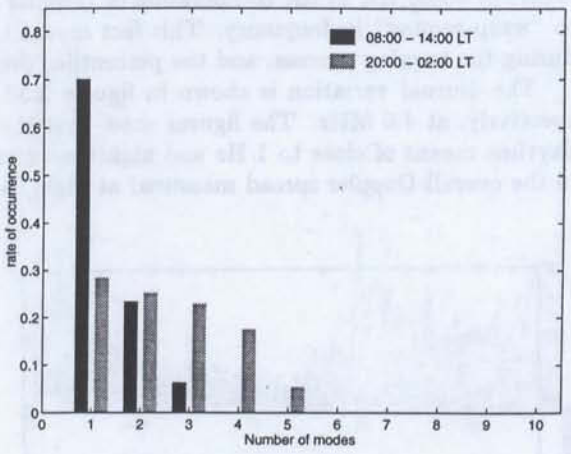


Figure 3.35: Distribution of number of modes at 11.2 MHz, day and night, May, 1995

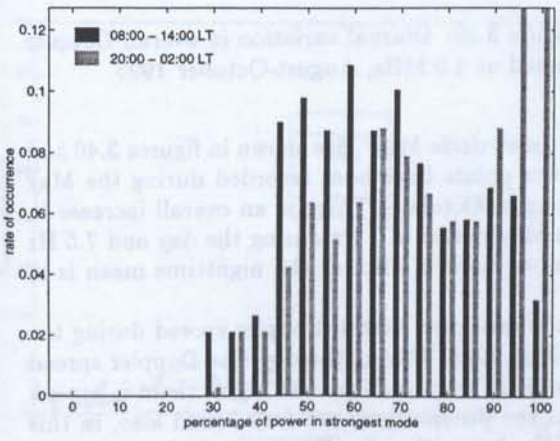


Figure 3.36: Distribution of percentage of power in strongest mode at 11.2 MHz, day and night, August-October, 1995

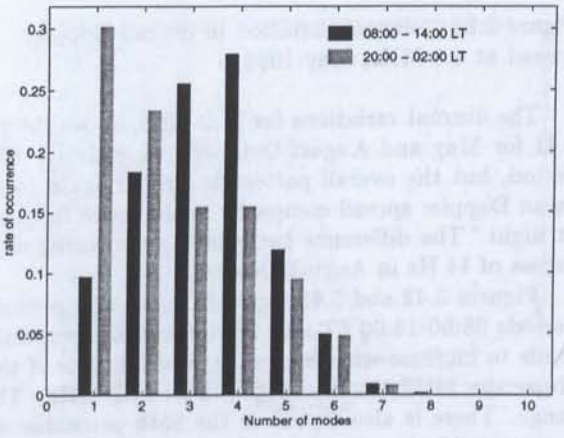


Figure 3.37: Distribution of number of modes at 11.2 MHz, day and night, August-October, 1995

The distribution of the overall Doppler spread varies considerably with time-of-day and season, as well as with frequency, on the Harstad-Kiruna link. Note that the Doppler spread cannot be measured reliably in excess of 40-50 Hz, as the combination of Doppler spread and Doppler shift may cause the power spectrum to "wrap-around" in frequency. This fact means that some of the more extreme characteristics are missed during the tagging process, and the percentiles presented here may be lower than the true values.

The diurnal variation is shown in figures 3.38 and 3.39 for the periods May and August-October, respectively, at 4.0 MHz. The figures show that the characteristics during the two periods are similar, with daytime means of close to 1 Hz and nighttime means near 3 Hz. There is also significantly more variation in the overall Doppler spread measured at night, particularly during the August-October period.

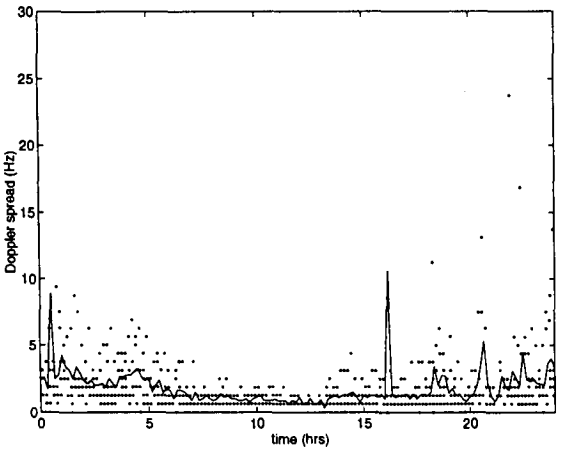


Figure 3.38: Diurnal variation in overall Doppler spread at 4.0 MHz, May 1995

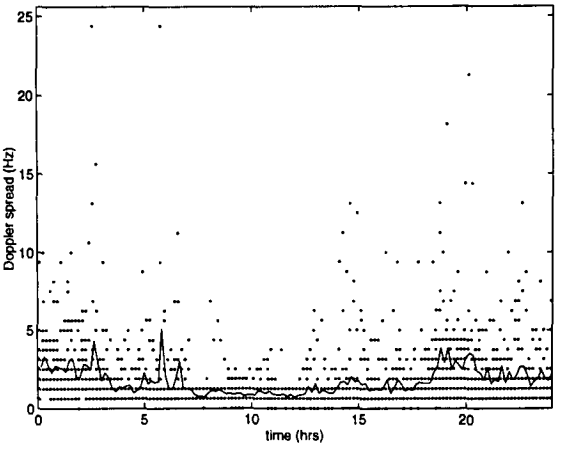


Figure 3.39: Diurnal variation in overall Doppler spread at 4.0 MHz, August-October 1995

The diurnal variations for 11.2 MHz, above the predicted great-circle MUF, are shown in figures 3.40 and 3.41 for May and August-October, respectively. Clearly, fewer points have been recorded during the May period, but the overall pattern is similar again to that in August-October. There is an overall increase in mean Doppler spread compared to the lower frequency, with May means of 3 Hz during the day and 7.5 Hz at night. The difference between the two times of year is more marked, also, as the nighttime mean is in excess of 14 Hz in August-October.

Figures 3.42 and 3.43 show the mean and percentiles of the measured overall Doppler spread during the periods 08:00-14:00 LT and 20:00-02:00 LT, respectively, in May 1995. During the day, the Doppler spread tends to increase with frequency, and the tails of the distributions become wider. At night, there is a peak above the MUF, in the range 6.8 to 11.2 MHz. The tails of the distributions are very broad also, in this range. There is also a peak in the 95th percentile at 19.1 MHz, but with only slightly more than 100 data points at this frequency and time period, this is not a reliable estimate.

In figures 3.44 and3.45, the variation in the mean and percentiles across the frequencies is shown for daytime and nighttime in the August-October period. There is a significant broadening of the tails of the distributions at 6.8 MHz and 9.0 MHz, just above the predicted MUF, during the daytime. At night, the distributions are broad for all frequencies above the MUF. In particular, the 90th and 95th percentiles are

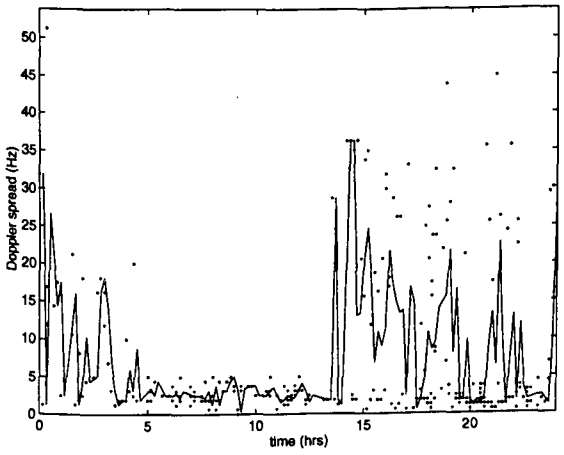


Figure 3.40: Diurnal variation in overall Doppler spread at 11.2 MHz, May 1995

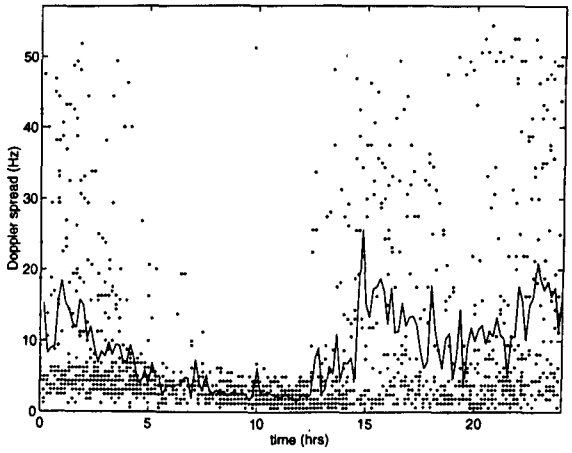


Figure 3.41: Diurnal variation in overall Doppler spread at 11.2 MHz, August-October 1995

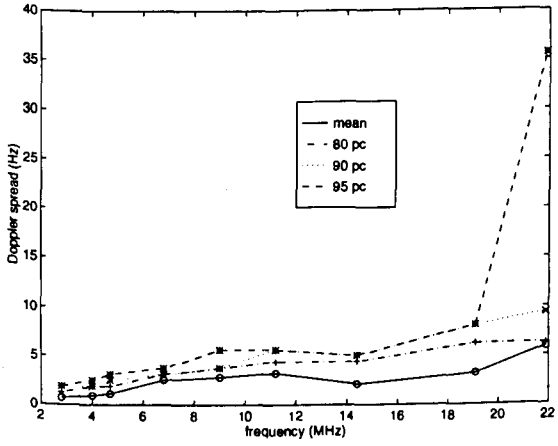


Figure 3.42: Variation in Doppler spread, 08:00 - 14:00 LT, May 1995

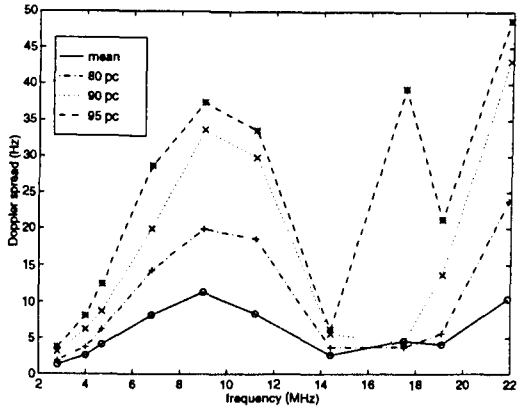


Figure 3.43: Variation in Doppler spread, 20:00 - 02:00 LT, May 1995

close to, or exceed, the reliable limit of the measurement system at and above 11.2 MHz. For clarity, the 90th percentiles of the overall Doppler spread are reproduced in table 3.2.

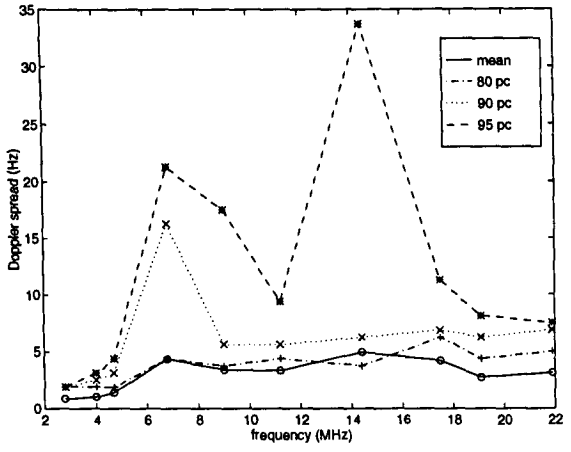


Figure 3.44: Variation in Doppler spread, 08:00 - 14:00 LT, August-October 1995

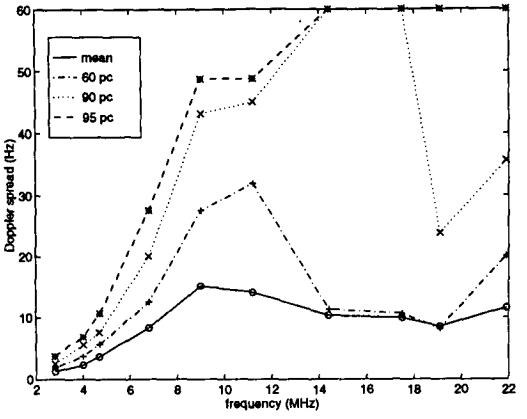


Figure 3.45: Variation in Doppler spread, 20:00 - 02:00 LT, August-October 1995

| frequency (MHz) | May | | August-October | |
|---|---|---|---|---|
| | 08:00-14:00 | 20:00-02:00 | 08:00-14:00 | 20:00-02:00 |
| 2.8 | 1.9 | 3.1 | 1.9 | 2.5 |
| 4.0 | 1.9 | 6.9 | 2.5 | 5.6 |
| 4.7 | 2.5 | 9.4 | 3.1 | 7.5 |
| 6.8 | 3.8 | 18.8 | 17.5 | 18.8 |
| 9.0 | 4.4 | 37.5 | 5.6 | 43.1 |
| 11.2 | 5.0 | 28.1 | 5.6 | 45.0 |
| 14.4 | 5.0 | 6.3 | 33.8 | $> 50$ |
| 17.5 | - | 4.4 | 6.9 | $> 50$ |
| 19.1 | 8.1 | 20.0 | 6.3 | 25.0 |
| 21.9 | 9.4 | 43.1 | 6.9 | 37.5 |

Table 3.2: 90th percentiles of overall Doppler spread

In many cases, the overall Doppler spread is the combination of two or more modes, which often have different measured Doppler characteristics. As it is likely to be the Doppler spread on each individual mode that affects the performance of a data modem, rather than the combination, the Doppler spreads on the strongest and second strongest modes are compared here.

Figures 3.46 and 3.47 show the mean and percentiles of the Doppler spread on the strongest and second strongest modes in the daytime during May. While the plots for the strongest mode closely follow the overall Doppler spread (figure 3.42), as would be expected, the characteristics seen on the second strongest mode are quite different at some frequencies. The mean on the second strongest mode is fairly constant above the

MUF, although the tails of the distribution are particularly broad at 6.8 MHz.

At night during May, figures 3.48 and 3.49, the strongest and second strongest modes have similar Doppler spread distributions across the frequency band, although the mean on the second strongest mode is generally smaller, e.g. 6.8 Hz compared to 9.8 Hz at 9.0 MHz. Note that the dsitributions are not as smooth for the second strongest mode as there are fewer data points.

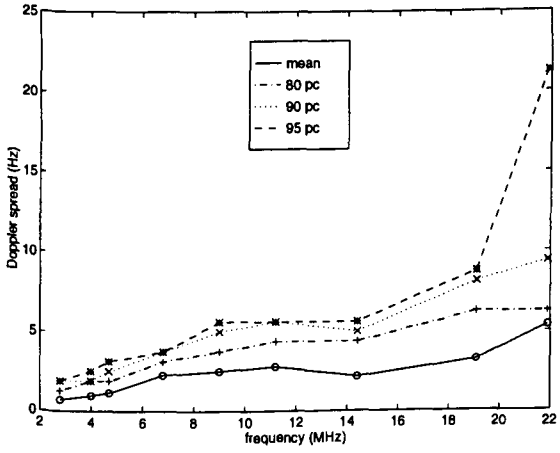


Figure 3.46: Variation in Doppler spread on strongest mode, 08:00-14:00 LT, May 1995

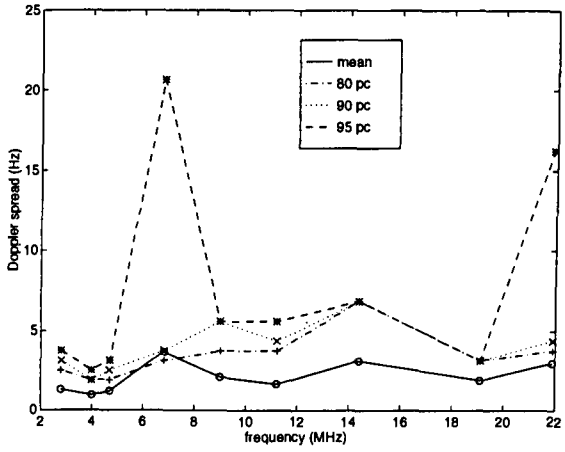


Figure 3.47: Variation in Doppler spread on second strongest mode, 08:00-14:00 LT, May 1995

In the August-October period during the hours of daylight at frequencies below the predicted MUF, the Doppler spread is slightly larger on the second strongest mode. Above the MUF, the reverse is generally true, as seen in figures 3.50 and 3.51. As in May, there is a broadening of the distributions just above the predicted MUF, with the 90th percentile at 14 Hz and 5 Hz on the strongest and second strongest modes, respectively, at 6.8 MHz. Note that for both the strongest and second strongest modes at 14.4 MHz, the 95th percentile is less than 5 Hz. In figure 3.44, it was seen that the 95th percentile of the overall Doppler spread is in excess of 30 Hz. Here is an indication that either there are weaker modes with significant Doppler spread, or that one of the two modes considered has considerable Doppler shift, which is exaggerating the overall Doppler spread.

At night, figures 3.52 and 3.53, the 90th and 95th percentiles are quite removed from the 80th above the MUF, indicating that the distribution has very broad tails. Again, the Doppler spread is larger on the strongest mode with the 90th percentile exceeding the system capabilities for several frequencies above the MUF.

## 3.4 DOPPLER SHIFT

The diurnal variation of the Doppler shift on the strongest and second strongest modes at 4.0 MHz is shown in figures 3.54 and 3.55 for May, and in figures 3.56 and 3.57 for August-October. At both times of year, and on both modes, the variation is more marked during darkness although this is most significant in August-October. There is no tendency for the mean Doppler shift to be either positive or negative in any of these data sets.

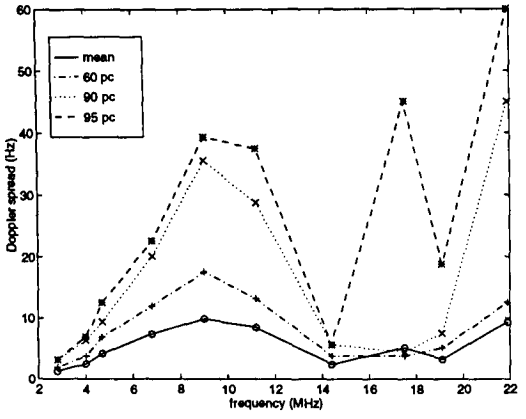


Figure 3.48: Variation in Doppler spread on strongest mode, 20:00-02:00 LT, May 1995

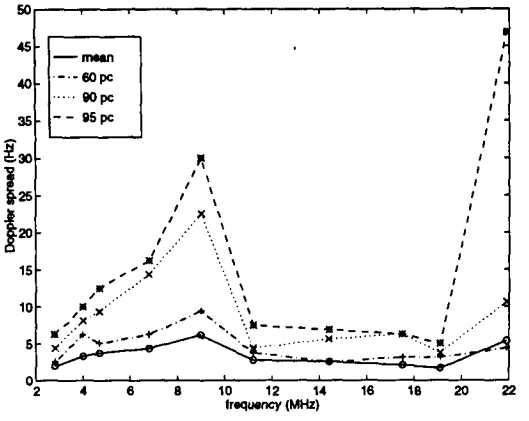


Figure 3.49: Variation in Doppler spread on second strongest mode, 20:00-02:00 LT, May 1995

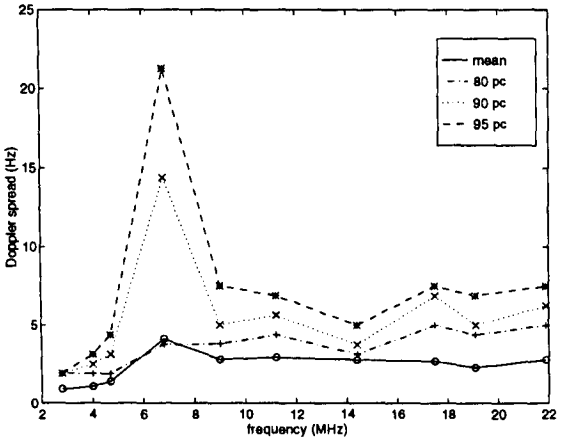


Figure 3.50: Variation in Doppler spread on strongest mode, 08:00-14:00 LT, August-October 1995

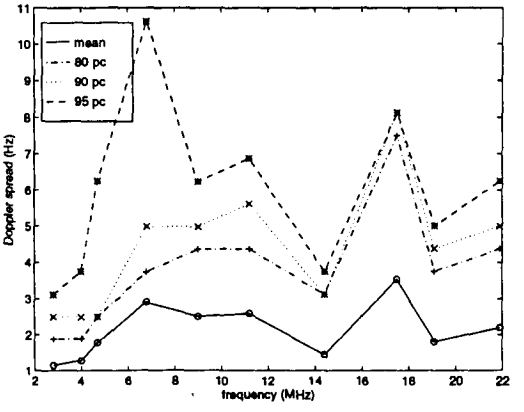


Figure 3.51: Variation in Doppler spread on second strongest mode, 08:00-14:00 LT, August-October 1995

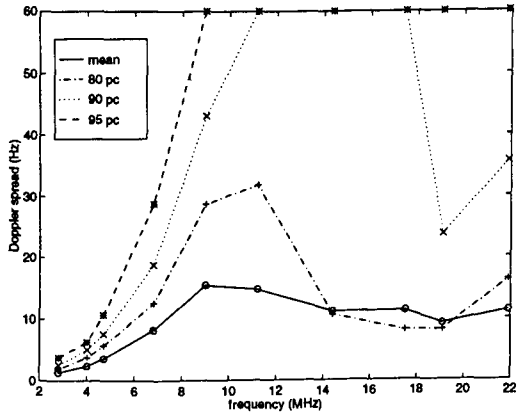


Figure 3.52: Variation in Doppler spread on strongest mode, 20:00-02:00 LT, August-October 1995

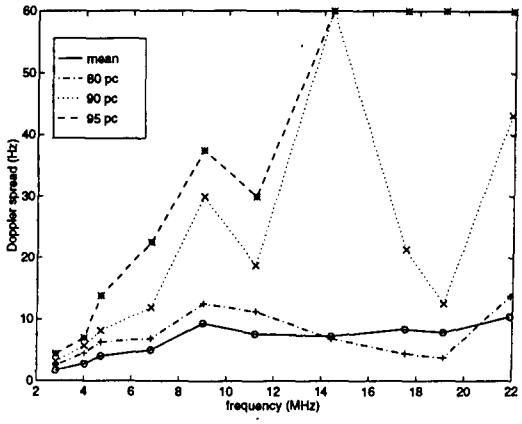


Figure 3.53: Variation in Doppler spread on second strongest mode, 20:00-02:00 LT, August-October 1995

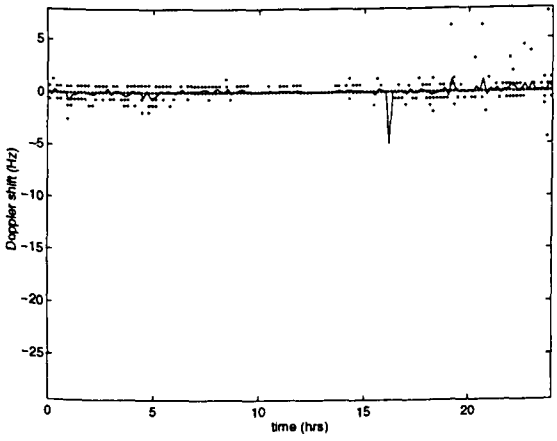


Figure 3.54: Diurnal variation in Doppler shift on the strongest mode at 4.0 MHz, May 1995

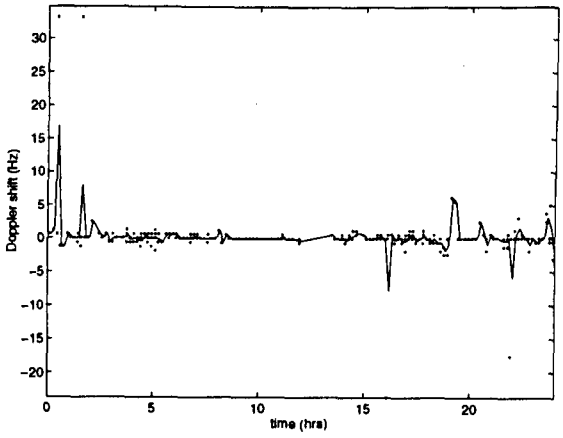


Figure 3.55: Diurnal variation in Doppler shift on the second strongest mode at 4.0 MHz, May 1995

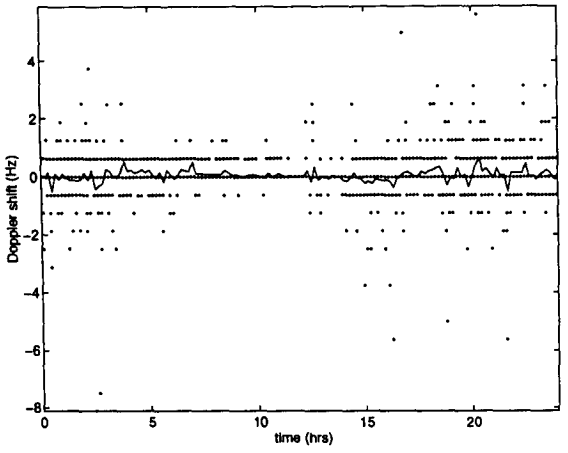


Figure 3.56: Diurnal variation in Doppler shift on the strongest mode at 4.0 MHz, August-October 1995

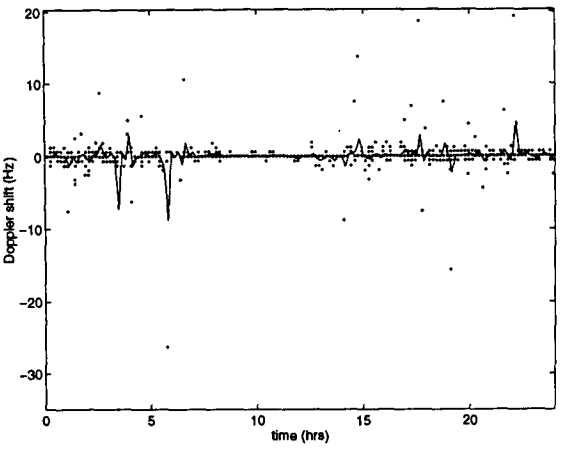


Figure 3.57: Diurnal variation in Doppler shift on the second strongest mode at 4.0 MHz, August-October 1995

Figures 3.58 to 3.61 show the diurnal variation of the Doppler shift on the strongest and second strongest modes at 11.2 MHz for May and August-October. There is considerably more variation seen on this frequency than below the MUF. In particular, there are often large positive Doppler shifts measured on the strongest mode around late afternoon to early evening, at both times of year. There are also some large negative Doppler shifts observed on the same mode during the night in August-October. While this behaviour is mirrored to some extent on the second strongest mode, the mean shows less deviation from 0 Hz overall.

The means and percentiles for the distributions of Doppler shift on the strongest and second strongest modes during daylight hours (08:00 to 14:00 LT) in May are shown in figure 3.62 and 3.63. Figures 3.64 and 3.65 show the corresponding plots for 20:00 - 02:00 LT. On both modes and for both time periods, there is little variation on frequencies below the predicted MUF, i.e. below about 6.0 MHz. Above this frequency, the distributions broaden; this effect is more consistent across the frequencies in the 20:00 to 02:00 period on the strongest mode. Note that the number of data points at night at 17.5 MHz is less than 10, hence the points have been omitted for this frequency. The tails of the distributions tend to be biased towards negative Doppler shifts.

For the August-October period, the means and percentiles are shown in figures 3.66 and 3.67 for daylight hours, and in figures 3.68 and 3.69 for nighttime. As with the May observations, there is least variation seen at the frequencies below the predicted MUF. In addition, the distributions are quite narrow for most frequencies on the second strongest mode during the daytime. At night, there is a tendency again for more negative Doppler shifts. Note that 17.5 MHz again has few data points. Overall, the daytime measurements are similar to those seen during the daytime in May, however the nighttime measurements have more extreme values in August-October.

## 3.5 PARAMETER INTERACTION

In this section, there will be a brief discussion of the interaction of Doppler spread, multipath spread and Doppler shift. As the SNR measurements in the DAMSON system are currently derived from the CW

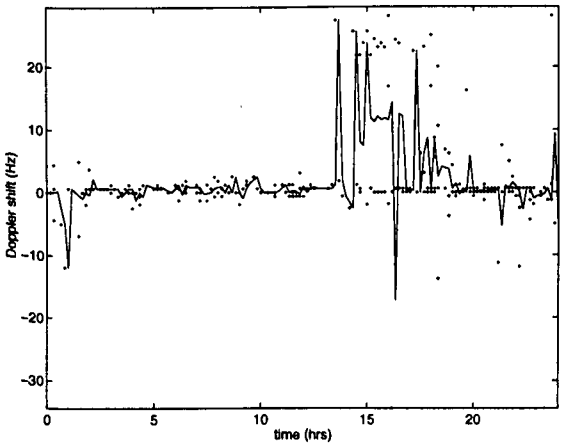


Figure 3.58: Diurnal variation in Doppler shift on the strongest mode at 11.2 MHz, May 1995

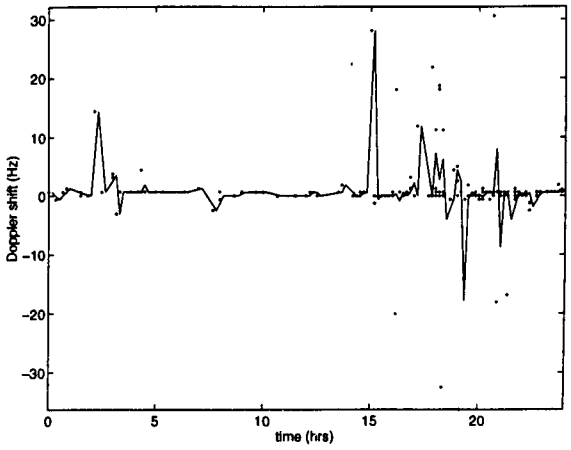


Figure 3.59: Diurnal variation in Doppler shift on the second strongest mode at 11.2 MHz, May 1995

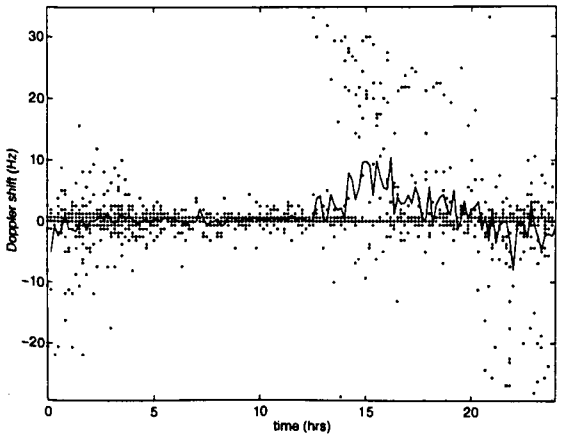


Figure 3.60: Diurnal variation in Doppler shift on the strongest mode at 11.2 MHz, August-October 1995

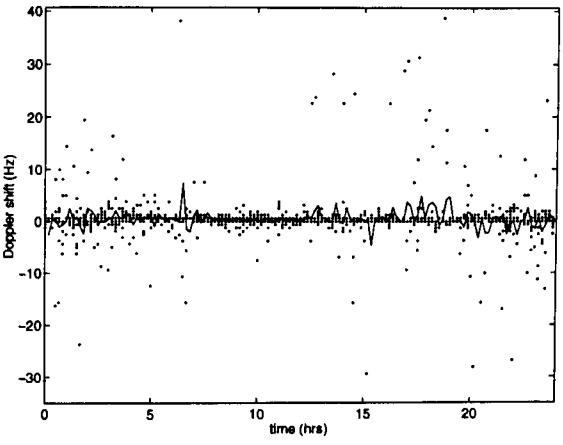


Figure 3.61: Diurnal variation in Doppler shift on the second strongest mode at 11.2 MHz, August-October 1995

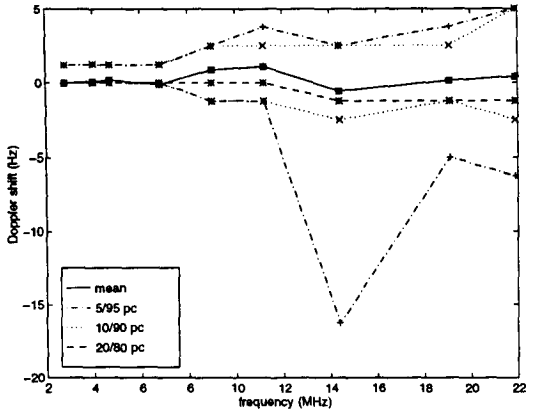


Figure 3.62: Variation in Doppler shift on the strongest mode, 08:00 - 14:00 LT, May 1995

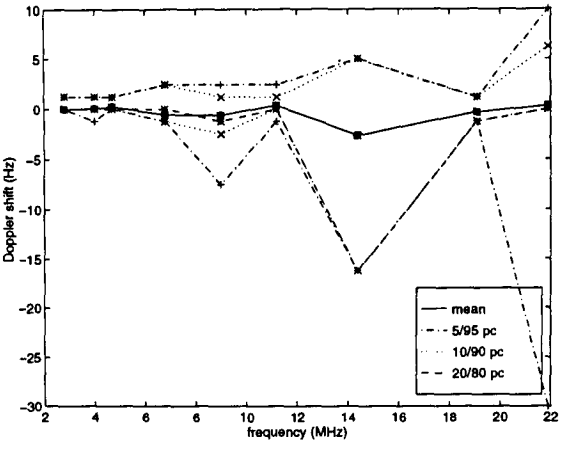


Figure 3.63: Variation in Doppler shift on the second strongest mode, 08:00 - 14:00 LT, May 1995

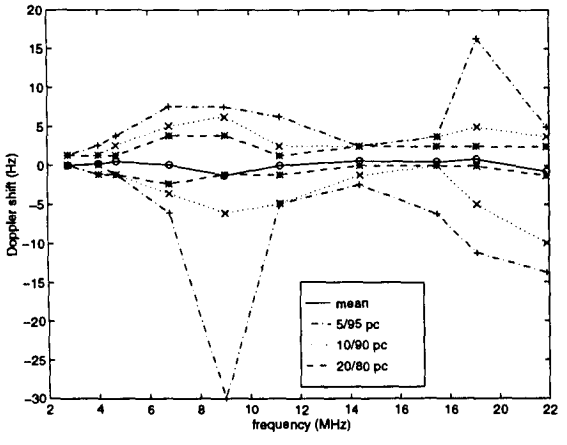


Figure 3.64: Variation in Doppler shift on the strongest mode, 20:00 - 02:00 LT, May 1995

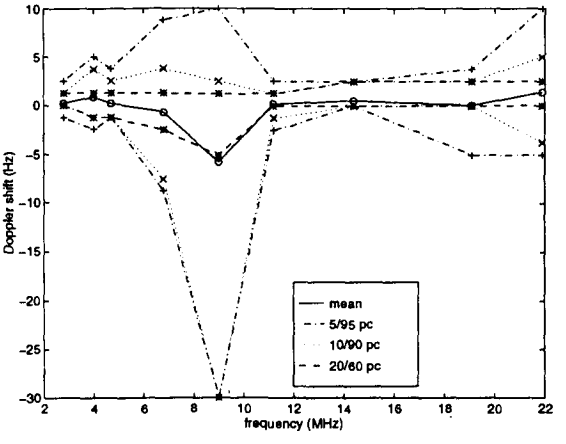


Figure 3.65: Variation in Doppler shift on the second strongest mode, 20:00 - 02:00 LT, May 1995

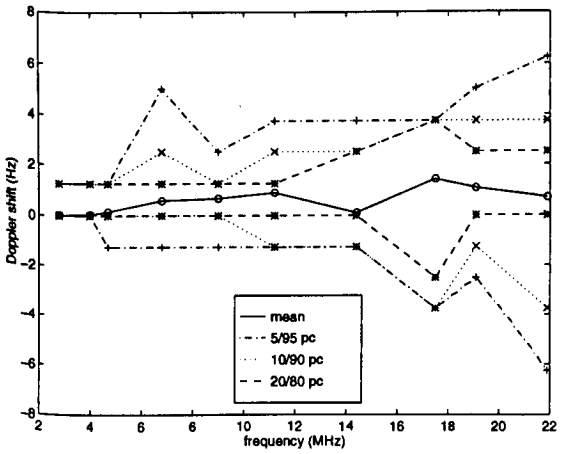


Figure 3.66: Variation in Doppler shift on the strongest mode, 08:00 - 14:00 LT, August-October 1995

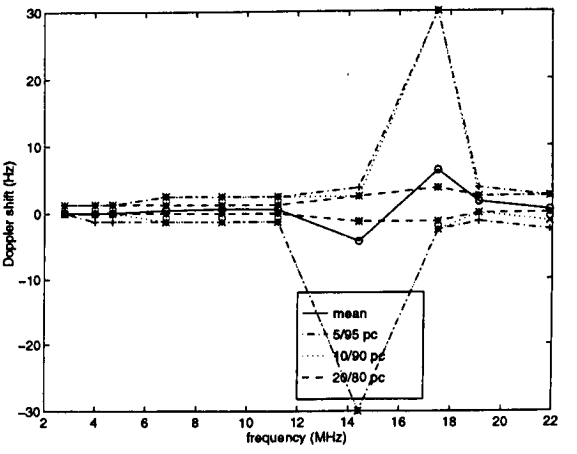


Figure 3.67: Variation in Doppler shift on the second strongest mode, 08:00 - 14:00 LT, August-October 1995

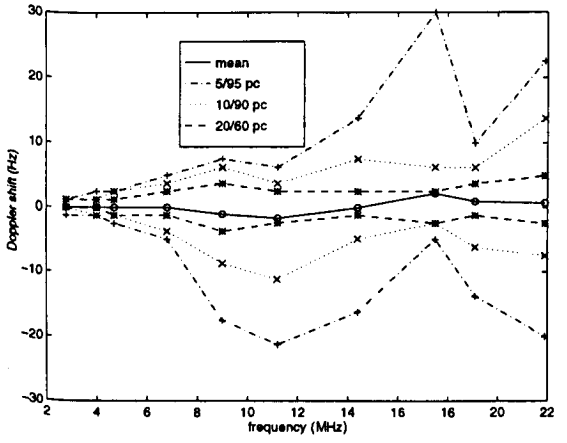


Figure 3.68: Variation in Doppler shift on the strongest mode, 20:00 - 02:00 LT, August-October 1995

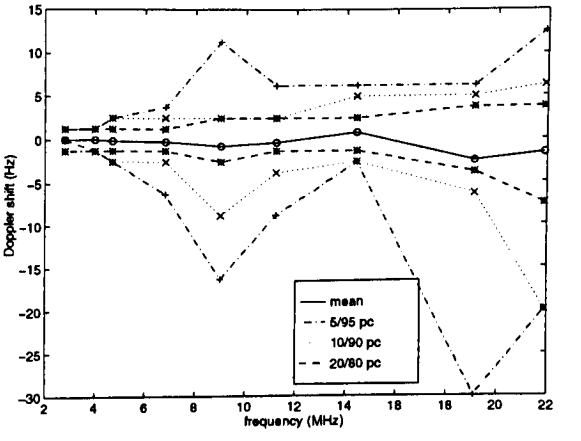


Figure 3.69: Variation in Doppler shift on the second strongest mode, 20:00 - 02:00 LT, August-October 1995

portion of the signal, the values cannot be reliably mapped to the delay-Doppler portion.

### 3.5.1 Doppler spread on two modes

The joint distributions of the Doppler spreads measured on the strongest and second strongest modes at 4.0 MHz are shown in figures 3.70 and 3.71 for daylight and darkness in May, and in figures 3.72 and 3.73 for the same times of day in August-October. All the plots show that there is little difference in the Doppler spreads on the two modes. Even at night during the August-October period, when the Doppler spreads measured are most severe, the distribution is fairly uniform between the two modes.

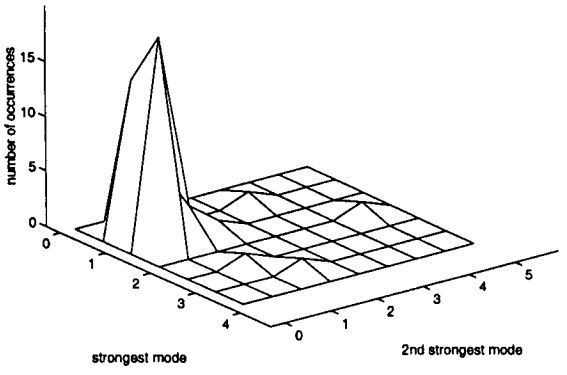


Figure 3.70: Joint distribution of Doppler spread on strongest and second strongest modes, 4.0 MHz, 08:00 - 14:00 May 1995

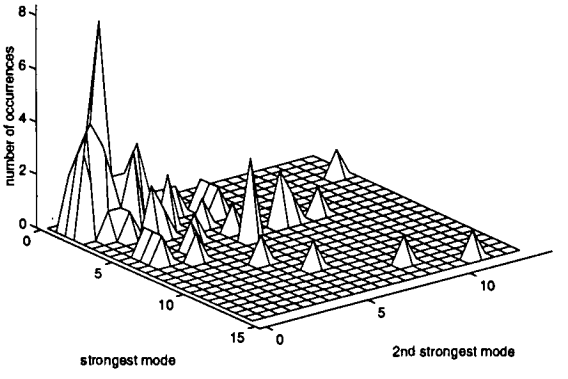


Figure 3.71: Joint distribution of Doppler spread on strongest and second strongest modes, 4.0 MHz, 20:00 - 02:00 May 1995

In figures 3.74 to 3.77, the joint distributions of Doppler spread on the strongest and second strongest modes are shown for daytime and nighttime during May and August-October at 11.2 MHz. During the day in May, there are insufficient data points to draw conclusions, however in August-October, there is elongation along both axes, which indicates that only one of the modes has a large Doppler spread, while the other is quite small. The uniformity along both axes suggests that two propagation modes with very different Doppler spread characteristics are being received with similar powers. In any given measurement, either can be identified as the stronger. This is in line with the finding in section 3.2.1 which showed that the strongest mode tends to have less of the total power than at other times of the day or year. During the night in August-October, there is an elongation along the strongest mode axis. This imbalance indicates that the same propagation mode is being selected as the strongest mode for most of the measurement points in this set. This difference from day to night is supported by the results in section 3.2.1, which showed that at night in August-October, the strongest mode tends to contain a larger proportion of the total received signal power. This suggests one propagation mode is significantly stronger than the others, and clearly this mode has larger Doppler spreads than the other modes. It is possible that this effect is caused by more of the tails of the power spectrum of the strongest mode being above the estimation threshold. However, anecdotal evidence from the tagging process suggests that the power spectrum of one mode is often markedly different from that of another.

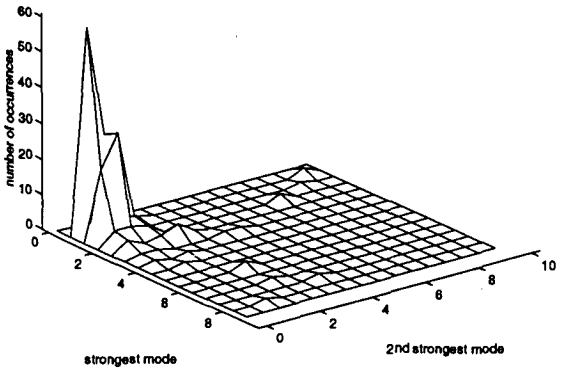


Figure 3.72: Joint distribution of Doppler spread on strongest and second strongest modes, 4.0 MHz, 08:00 - 14:00 August-October 1995

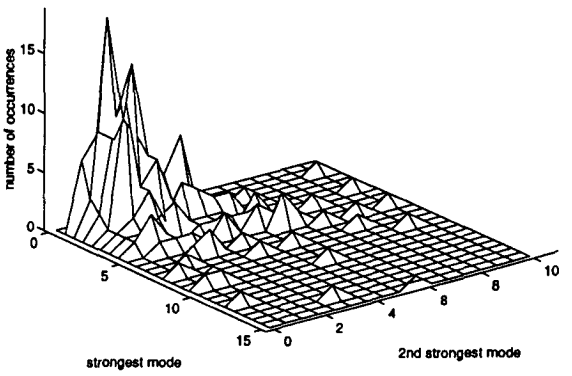


Figure 3.73: Joint distribution of Doppler spread on strongest and second strongest modes, 4.0 MHz, 20:00 - 02:00 August-October 1995

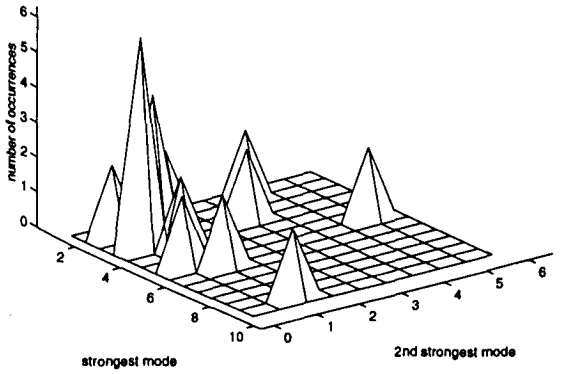


Figure 3.74: Joint distribution of Doppler spread on strongest and second strongest modes, 11.2 MHz, 08:00 - 14:00 May 1995

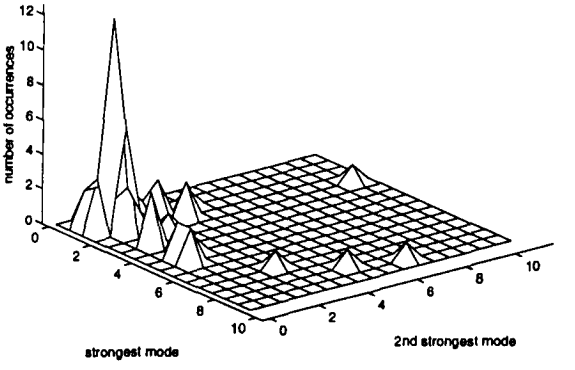


Figure 3.75: Joint distribution of Doppler spread on strongest and second strongest modes, 11.2 MHz, 20:00 - 02:00 May 1995

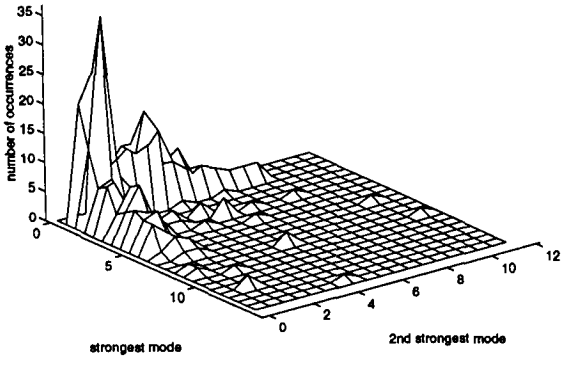


Figure 3.76: Joint distribution of Doppler spread on strongest and second strongest modes, 11.2 MHz, 08:00 - 14:00 August-October 1995

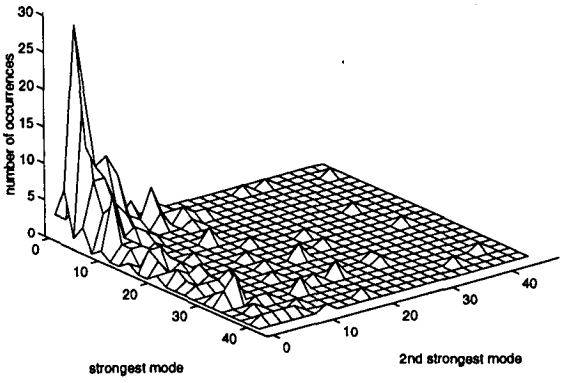


Figure 3.77: Joint distribution of Doppler spread on strongest and second strongest modes, 11.2 MHz, 20:00 - 02:00 August-October 1995

### 3.5.2 Doppler spread and multipath spread interaction

In this section, the joint distribution of the overall Doppler spread and the multipath spread is considered. Figure 3.78 shows the distribution for 08:00 to 14:00 in May, at 4.0 MHz. There are a few points with multipath spreads at the limit of the DAMSON measurement system, but the majority are concentrated with fairly small multipath spread (2-3 ms) over a range of Doppler spreads up to 4 Hz. At night, the distribution shows more points with larger Doppler spreads and multipath spreads, figure 3.79, but there is no clear pattern indicating a specific relationship.

In the August-October period, larger multipath spreads and Doppler spreads were recorded (sections 3.1 and 3.3). Figures 3.80 and 3.81 show the joint distributions during daylight and darkness, respectively. While the distribution is dominated by points with relatively small Doppler spread and multipath spread, there is an elongation along both axes, although this is more marked at night. This indicates that, where the Doppler spread is large, the multipath spread is likely to be small, and vice versa.

This effect is much more evident at frequencies above the MUF in both May and August-October, for example at 11.2 MHz as shown in figures 3.82 to 3.85. In the daytime in May, figure 3.82, the multipath tends to be small, up to 4 ms, while the Doppler spread ranges fairly uniformly up to 6 Hz. At night during the same period, figure 3.83, multipath spreads are recorded up to 8.5 ms, with some at the limits of the DAMSON system, while only a few Doppler measurements exceed 6 Hz. Note that the small number of data points precludes firm conclusions from being drawn.

In figure 3.84, it is seen that a large proportion of multipath spread measurements approach and exceed the system capabilities as shown in section 3.1. The Doppler spreads measured at these times ranges up to about 7 Hz. With the small number of points with smaller multipath spreads, up to 6 ms, it appears that there may be a tendency again to see either larger multipath spreads or Doppler spreads. At night, figure 3.85, a peak in the distribution occurs for Doppler spreads of less than 10 Hz and multipath spreads less than 3 ms. However, there is evidence of elongation along the multipath axis. In addition, a great deal of "noise" indicates a significant proportion of data points with no specific relationship between Doppler

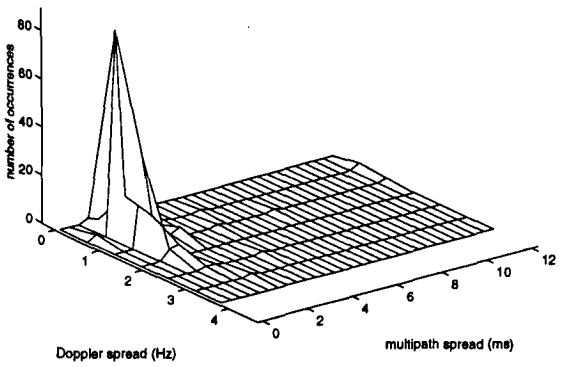


Figure 3.78: Joint distribution of overall Doppler spread and multipath spread, 4.0 MHz, 08:00 - 14:00 May 1995

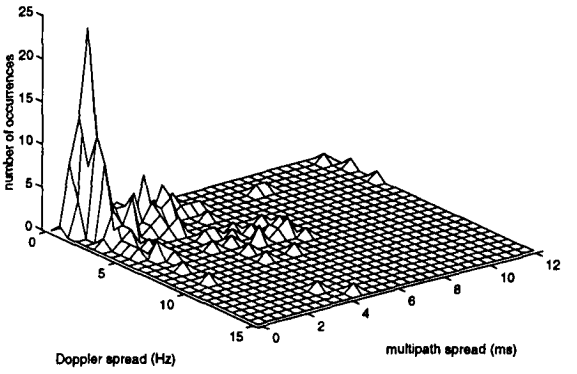


Figure 3.79: Joint distribution of overall Doppler spread and multipath spread, 4.0 MHz, 20:00 - 02:00 May 1995

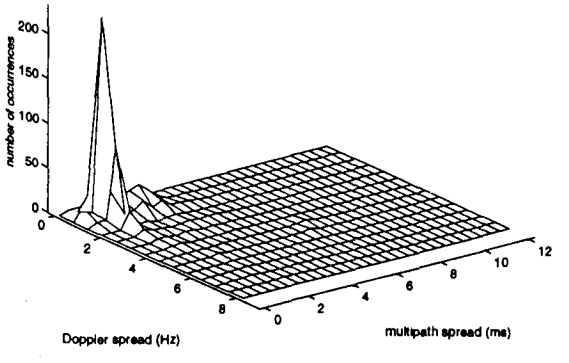


Figure 3.80: Joint distribution of overall Doppler spread and multipath spread, 4.0 MHz, 08:00 - 14:00 August-October 1995

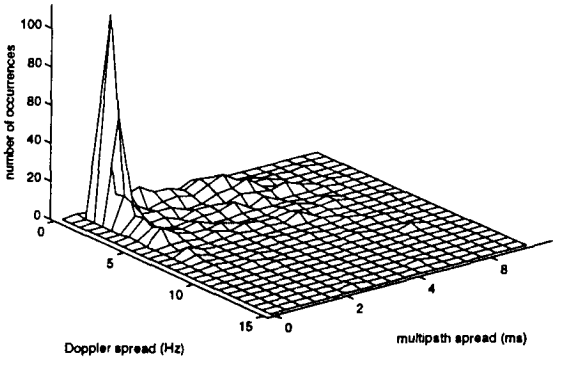


Figure 3.81: Joint distribution of overall Doppler spread and multipath spread, 4.0 MHz, 20:00 - 02:00 August-October 1995

spread and multipath spread.

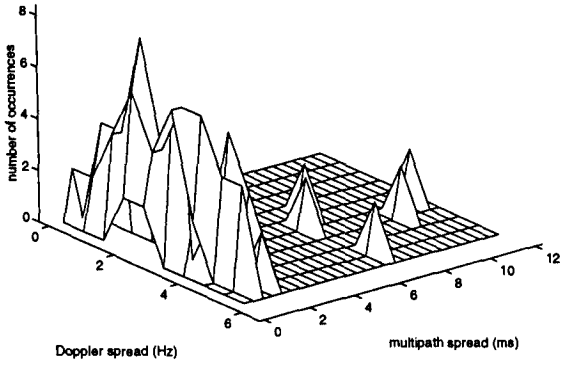


Figure 3.82: Joint distribution of overall Doppler spread and multipath spread, 11.2 MHz, 08:00 - 14:00 May 1995

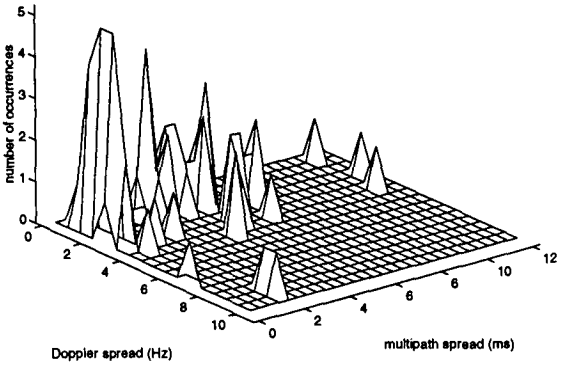


Figure 3.83: Joint distribution of overall Doppler spread and multipath spread, 11.2 MHz, 20:00 - 02:00 May 1995

### 3.5.3 Doppler shift and multipath spread interaction

The interaction of Doppler shift (taken as the absolute difference between the strongest and second strongest modes) and multipath spread has also been examined for frequencies above and below the predicted MUF. There was no evidence of a relationship between the two; on average the Doppler shift is quite small, as seen in section 3.4, and does not vary with multipath spread.

## 3.6 SUMMARY

The Harstad-Kiruna link is short, and approximately parallel to the edge of the auroral zone. At some times, the great-circle path has a reflection point inside the auroral zone, at others it is slightly further south. This geography causes some very interesting propagation characteristics which pose severe problems for the modem designer. The model is not well-predicted by standard programs such as ICEPAC which consider only great-circle propagation. Significant propagation is seen above the predicted MUF. The multipath spread is typically quite large, particularly in the 6 MHz above the predicted MUF, where it is often extreme. Multipath spreads in this frequency range show a tendency to fall into bands of 6 ms to the 12 ms limit of the measurement system. The number of modes detected does not increase significantly, and the main cause of the large multipath spread is that the modes can be very elongated. In May, the largest multipath spreads are seen at night, whereas in the August-October period, they occur during the daytime, in the 6 MHz range above the predicted MUF.

The SNR decreases with frequency above the predicted MUF, and the power tends to be more uniformly distributed among the modes above the MUF, particularly in the August-October period. Above the MUF, the nighttime SNRs are greater than the daytime values, but stronger signals are seen below the MUF in the daytime.

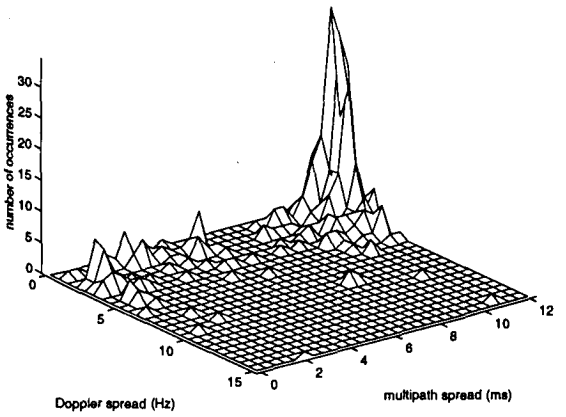


Figure 3.84: Joint distribution of overall Doppler spread and multipath spread, 11.2 MHz, 08:00 - 14:00 August-October 1995

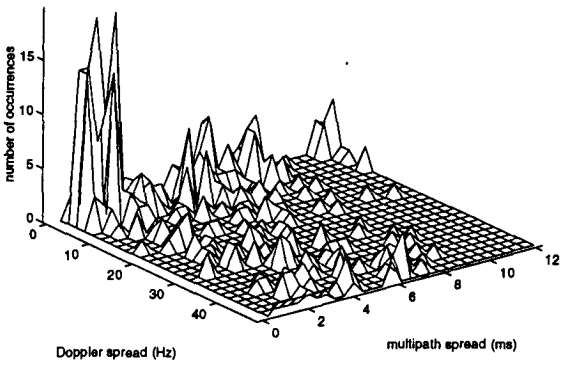


Figure 3.85: Joint distribution of overall Doppler spread and multipath spread, 11.2 MHz, 20:00 - 02:00 August-October 1995

The Doppler spread tends to be more severe at night, particularly above the predicted MUF. In May, the largest nighttime Doppler spreads are seen in the 6 MHz above the predicted MUF, where the 90th percentile exceeds 30 Hz. In the August-October period, the Doppler spreads at night are severe on all frequencies above the MUF, with 90th percentiles exceeding 40 Hz. The strongest propagation mode tends to exhibit the worst characteristics, although it is not clear if this is an artifact introduced by the measurement system. Doppler shifts up to $\pm 5$ Hz are also detected, again particularly above the predicted MUF. There is a tendency for the Doppler shifts to be negative at night.

The observations on this link indicate that the ICEPAC predictions for the MUF are quite good. The measurements of multipath spread and number of modes detected support the predictions of propagation modes, to the extent that it is possible with the limited information. The ICEPAC program relies only on a great-circle model, and cannot predict the behaviour above the MUF. The observations at frequencies above 6 MHz are strongly indicative of off-great-circle propagation, with scatter off the edge of the auroral zone.

# 4.0 ISFJORD-TUENTANGEN

The path from Isfjord to Tuentangen is 2016 km long, at an azimuth of 184°. There are 30 days of measurements in 1995, seven from April, five in May, seven in July, five August and six in September. The data sets will be divided into the April-May period and the July-September period. The number of data points at each frequency during each of these periods is shown in table 4.1.

| frequency | SNR | | Doppler & multipath | |
|---|---|---|---|---|
| (MHz) | Apr-May | Jul-Sep | Apr-May | Jul-Sep |
| 2.8 | 0 | 16 | 0 | 9 |
| 4.0 | 246 | 436 | 232 | 393 |
| 4.7 | 592 | 1194 | 549 | 1152 |
| 6.8 | 944 | 1396 | 929 | 1369 |
| 9.0 | 986 | 1396 | 991 | 1390 |
| 11.2 | 992 | 1443 | 998 | 1448 |
| 14.4 | 943 | 1337 | 947 | 1344 |
| 17.5 | 738 | 1039 | 748 | 1047 |
| 19.1 | 485 | 777 | 495 | 797 |
| 21.9 | 393 | 636 | 398 | 649 |
| total | 6319 | 9670 | 6287 | 9598 |

Table 4.1: Number of data points on Isfjord-Tuentangen link for SNR and Doppler/multipath analysis

The predicted LUFs and MUFs for this path, generated using ICEPAC for May and August 1995, using smoothed sunspot numbers of 19 and 16, respectively, are shown in figure 4.1.

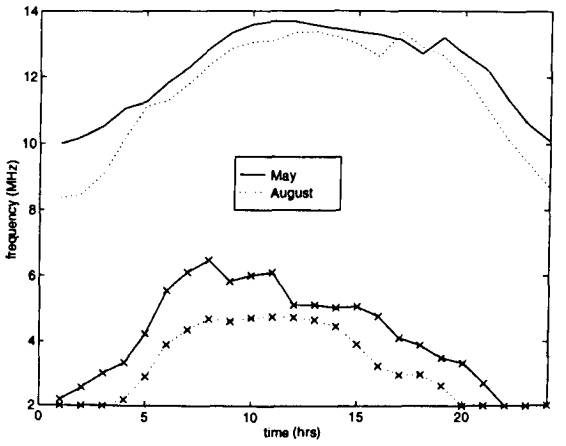


Figure 4.1: Predicted LUFs/MUFs for May and August 1995

## 4.1 MULTIPATH SPREAD

The prediction program ICEPAC has been used to determine the expected propagation modes thoughout the day on each frequency. Figures 4.2 and 4.3 show the predicted modes at 4.0 MHz in May and August, respectively. Note that both these plots omit the single and two-hop sporadic-E modes that are predicted to be possible at all times of day, at 6.8 ms and 6.9 ms delay. This frequency is below the predicted LUF in both months during daylight hours. This is reflected by the low-reliability multihop E-modes which are predicted, while no F-layer propagation is supported. At night, when the LUF is below 4.0 MHz, multihop F2-layer propagation is predicted.

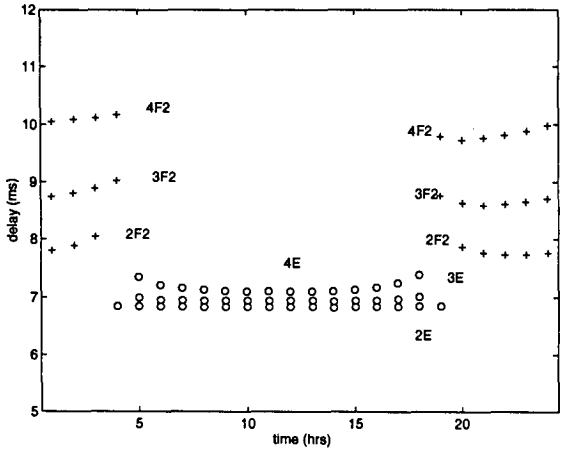


Figure 4.2: Predicted propagating modes at 4.0 MHz for May, 1995

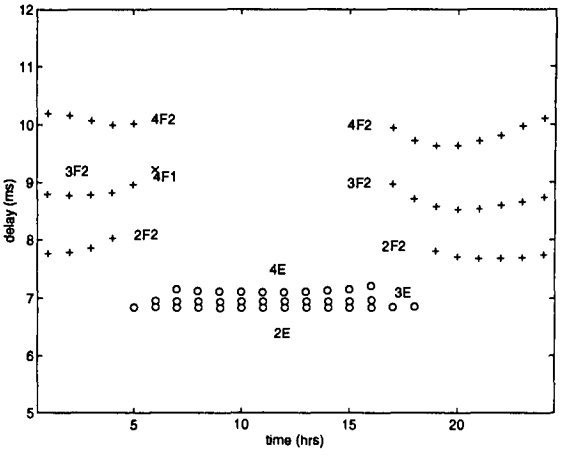


Figure 4.3: Predicted propagating modes at 4.0 MHz for August, 1995

The diurnal variations in multipath spread at 4.0 MHz observed in the April-May and July-September periods are shown in figures 4.4 and 4.5, respectively. Note that no propagation is seen during the periods 05:00-15:30 in April-May, and 10:00-14:30 in July-September, which correspond to the peak daylight hours, and to the period when this frequency is below the predicted LUF. During the hours when propagation is supported at this frequency, the measured multipath spread varies greatly, from under 1 ms to 6 ms. Only about 15 % of measurements detected three or more modes during both times of year, as shown in figure 4.6, which indicates that the delay spread on each mode is quite large. This is most likely due to multiple hops, which were predicted.

At 6.8 MHz, the predicted propagation is very different to that at 4.0 MHz. This frequency is between the LUF and MUF, as predicted by ICEPAC, for all times of day at both times of year considered here. In both May and August, some 3F2 propagation is expected for a few hours around the local geomagnetic 13:00, as shown in figures 4.7 and 4.8 where the 1Es and 2Es predictions have again been omitted for clarity. 1E and 2E propagation is expected during the day in May, but in August the main daytime support is obtained from the F1 layer. At night during both times of year, propagation via the F2 layer is expected.

The observed diurnal variation in multipath spread at 6.8 MHz is shown in figures 4.9 and 4.10 for April-May and July-September, respectively. During both times of year, the observed multipath spread is greater during daylight than darkness, and the variation in measurements is quite large. At night, between 75 %

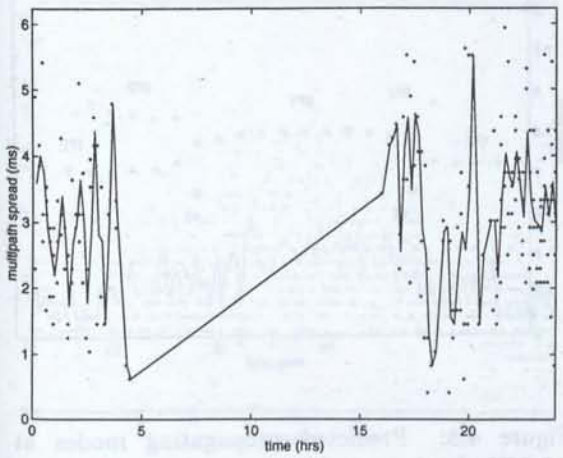


Figure 4.4: Diurnal variation in multipath spread at 4.0 MHz for April-May, 1995

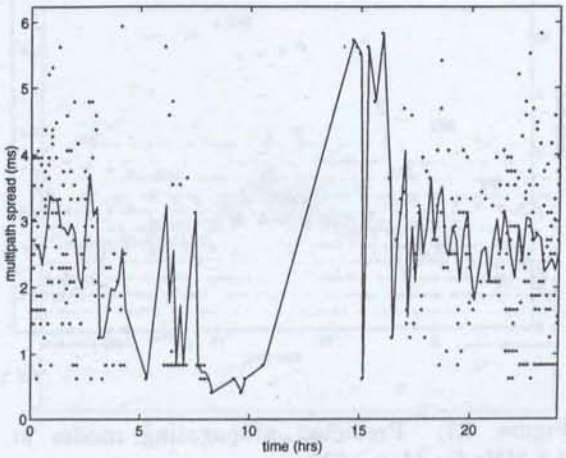


Figure 4.5: Diurnal variation in multipath spread at 4.0 MHz for July-September, 1995

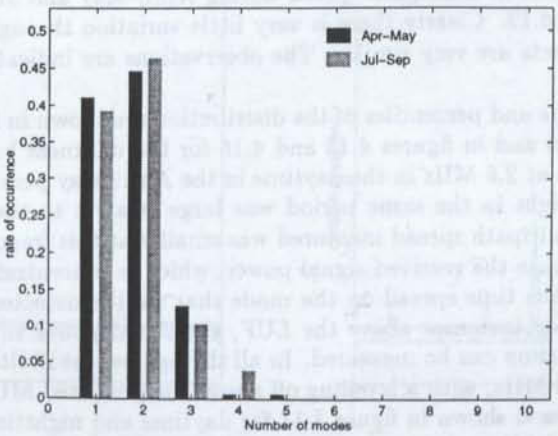


Figure 4.6: Distribution of the number of propagating modes detected 20:00 to 02:00 at 4.0 MHz, 1995

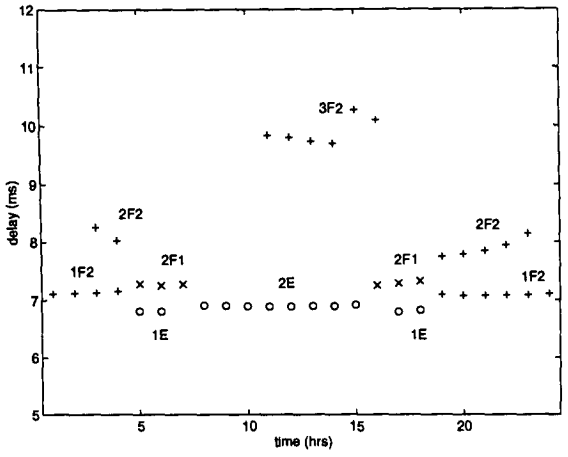


Figure 4.7: Predicted propagating modes at 6.8 MHz for May, 1995

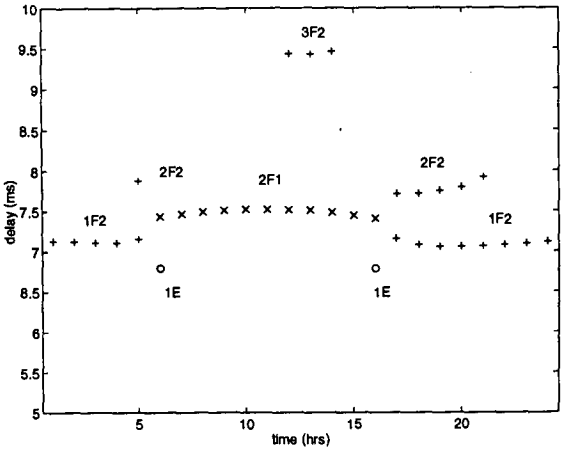


Figure 4.8: Predicted propagating modes at 6.8 MHz for August, 1995

and 80 % of the observations recorded only a single propagation mode, at both times of year, compared to 50 % during April-May and 20 % during July-September in daylight hours. Daytime multipath spreads of 3-4 ms support the prediction of 2E/2F1 and 3F2 propagation during this time. The nighttime propagation is most likely via the F2 layer, though it is not possible to determine whether it is one or two hops without angle of arrival information.

The frequency 17.5 MHz is above the predicted MUF, but was seen to be quite reliable, as shown in table 4.1. The diurnal variations in multipath spread during April-May and July-September at 17.5 MHz are shown in figures 4.11 and 4.12. Clearly there is very little variation throughout the 24 hours, and the spring and late summer data sets are very similar. The observations are indicative of predominantly single mode propagation.

The mean multipath spreads and percentiles of the distribution are shown in figures 4.13 and 4.14 for the daylight hours (08:00 to 14:00) and in figures 4.15 and 4.16 for the darkness hours (20:00 to 02:00). Note that there were no data points at 2.8 MHz in the daytime in the April-May period. The observed multipath spread at this frequency at night in the same period was large relative to the other frequencies. In the July-September period, the multipath spread measured was smaller at this frequency, 2.8 MHz, than at the other frequencies. This is because the received signal power, which is concentrated in a single mode at this frequency, is quite low hence the time spread on the mode that can be detected by the DAMSON system is very small. As the frequency increases above the LUF, the signal power in the mode increases, hence more of the tails of the distribution can be measured. In all the figures, the multipath spread decreases with increasing frequency above 6.8 MHz, with a levelling off above the predicted MUF.

The mean number of modes is shown in figure 4.17 for daytime and nighttime at the two times of year under consideration. Above 10 MHz, the average is very close to one, from peaks of less than two in the frequency range 4.7 MHz to 6.8 MHz.

The distributions of multipath spread and the number of modes are shown in figures 4.18 and 4.19 for all times of day in April-May. The plots are very similar to those generated for the July-September period which are not shown. Clearly the multipath spread and number of modes are very closely related, which

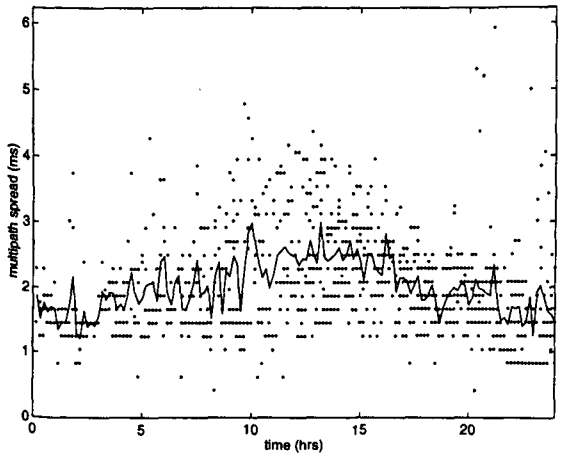


Figure 4.9: Diurnal variation in multipath spread at 6.8 MHz for May, 1995

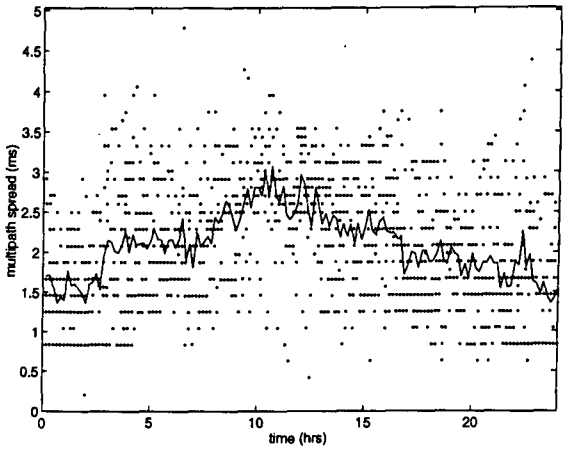


Figure 4.10: Diurnal variation in multipath spread at 6.8 MHz for August, 1995

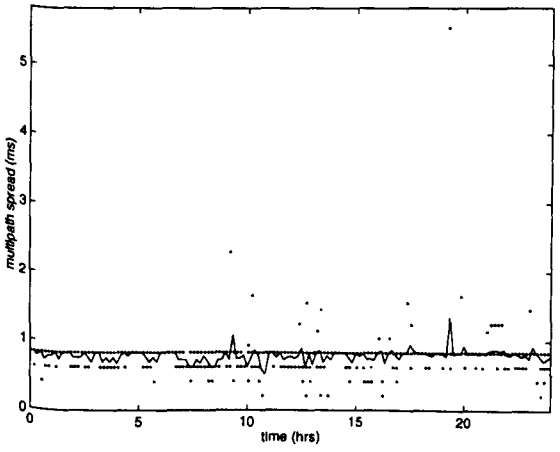


Figure 4.11: Diurnal variation in multipath spread at 17.5 MHz for May, 1995

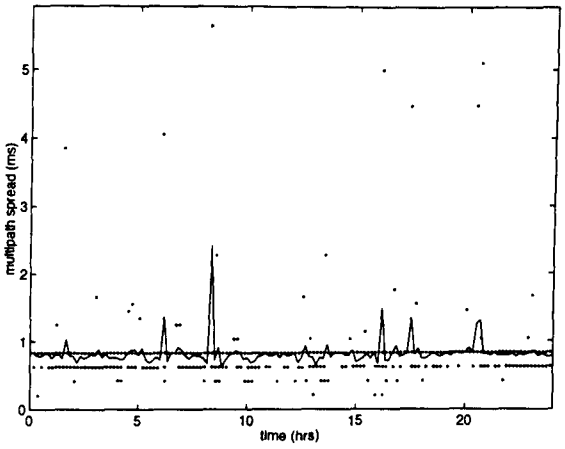


Figure 4.12: Diurnal variation in multipath spread at 17.5 MHz for August, 1995

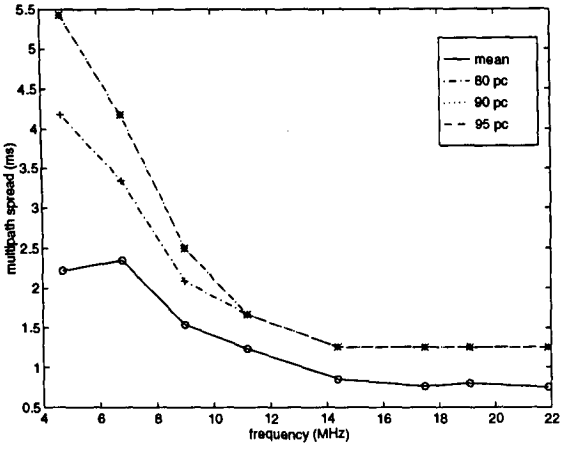


Figure 4.13: Percentiles of the multipath spread distribution for 08:00 to 14:00, April-May, 1995

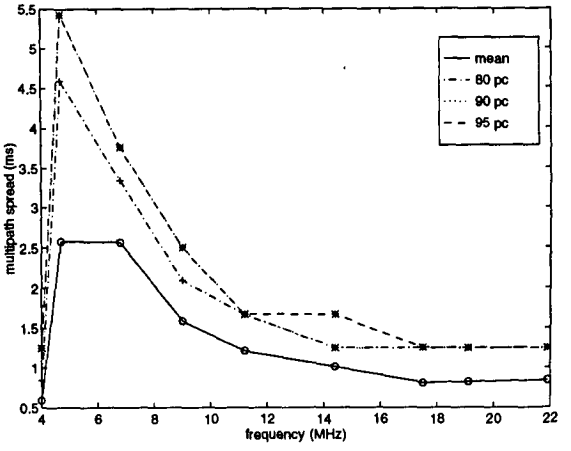


Figure 4.14: Percentiles of the multipath spread distribution for 08:00 to 14:00, July-September, 1995

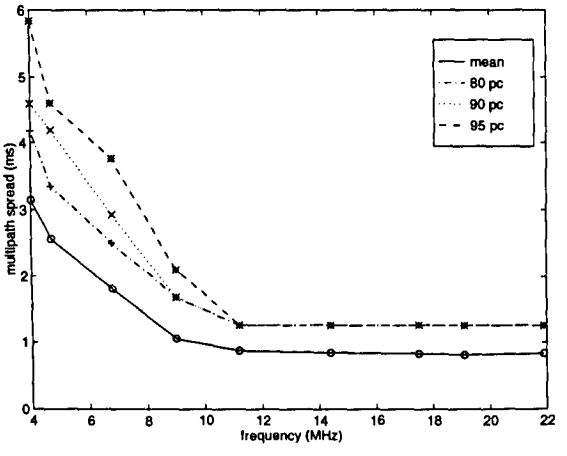


Figure 4.15: Percentiles of the multipath spread distribution for 20:00 to 02:00, April-May, 1995

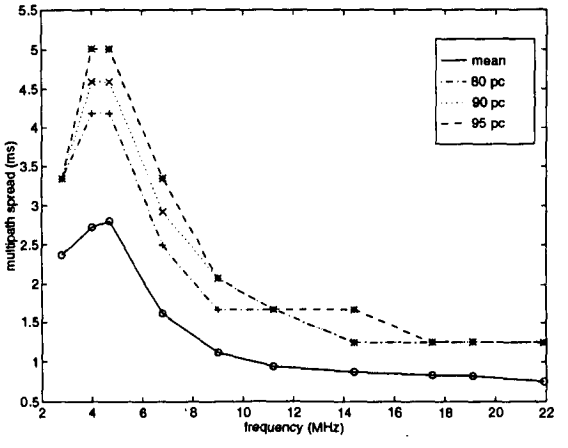


Figure 4.16: Percentiles of the multipath spread distribution for 20:00 to 02:00, July-September, 1995

is to be expected as elongated modes such as those seen on the Harstad-Kiruna link (section 3.1) are not common on the Isfjord-Tuentangen link.

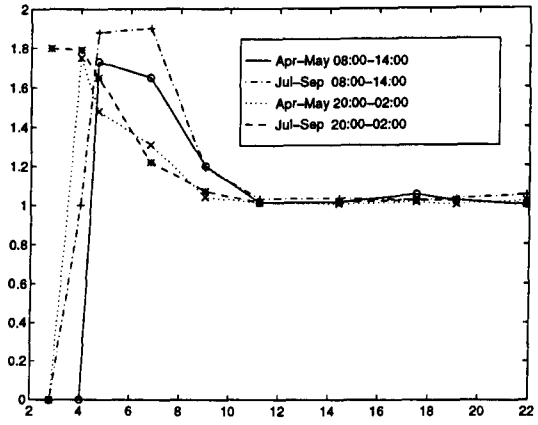


Figure 4.17: Mean number of modes detected

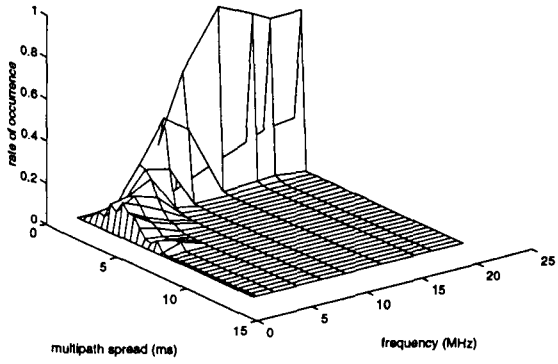


Figure 4.18: Distribution of multipath spreads for April-May, 1995

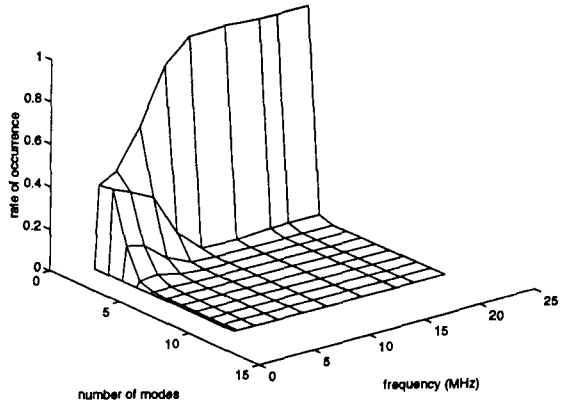


Figure 4.19: Distribution of number of modes for April-May, 1995

## 4.2 SNR

The diurnal variation in the measured SNR at 6.8 MHz is shown in figure 4.20 for April-May and in figure 4.21 for July-September. There is considerable variation in the measurements at all times of the day, but the overall mean remains fairly constant throughout the 24 hours.

Above the predicted MUF, there is considerably more variation in SNR throughout the day, as seen in figures 4.22 and 4.23. In April-May, the SNR is significantly greater from late-afternoon to midnight, local

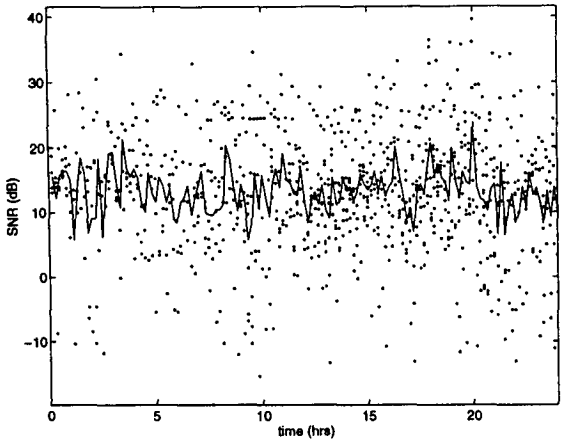


Figure 4.20: Diurnal variation in SNR at 6.8 MHz, April-May, 1995

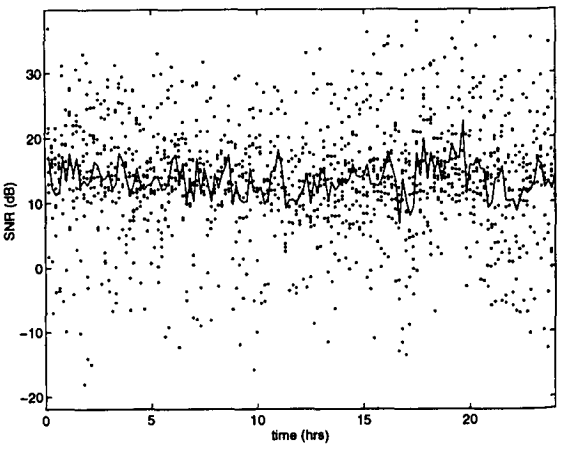


Figure 4.21: Diurnal variation in SNR at 6.8 MHz, July-September, 1995

time. For six hours around the local geomagnetic noon, the mean SNR is very low, about 25 dB lower than the mean pre-midnight values. In the July-September period, there is less variation than in April-May, however there is still a tendency to measure lower SNRs during the daytime.

The mean and percentiles of the SNR are shown in figures 4.24 and 4.25 for the daylight period in April-May and July-September, respectively. There is a peak in the distributions corresponding quite closely to the frequencies between the predicted LUF and MUF. The means in this region are between 10 and 20 dB. The distributions are broader at the highest frequencies, and the means are seen to increase with frequency, but there are insufficient frequencies available in this range to determine if this is a real effect or is caused by a shortage of measurement data.

Figures 4.26 and 4.27 show the mean and percentiles for the nighttime at the same times of year. The means are higher in the April-May period above the MUF and below the predicted LUF, between 5 and 15 dB. This is also true for frequencies below the LUF in July-September. Overall, the distributions are broader at night than during the day.

### 4.2.1 Distribution of signal power

As was seen in section 4.1, the only frequencies on which more than one mode was detected are between the predicted LUF and MUF. The distribution of the percentage of total signal power which was received in the strongest mode is shown in figure 4.28 for April-May and July-September in the time period 08:00 to 14:00 LT. Figure 4.29 shows the corresponding distribution for 20:00 to 02:00 LT. There is little difference in the two distributions which show that, on average, 75-80 % of the total signal power is received in the strongest mode.

## 4.3 DOPPLER SPREAD

As was seen in section 4.1, a large proportion of the observations indicated only one propagating mode, hence there are insufficient data points with a second mode to make reliable statistical conclusions. Thus,

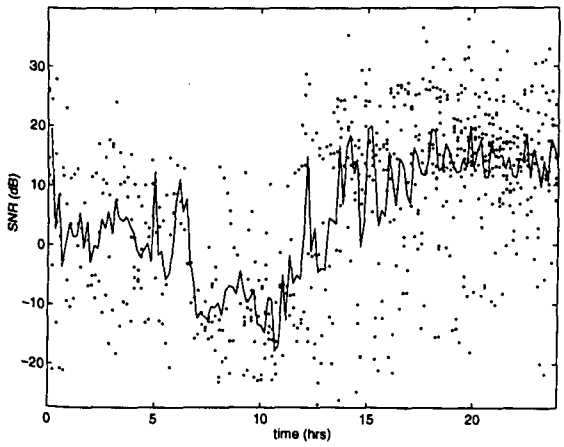


Figure 4.22: Diurnal variation in SNR at 17.5 MHz, April-May, 1995

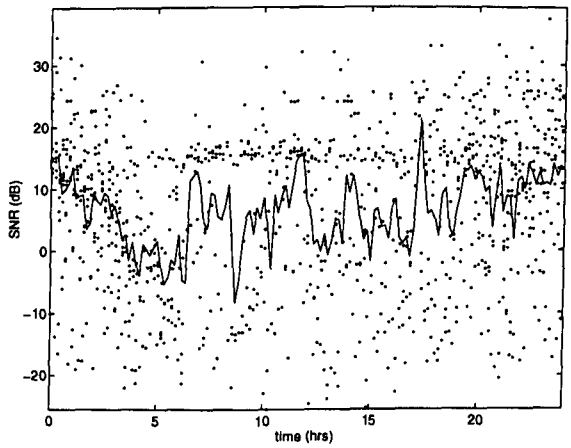


Figure 4.23: Diurnal variation in SNR at 17.5 MHz, July-September, 1995

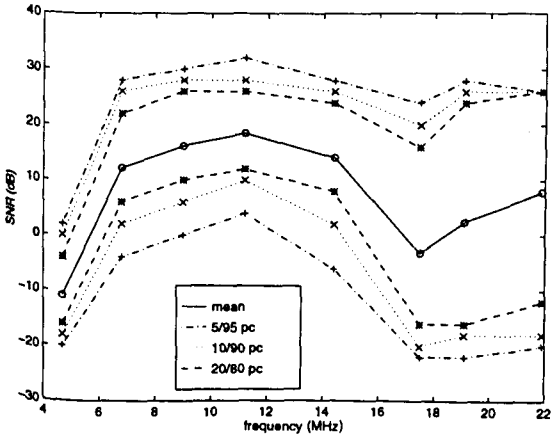


Figure 4.24: Percentiles of SNR for 08:00 - 14:00, April-May, 1995

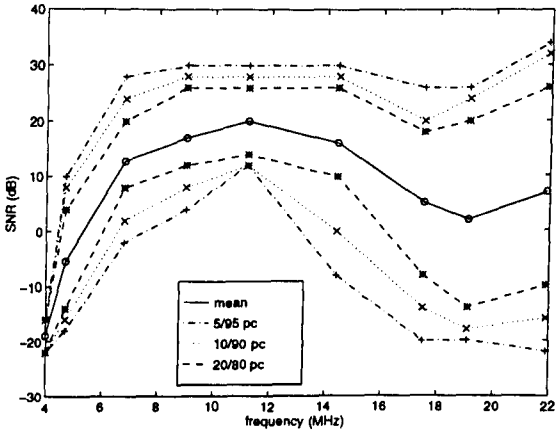


Figure 4.25: Percentiles of SNR for 08:00 - 14:00, July-September, 1995

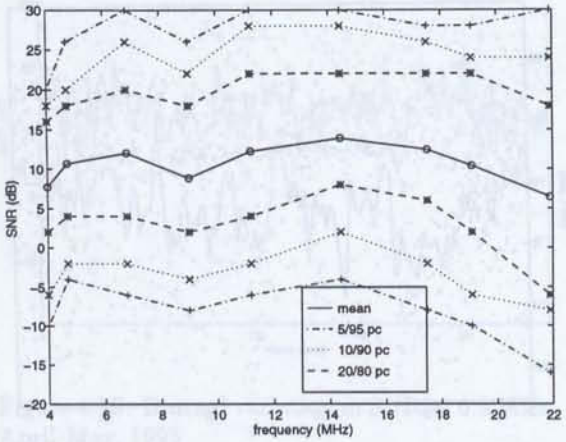


Figure 4.26: Percentiles of SNR for 20:00 - 02:00, April-May, 1995

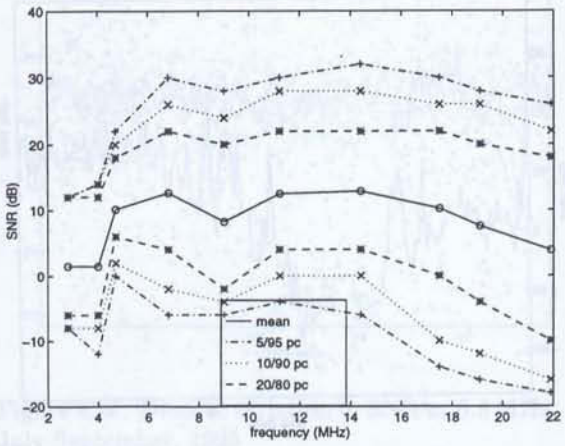


Figure 4.27: Percentiles of SNR for 20:00 - 02:00, July-September, 1995

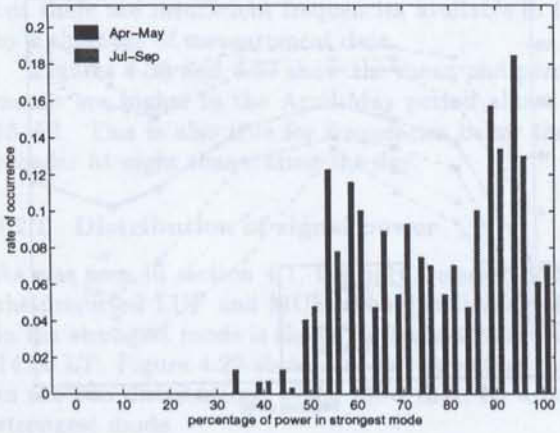


Figure 4.28: Distribution of percentage of power in strongest mode at 6.8 MHz, 08:00 - 14:00, 1995

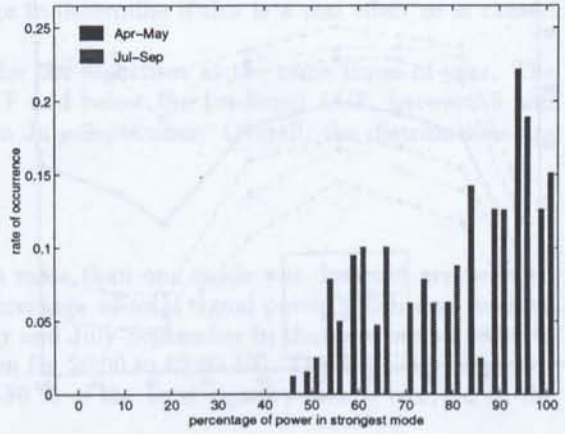


Figure 4.29: Distribution of percentage of power in strongest mode at 6.8 MHz, 20:00 - 02:00, 1995

in this section, only the overall Doppler spread will be considered.

The diurnal variation in Doppler spread at 6.8 MHz is shown in figure 4.30 for the April-May period, and in figure 4.31 for July-September. There is a slight increase in the mean Doppler spread observed during the night in the April-May period, but this tendency is more marked during July-September, when the daytime mean is 1-3 Hz and the nighttime mean is close to 5 Hz. In addition, there is a great deal more variability in the observed Doppler spread at night than during the day in July-September. The greatest variability is seen during the night in April-May, when the ten-minute means vary up to 10 Hz in the space of one hour.

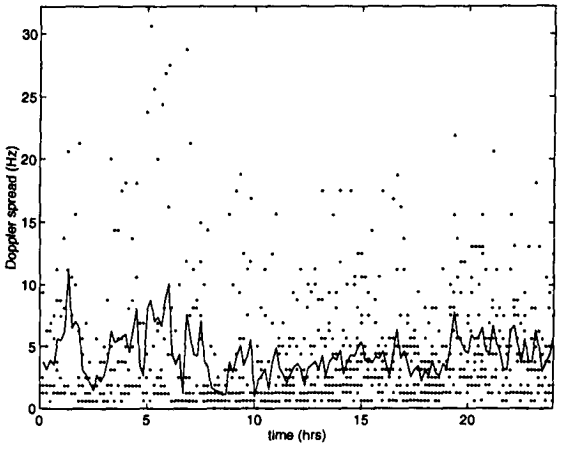


Figure 4.30: Diurnal variation in overall Doppler spread at 6.8 MHz, April-May, 1995

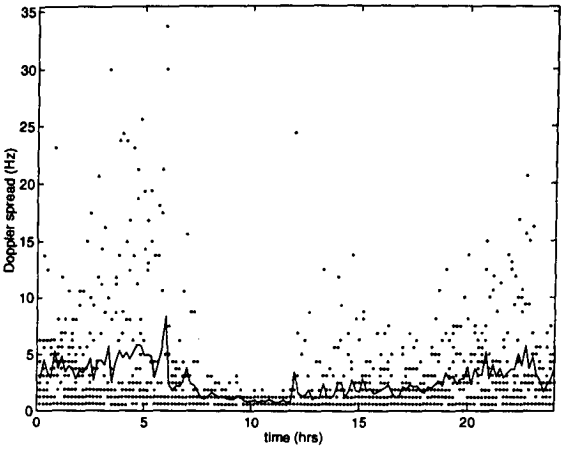


Figure 4.31: Diurnal variation in overall Doppler spread at 6.8 MHz, July-September, 1995

For propagation above the predicted MUF, the frequency 17.5 MHz is again considered. The diurnal variations are shown in figures 4.32 and 4.33 for the two times of year. Again, the Doppler spread is worse during the hours of darkness, and at this frequency this effect is noted also during April-May.

The mean and percentiles of the Doppler spread distributions are shown in figures 4.34 and 4.35 for the period 08:00 - 14:00 in April-May and August-September, respectively. Note that the distributions are much broader in the spring months, especially below the MUF, with the 90th percentile at 6.8 MHz exceeding 9 Hz. In the late summer, however, the distributions are narrow, and the resolution limitations of the DAMSON system result in the step-like functions seen in figure 4.35. In general, the Doppler spreads are largest below the MUF, and decrease with frequency above it.

The percentiles of the overall Doppler spread distributions for the period 20:00 - 02:00 are shown in figures 4.36 and 4.37 for April-May and July-September, respectively. The mean nighttime Doppler spreads are higher at all frequencies than during the day. In the spring months, the mean Doppler spread decreases as the frequency increases below the MUF, and then increases gradually with frequency above it. In July-September, the Doppler spread distributions decrease with frequency from a peak at 4.7 MHz, which is close to the predicted LUF.

## 4.4 DOPPLER SHIFT

The variation in Doppler shift with frequency is shown in figures 4.38 and 4.39 for the daylight hours 08:00 to 14:00 LT in April-May and July-September, respectively. The trend is for increasingly negative mean

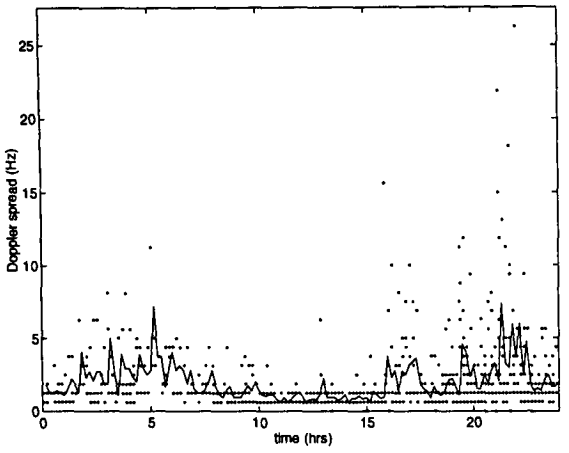


Figure 4.32: Diurnal variation in overall Doppler spread at 17.5 MHz, April-May, 1995

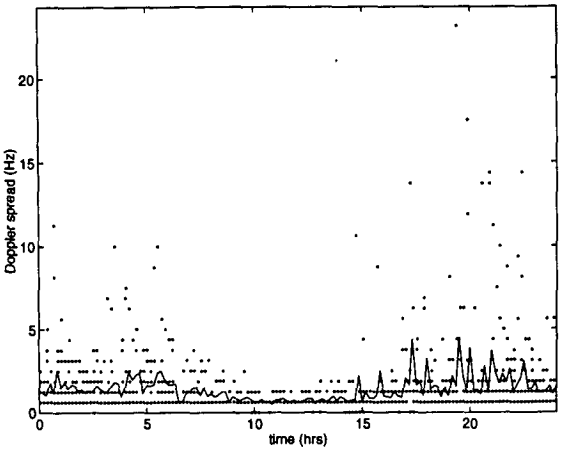


Figure 4.33: Diurnal variation in overall Doppler spread at 17.5 MHz, July-September, 1995

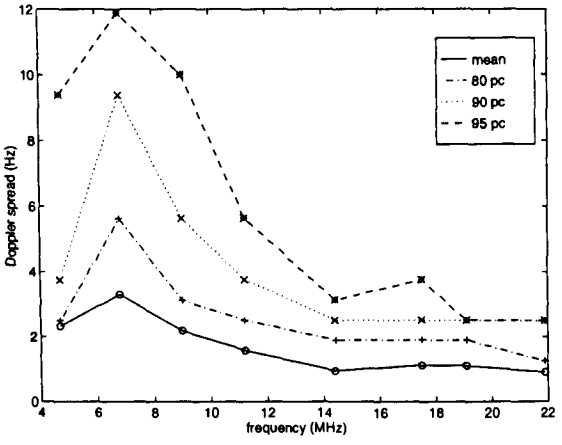


Figure 4.34: Percentiles of the overall Doppler spread for 08:00 to 14:00, April-May, 1995

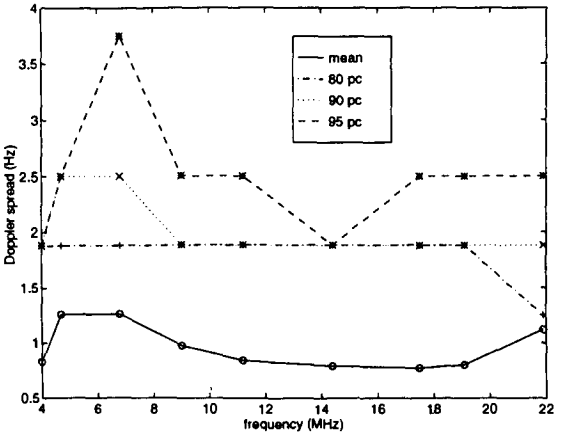


Figure 4.35: Percentiles of the overall Doppler spread for 08:00 to 14:00, July-September, 1995

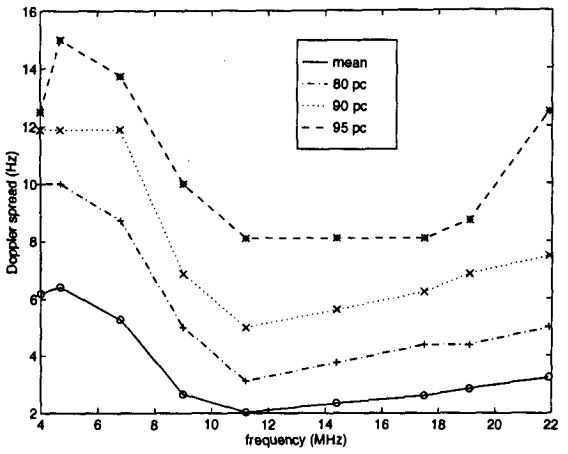


Figure 4.36: Percentiles of the overall Doppler spread for 20:00 to 02:00, April-May, 1995

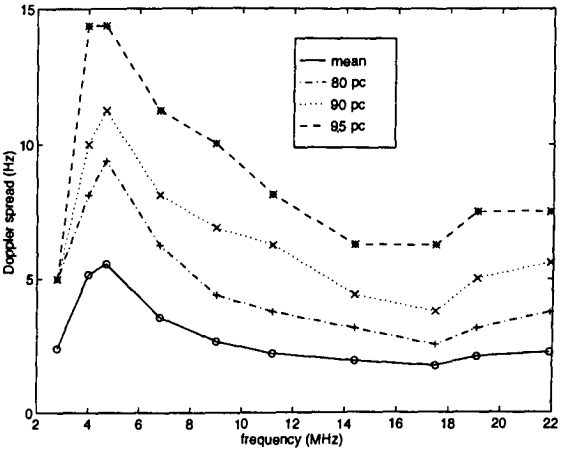


Figure 4.37: Percentiles of the overall Doppler spread for 20:00 to 02:00, July-September, 1995

Doppler shifts with increasing frequency. The largest mean Doppler shift is approximately -0.5 Hz, and the distributions are very narrow. At night, 20:00 to 02:00 LT, the same trend is seen (figures 4.40 and 4.41), and the distributions tend to be wider. The Doppler shifts at night in the April-May period are similar to that during the day, however in July-September, the mean nighttime Doppler shifts are almost a factor of two larger than during the day.

## 4.5 PARAMETER INTERACTION

### 4.5.1 Doppler spread on two modes

Below the MUF during the day in the July-September period, multiple modes were detected. The joint distribution of the Doppler spread on the two strongest modes is shown in figure 4.42 for 6.8 MHz in the time range 08:00 - 14:00. The dominant feature shows that the Doppler spreads on the two modes tend to be very similar, however there is a slight elongation along the strongest mode axis, which indicates that the strongest mode does have larger Doppler spreads at some times. As was seen in section 4.1, above the MUF only one propagation mode is usually detected.

### 4.5.2 Doppler spread and multipath spread interaction

Above the MUF, there appears to be no particular relationship between the overall Doppler spread and multipath spread. However, below the MUF there seems to be a tendency to see either large Doppler spreads or large multipath spreads. This is seen in figure 4.43 which shows the joint distribution of Doppler spread and multipath spread taken over all times of day and all times of year at 6.8 MHz. There is clearly some elongation along both the Doppler spread axis and the multipath spread. A possible cause of this is a propagation mode which, when present, is strong with small Doppler spread, combined with a weaker mode with large Doppler spread. When the slow fading mode is not present, the overall Doppler spread reflects that of the (possibly) single mode, with correspondingly small multipath spread. When the additional mode

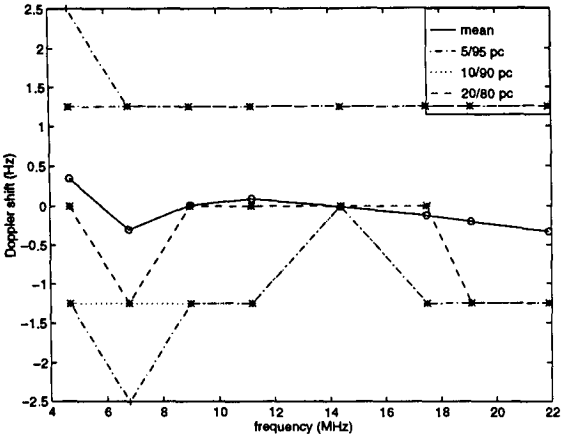


Figure 4.38: Percentiles of Doppler shift distributions on strongest mode for 08:00 to 14:00, April-May, 1995

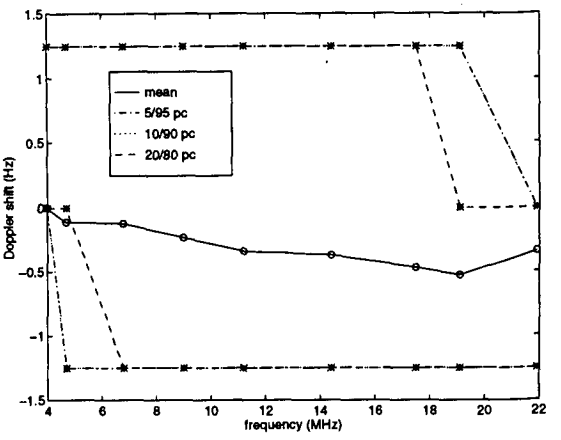


Figure 4.39: Percentiles of Doppler shift distributions on strongest mode for 08:00 to 14:00, July-September, 1995

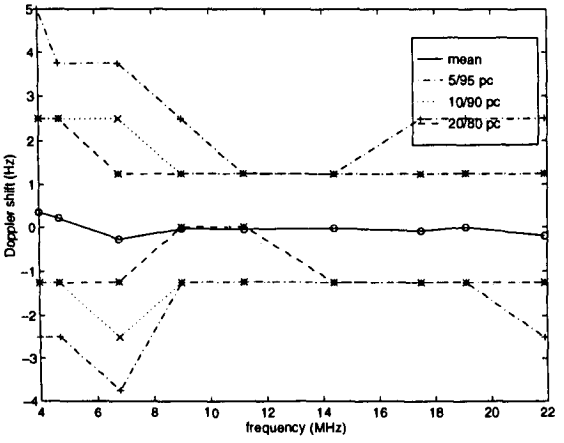


Figure 4.40: Percentiles of Doppler shift distributions on strongest mode for 20:00 to 08:00, April-May, 1995

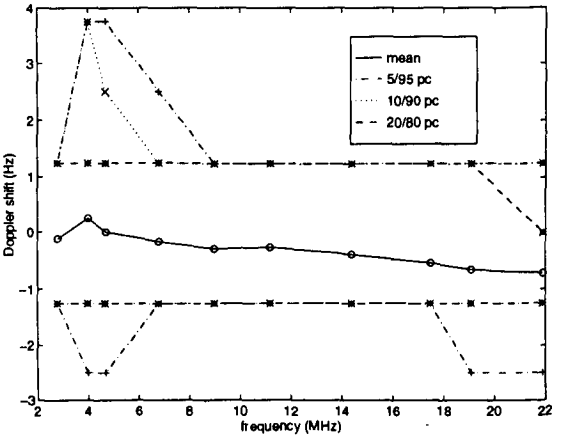


Figure 4.41: Percentiles of Doppler shift distributions on strongest mode for 20:00 to 08:00, July-September, 1995

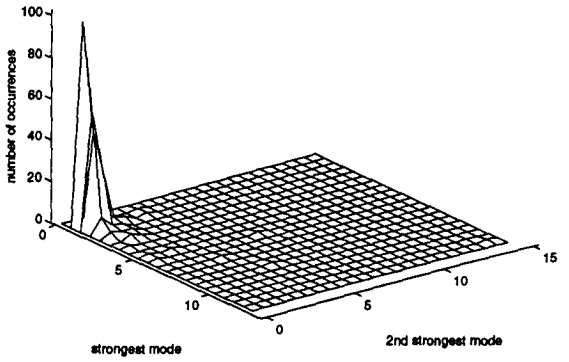


Figure 4.42: Joint distribution of Doppler spread on strongest and second strongest modes at 6.8 MHz, 08:00 - 14:00, July-September 1995

is propagating, it dominates the overall Doppler spread which is then relatively small, while the multipath spread is increased.

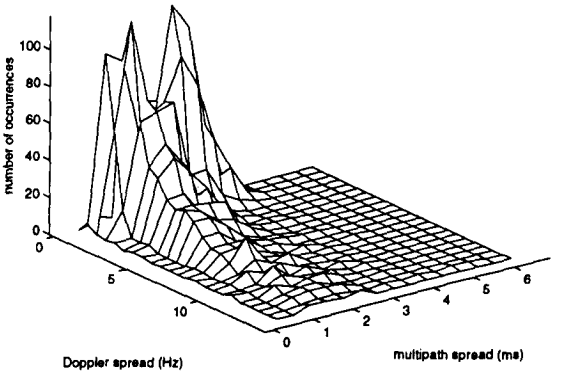


Figure 4.43: Joint distribution of Doppler spread and multipath spread at 6.8 MHz, all times of day and year

### 4.5.3 Doppler shift and multipath spread interaction

The variation in Doppler shift is small, and there is no discernible relationship between this parameter and the multipath spread at any of the frequencies in the DAMSON range.

## 4.6 SUMMARY

The Isfjord-Tuentangen link is the longest of the four considered, and has a north-south direction. The reflection points may be in the polar cap or auroral zone for multiple-hop propagation, or south of the auroral zone for fairly quiescent goemagnetic periods. As the $K_p$ values and sunspot numbers are quite low for the period being considered here, the southerly edge of the auroral zone is quite far north, and its effects are unlikely to be as pronounced as when the solar activity is higher.

The program ICEPAC has effectively predicted the LUF, which is often above the lowest DAMSON frequency, on which very little propagation is seen. The main difference in the predicted propagation modes in the LUF/MUF window was due to the different lengths of daylight, and the measurement data shows that multipath spread and SNR were quite similar for the two times of year when considered in terms of daylight and darkness. In general, multiple propagation modes were detected only below the MUF; above that frequency, the multipath spread was consistently small. The SNR measurements across the frequency band clearly show a LUF and MUF in the range predicted by ICEPAC.

The Doppler spread is significantly higher at night than during daylight at both times of year. The Doppler spread is greatest at the lower frequencies, just above the LUF. The most significant difference between the spring and late summer data is in the daytime Doppler spreads, which are a factor two larger in April-May than in July-September. The mean Doppler shifts are small, but increasingly negative with increasing frequency. The large Doppler spread suggests that the reflection points are in the auroral zone, where disturbances in the ionosphere cause scattering of the reflected signal.

# 5.0 ISFJORD-KIRUNA

The path from Isfjord to Kiruna is 1155 km long, at an azimuth of 166°. Measurements were made on four days in April, three days in May and nine days in August 1995, for a total of 10,900 data points for SNR analysis and 10,947 for Doppler and multipath analysis. The data sets will be divided into the April-May period and the August period for this analysis. The number of data points at each frequency during each of these periods is shown in table 5.1.

| frequency | SNR | | Doppler & multipath | |
|---|---|---|---|---|
| (MHz) | Apr-May | August | Apr-May | August |
| 2.8 | 231 | 393 | 240 | 386 |
| 4.0 | 589 | 746 | 589 | 734 |
| 4.7 | 691 | 849 | 687 | 833 |
| 6.8 | 742 | 848 | 746 | 846 |
| 9.0 | 538 | 798 | 544 | 796 |
| 11.2 | 686 | 799 | 700 | 789 |
| 14.4 | 331 | 485 | 348 | 494 |
| 17.5 | 237 | 300 | 248 | 237 |
| 19.1 | 233 | 339 | 247 | 341 |
| 21.9 | 470 | 595 | 548 | 594 |
| total | 4748 | 6152 | 4897 | 6050 |

Table 5.1: Number of data points on Isfjord-Kiruna link for SNR and Doppler/multipath analysis

The LUFs and MUFs were predicted using ICEPAC for May and August, using the smoothed sunspot numbers 19 and 16, respectively. The prediction results are shown in figure 5.1.

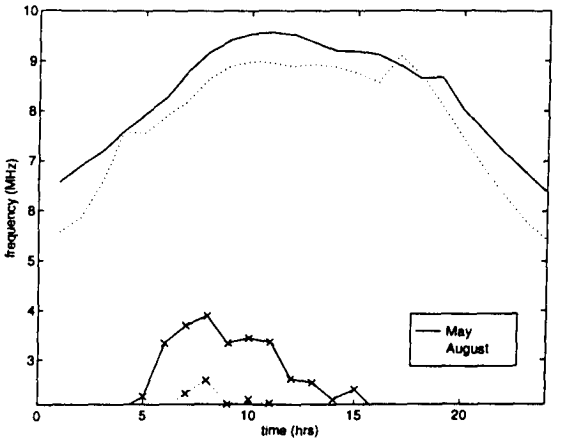


Figure 5.1: Predicted LUFs and MUFs for May and August 1995

## 5.1 MULTIPATH SPREAD

The LUF/MUF plot shown in figure 5.1 indicates that the 2.8 MHz and 4.0 MHz are below the peak LUF frequency in May, and 2.8 MHz is very close to the peak LUF in August. During daylight hours, when the LUF is at its highest, ICEPAC predicts unreliable propagation via the E and Es layers at 2.8 MHz and 4.0 MHz. At night, more reliable propagation support is predicted from the F2 layer.

The predicted modes are shown in figures 5.2 and 5.3 for 4.7 MHz in May and August, respectively, where the Es modes are omitted for clarity. The predictions are quite different, in that 2F1 propagation is predicted throughout the day in May, but only in the early morning and late afternoon in August, while multihop E layer propagation is predicted in daylight in August. The 3F2 mode is also active longer in May. Overall, the predictions show that multipath spreads on the order of 4-6 ms can be expected during the hours of daylight, with fewer modes and smaller multipath spreads in darkness, especially in the late summer.

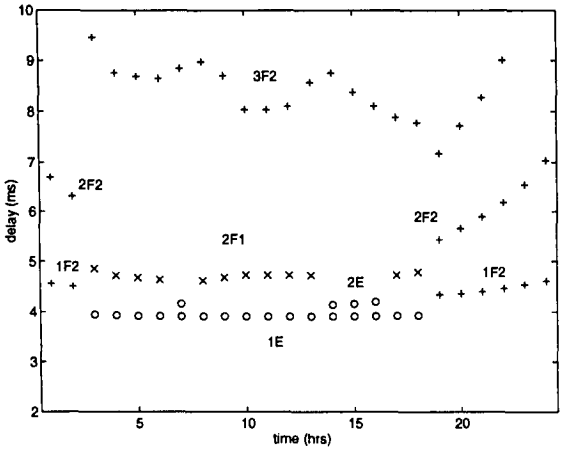


Figure 5.2: Predicted propagating modes at 4.7 MHz for May, 1995

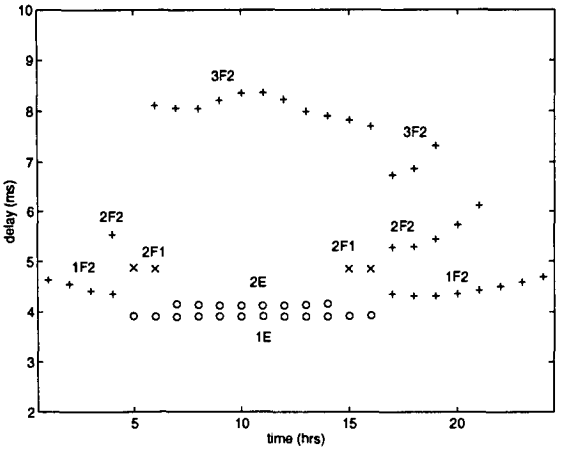


Figure 5.3: Predicted propagating modes at 4.7 MHz for August, 1995

The diurnal variations observed in the multipath spread are shown in figures 5.4 and 5.5 for 4.7 MHz in April-May and August, respectively. The multipath spread is greatest during the daylight hours at both times of year, although it tends to be larger in August when means of 4-5 ms are seen, compared to 3-4 ms in April-May. At night, the mean multipath spreads are in the range 1-2 ms in April-May and 2-2.5 ms in August.

Above the MUF, the multipath spread tends to be small, as propagation is generally limited to a single mode. The diurnal variation at 14.4 MHz is shown in figure 5.6 for April-May and in figure 5.7 for August. Note that there is very little propagation around noon, local time, particularly in April-May. This is the case for most of the frequencies above the MUF during daylight. When propagation does occur, the multipath spread tends to be large. The small multipath spreads at night indicate that single mode propagation is the norm.

The mean number of modes detected at each frequency during daylight and darkness hours is shown in figure 5.8. Note that the peak at 17.5 MHz for 08:00 to 14:00 is most likely an anomoly caused by too few

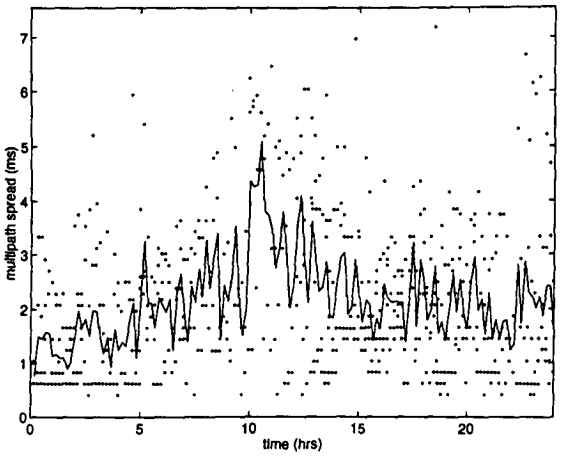


Figure 5.4: Diurnal variation in multipath spread at 4.7 MHz for April-May, 1995

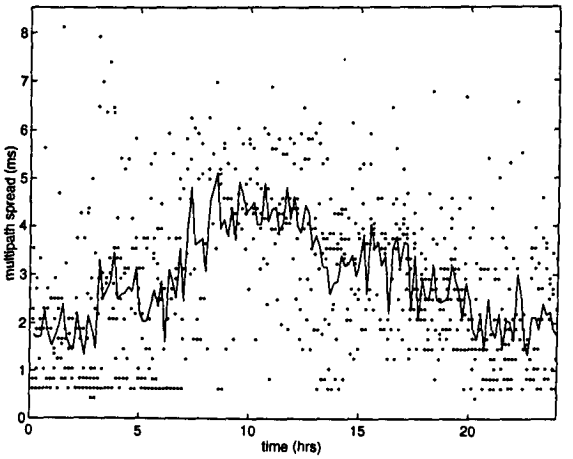


Figure 5.5: Diurnal variation in multipath spread at 4.7 MHz for August, 1995

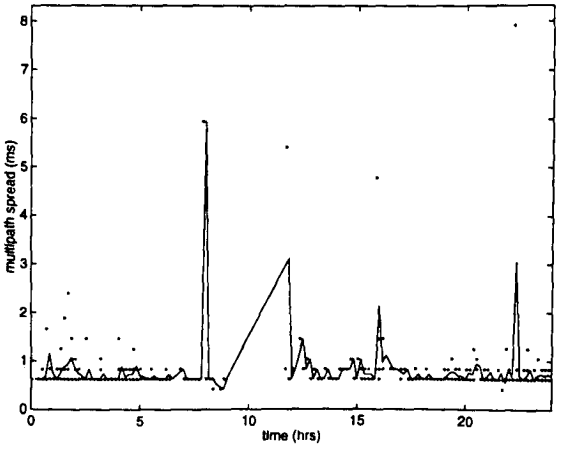


Figure 5.6: Diurnal variation in multipath spread at 14.4 MHz for April-May, 1995

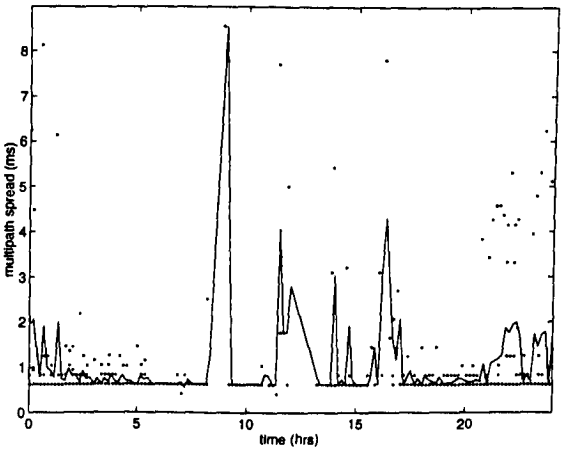


Figure 5.7: Diurnal variation in multipath spread at 14.4 MHz for August, 1995

data points. In general, frequencies between the predicted LUF and MUF have average numbers of modes between 1.5 and 2.5, whereas above the MUF multimode propagation is rare. Note also that the number of modes detected between the predicted LUF and MUF is greater during the daylight than during darkness.

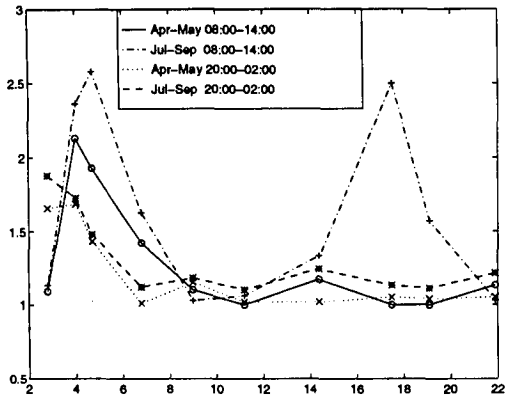


Figure 5.8: Mean number of propagation modes detected

The mean and percentiles of the multipath spread across the frequencies are shown in figures 5.9 and 5.10 for the daylight hours (08:00 - 14:00 LT) in April-May and August, respectively. The corresponding plots for nighttime (20:00 - 02:00 LT) are in figures 5.11 and 5.12. Again the peak at 17.5 MHz in daylight in August is given no statistical weight. Overall, the multipath spread is greatest between the predicted LUF and MUF, corresponding to multimodal propagation. Smaller multipath spreads are seen above the MUF when single modes are usually observed. The distributions are also broader when the mean multipath spreads are greater.

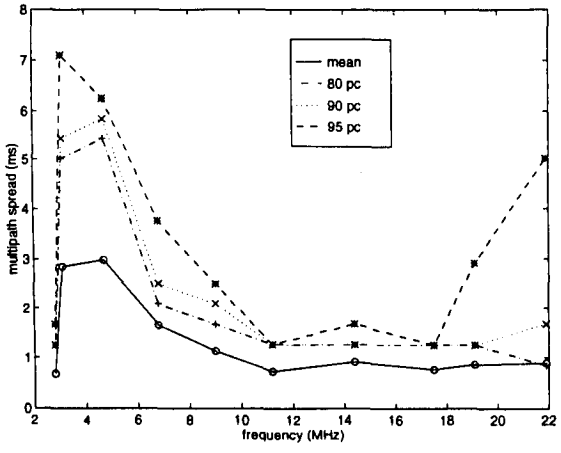


Figure 5.9: Percentiles of the multipath spread distribution for 08:00 to 14:00 for April-May, 1995

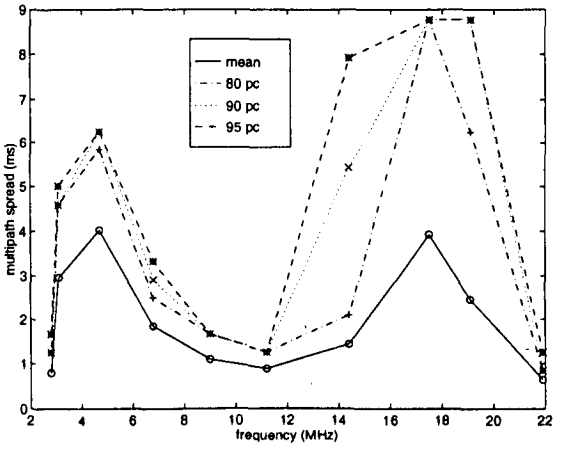


Figure 5.10: Percentiles of the multipath spread distribution for 08:00 to 14:00 for August, 1995

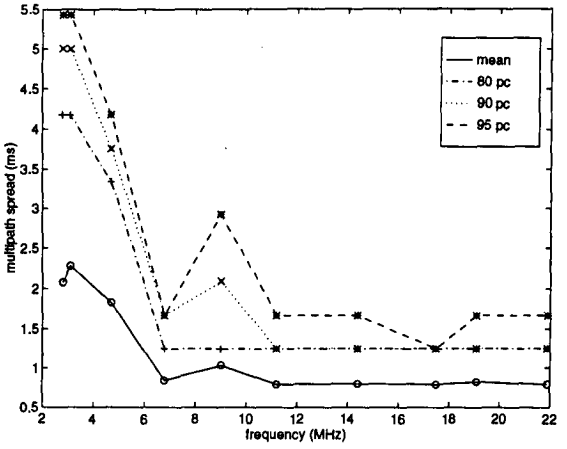


Figure 5.11: Percentiles of the multipath spread distribution for 20:00 to 02:00 for April-May, 1995

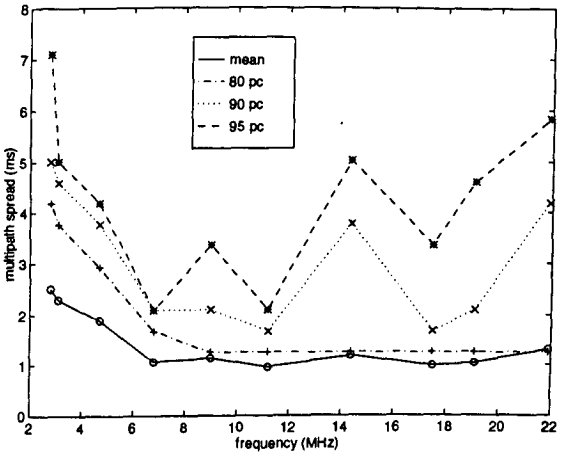


Figure 5.12: Percentiles of the multipath spread distribution for 20:00 to 02:00 for August, 1995

The distribution of multipath spread across the DAMSON frequencies is shown in figure 5.13 for all times of day in August. The figure beside it, figure 5.14, shows the distribution of the number of modes detected at each frequency. It is clear that the number of modes and the multipath spread tends to be larger in the predicted LUF/MUF window.

## 5.2 SNR

The diurnal variation for 4.7 MHz is shown in figure 5.15 for April-May and in figure 5.16 for August. At both times of year, the mean SNR is slightly greater during daylight than darkness, and the overall observations are very scattered, due in part to the short measurement period.

Above the MUF, the daytime propagation is reduced. This is seen in the diurnal variation in SNR at 14.4 MHz (figures 5.17 and 5.18), where the SNR decreases around dawn, and increases again as propagation resumes around dusk.

The mean and percentiles of the SNR distributions across the frequencies are shown in figures 5.19 and 5.20 for 08:00 - 14:00 in April-May and August, respectively, and in figures 5.21 and 5.22 for 20:00 - 02:00 for the same times of year. Between the predicted LUF and MUF, the daytime SNR is greater in August than in April-May, while above the MUF there is little difference. The nighttime SNRs tend to be lower, on average, than the daytime values for frequencies below the MUF, but greater above. The distributions are also broader above the MUF at night.

### 5.2.1 Distribution of signal power

The results presented in section 5.1 showed that the number of detected modes is greater than one, on average, only between the LUF and MUF. In this section, the percentage of power in the strongest mode is considered at 4.7 MHz.

The distribution of the proportion of power in the strongest mode is shown in figure 5.23 for daytime (08:00 - 14:00 LT) in April-May and August. The mean is around 70 % in both cases. During the nighttime,

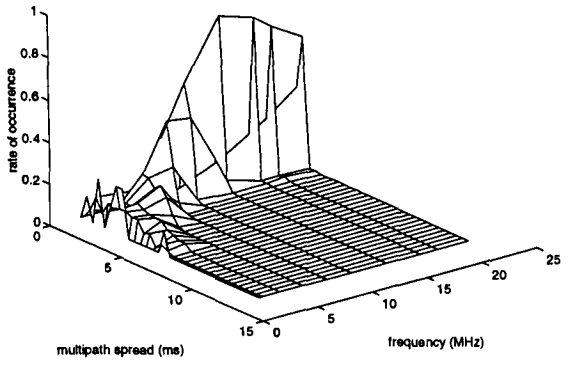


Figure 5.13: Distribution of multipath spreads for August, 1995

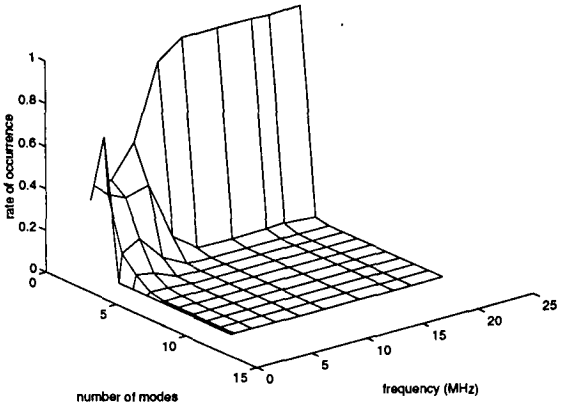


Figure 5.14: Distribution of number of modes for August, 1995

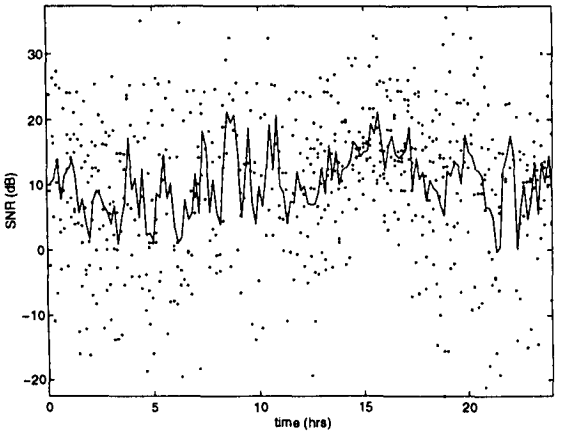


Figure 5.15: Diurnal variation in SNR at 4.7 MHz for April-May, 1995

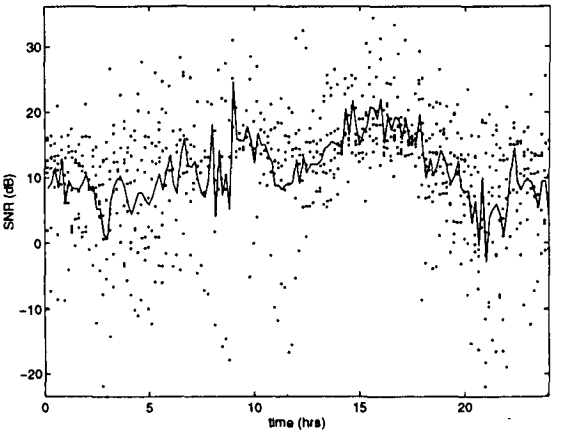


Figure 5.16: Diurnal variation in SNR at 4.7 MHz for August, 1995

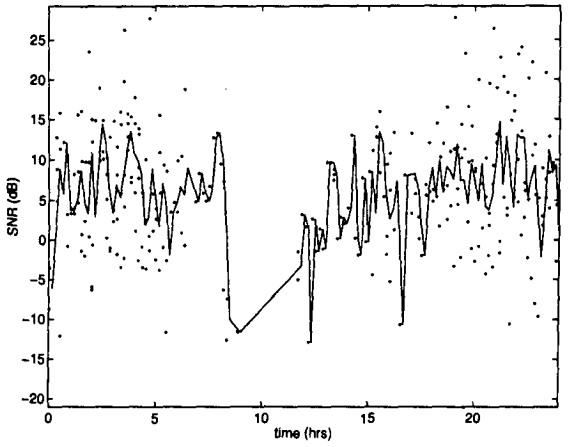


Figure 5.17: Diurnal variation in SNR at 14.4 MHz for April-May, 1995

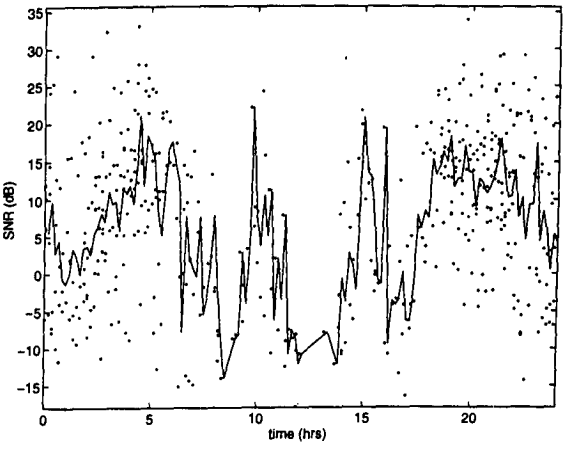


Figure 5.18: Diurnal variation in SNR at 14.4 MHz for August, 1995

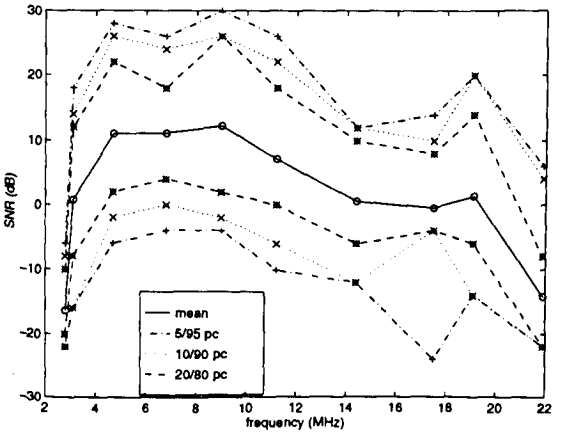


Figure 5.19: Percentiles of the SNR distribution for 08:00 to 14:00 for April-May, 1995

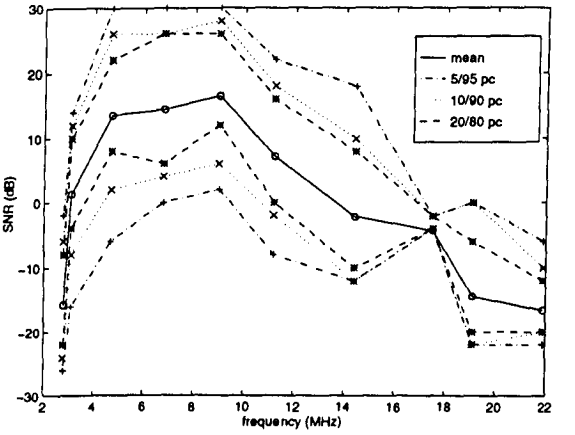


Figure 5.20: Percentiles of the SNR distribution for 08:00 to 14:00 for August, 1995

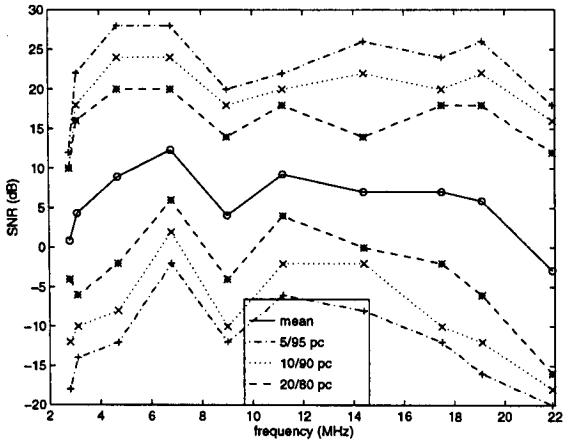


Figure 5.21: Percentiles of the SNR distribution for 20:00 to 02:00 for April-May, 1995

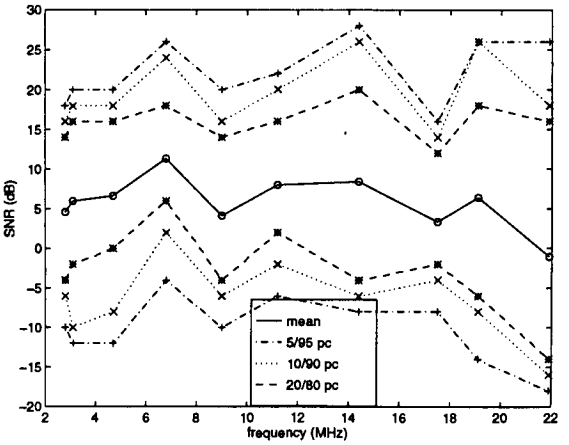


Figure 5.22: Percentiles of the SNR distribution for 20:00 to 02:00 for August, 1995

there tends to be more power in the strongest mode, as seen in figure 5.24, where the mean is close to 80 % for both times of year. This corresponds to the number of modes detected; when more modes are seen during daylight hours below the MUF, as discussed in section 5.1, the percentage of power in the strongest is expected to be lower than when only two modes are observed.

## 5.3 DOPPLER SPREAD

The number of propagating modes detected at each frequency was discussed in section 5.1, where it was seen that multimodal propagation occurs on only a few frequencies, for some times of day. Thus there are insufficient data points to make reliable conclusions about Doppler spreads on different modes, and the discussion in this section will concentrate on the overall Doppler spread.

The frequency 4.7 MHz is considered as it lies between the predicted LUF and MUF. The diurnal variation in the observed Doppler spread at this frequency is shown in figure 5.25 for April-May and in figure 5.26 for August. In April-May, the Doppler spread is very variable at all times of the day, with extreme values at 25 Hz. In August, there is a more obvious diurnal trend, with larger values being observed at night. The extreme values, of up to 35 Hz, are all recorded during the nighttime.

Above the MUF, the Doppler spreads observed tend to have a broader distribution than below. The diurnal variations for April-May and August at 14.4 MHz are shown in figures 5.27 and 5.28. Propagation is less reliable during daylight, and the Doppler spread is quite variable during those times when modes are detected.

The means and percentiles of the Doppler spread distributions are shown in figures 5.29 and 5.30 for 08:00 to 14:00 LT in April-May and August, respectively. The corresponding plots for 20:00 - 02:00 are shown in figures 5.31 and 5.32. The daytime peaks around 17.5 MHz are probably anomolous, as there are insufficient data points at these frequencies to determine statistical distributions. In general, the Doppler spread is greater at night. The nighttime means in August are slightly higher than in April-May, but at both times of year the distributions become broader as the frequency increases.

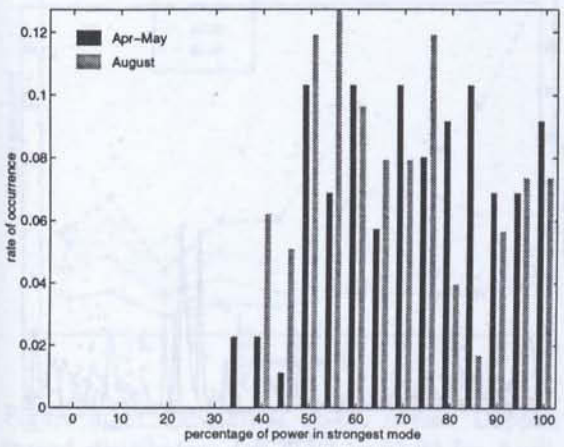


Figure 5.23: Distribution of percentage of power in strongest mode at 4.7 MHz, 08:00 - 14:00, 1995

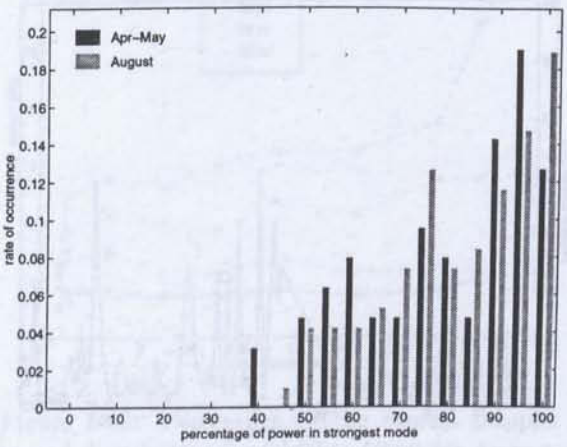


Figure 5.24: Distribution of percentage of power in strongest mode at 4.7 MHz, 20:00 - 02:00,1995

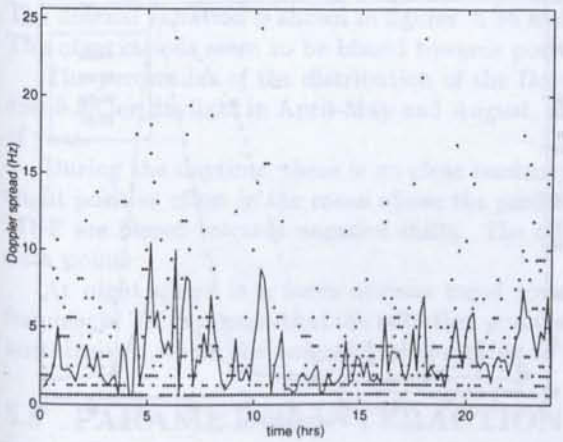


Figure 5.25: Diurnal variation in Doppler spread at 4.7 MHz for April-May, 1995

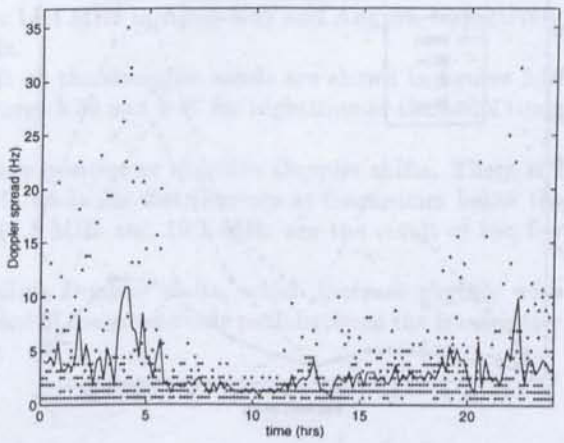


Figure 5.26: Diurnal variation in Doppler spread at 4.7 MHz for August, 1995

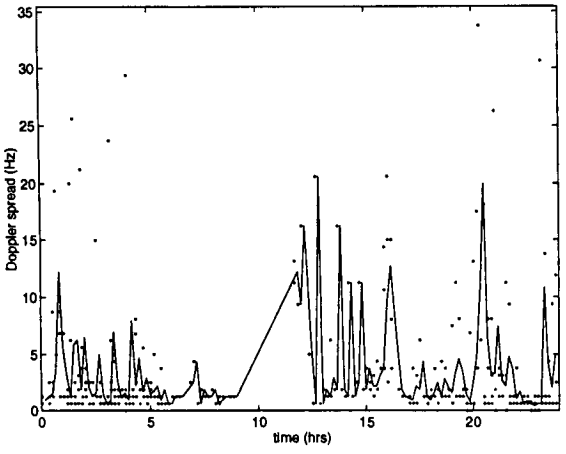


Figure 5.27: Diurnal variation in Doppler spread at 14.4 MHz for April-May, 1995

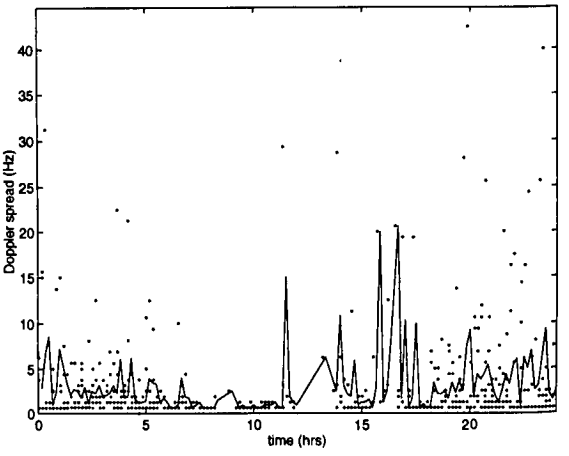


Figure 5.28: Diurnal variation in Doppler spread at 14.4 MHz for August, 1995

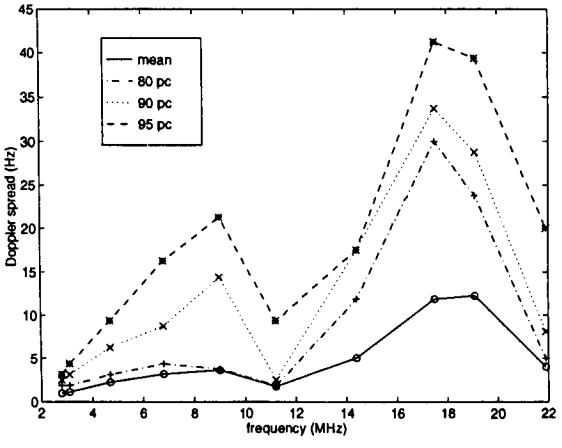


Figure 5.29: Percentiles of the overall Doppler spread distribution for 08:00 to 14:00 for April-May, 1995

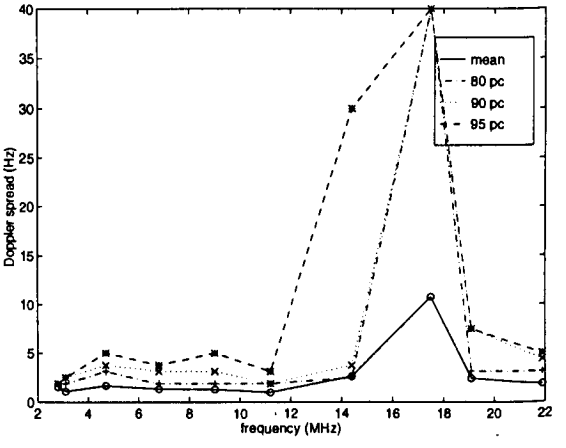


Figure 5.30: Percentiles of the overall Doppler spread distribution for 08:00 to 14:00 for August, 1995

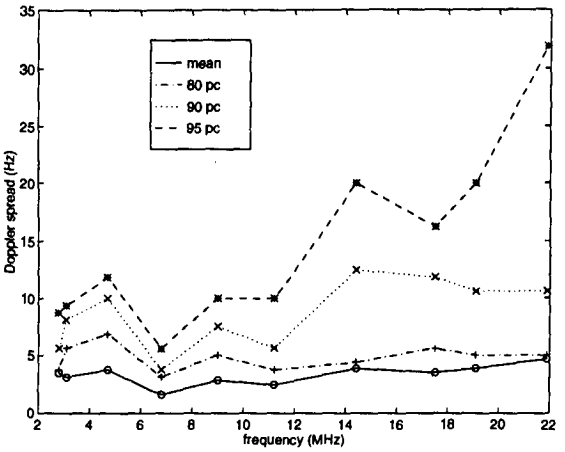


Figure 5.31: Percentiles of the overall Doppler spread distribution for 20:00 to 02:00 for April-May, 1995

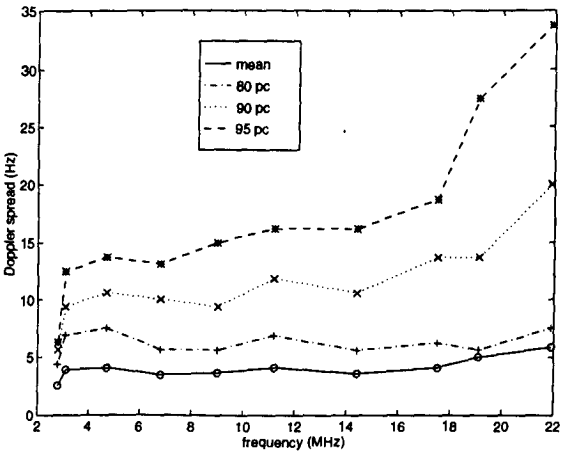


Figure 5.32: Percentiles of the overall Doppler spread distribution for 20:00 to 02:00 for August, 1995

## 5.4 DOPPLER SHIFT

The diurnal variation in the Doppler shift on the strongest mode is shown in figure 5.33 for April-May and in figure 5.34 for August at 4.7 MHz. In April-May, the shift is fairly uniform throughout the day. In August, the shift appears to be mainly positive in the early morning, and negative in the early evening.

Above the MUF, the shift tends to be more scattered in the daytime, when propagation is unreliable. The diurnal variation is shown in figures 5.35 and 5.36 for 14.4 MHz in April-May and August, respectively. The observations seem to be biased towards positive shifts.

The percentiles of the distribution of the Doppler shift on the strongest mode are shown in figures 5.37 and 5.38 for daylight in April-May and August, and in figures 5.39 and 5.40 for nighttime at the same times of year.

During the daytime, there is no clear tendency for either positive or negative Doppler shifts. There is a slight positive offset in the mean above the predicted MUF, while the distributions at frequencies below the MUF are biased towards negative shifts. The offsets at 17.5 MHz and 19.1 MHz are the result of too few data points.

At night, there is a more obvious trend towards positive Doppler shifts, which increase slightly with frequency. This suggests that the reflection point is to the east of the great-circle path between the transmitter and receiver, where the auroral oval is moving to the west.

## 5.5 PARAMETER INTERACTION

### 5.5.1 Doppler spread on two modes

Below the MUF, there are sufficient observations with two or more propagation modes detected to consider the interaction of Doppler spreads on the strongest and second strongest modes. The joint distribution of these estimates is shown in figures 5.41 and 5.42 for daytime (08:00 - 14:00 LT) in April-May and August,

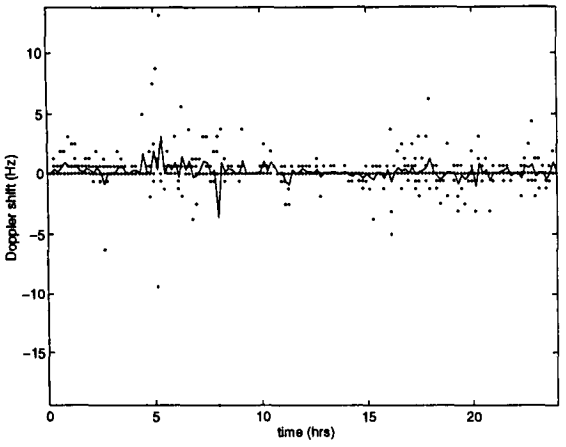


Figure 5.33: Diurnal variation in Doppler shift on strongest mode at 4.7 MHz for April-May, 1995

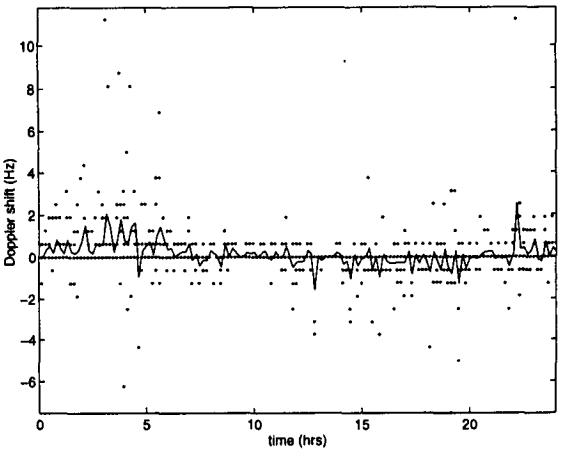


Figure 5.34: Diurnal variation in Doppler shift on strongest mode at 4.7 MHz for August, 1995

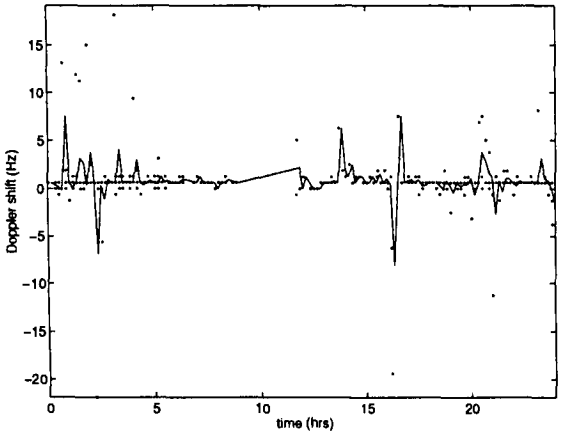


Figure 5.35: Diurnal variation in Doppler shift on strongest mode at 14.4 MHz for April-May, 1995

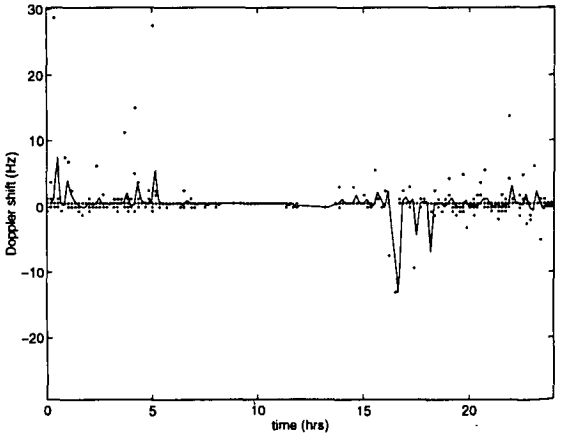


Figure 5.36: Diurnal variation in Doppler shift on strongest mode at 14.4 MHz for August, 1995

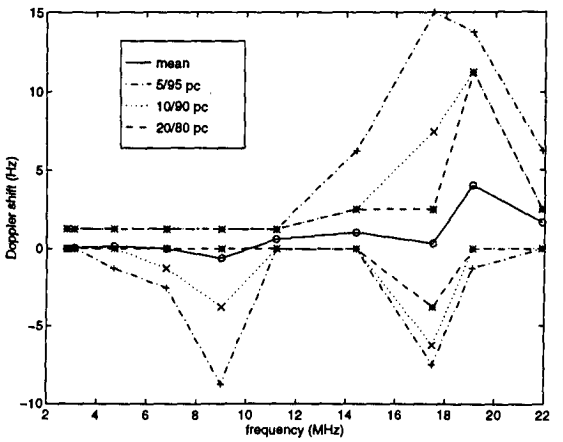


Figure 5.37: Percentiles of the Doppler shift distributions on strongest mode for 08:00 to 14:00 for April-May, 1995

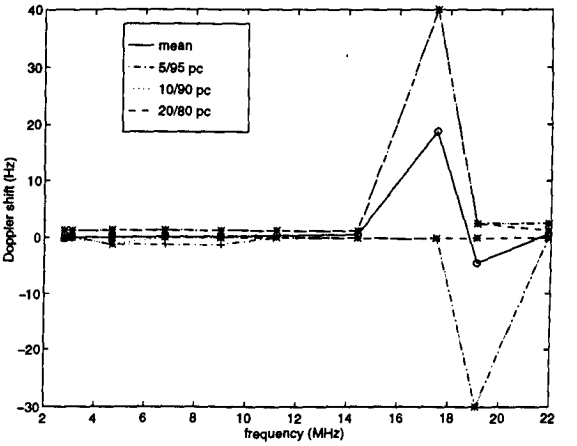


Figure 5.38: Percentiles of the Doppler shift distributions on strongest mode for 08:00 to 14:00 for August, 1995

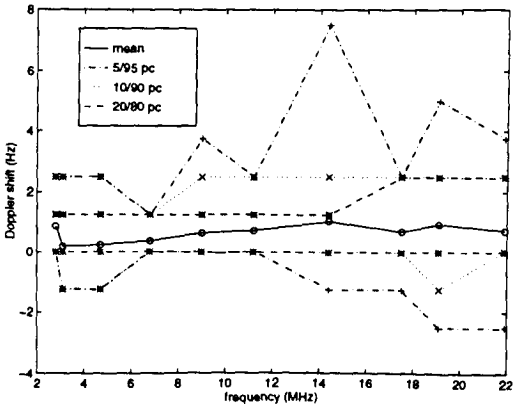


Figure 5.39: Percentiles of the Doppler shift distributions on strongest mode for 20:00 to 02:00 for April-May, 1995

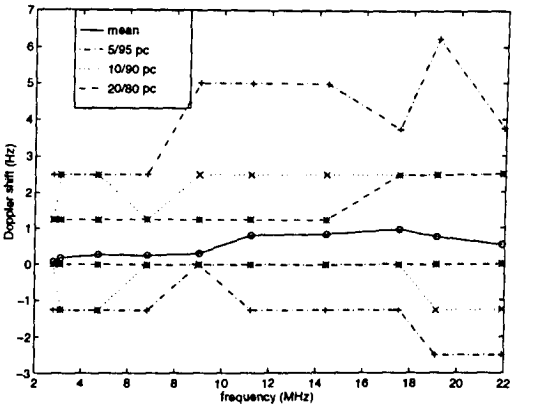


Figure 5.40: Percentiles of the Doppler shift distributions on strongest mode for 20:00 to 02:00 for August, 1995

respectively. There were insufficient data points with second modes at night to generate corresponding plots. It is seen that the Doppler spreads tend to be similar on both modes. In sections 5.1 and 5.2.1, it was seen that the mean number of modes is close to two, and that the strongest mode contains about 70 % of the total signal power. On the basis of this, it is reasonable to assume that there are typically two modes with only a small difference in signal power. At any given measurement instant, either mode may be identified as the stronger. This supposition is supported when the joint distribution over all times of year and all times of day is considered at this frequency, figure 5.43. There are elongations in the distribution along both the strongest mode axis and the second strongest mode axis, indicating that when the Doppler spread on one or other of the modes is large, it is small on the other.

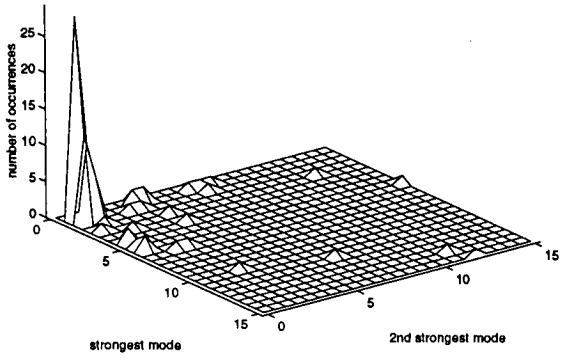


Figure 5.41: Joint distribution of Doppler spread on strongest and second strongest modes, 4.7 MHz, 08:00 - 14:00, April-May, 1995

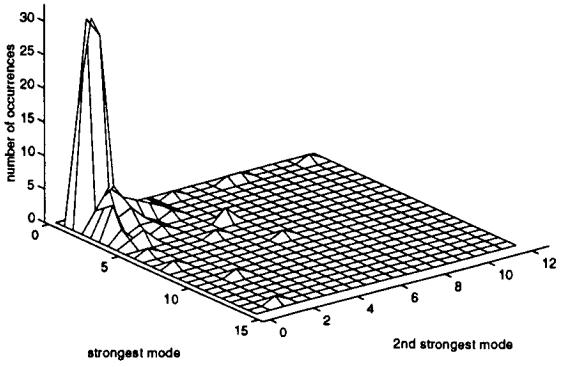


Figure 5.42: Joint distribution of Doppler spread on strongest and second strongest modes, 4.7 MHz, 08:00 - 14:00, August, 1995

Above the MUF, there are insufficient data points in which two or modes are detected to consider the joint distributions.

### 5.5.2 Doppler spread and multipath spread interaction

The joint distributions of the overall Doppler spread and multipath spread for daytime in April-May and August are shown in figures 5.44 and 5.45, respectively. There is no apparent relationship between the Doppler spread and multipath spread. At night, however, there is a clear trend for Doppler spread and multipath spread to increase together (figures 5.46 and 5.47). Note that this is unlikely to be caused by multiple modes with different Doppler shifts, as it was seen in section 5.1 that there are typically fewer propagating modes detected at night on this link.

The frequency 14.4 MHz is above the MUF, and it has been noted previously that there is reduced daytime propagation above the MUF. The joint distribution of Doppler spread and multipath spread does not vary greatly with time of year or time of day, and is typified by that shown in figure 5.48 which is taken over all times of year and all times of day. It is seen that the multipath spread is uniformly small for all values of Doppler spread.

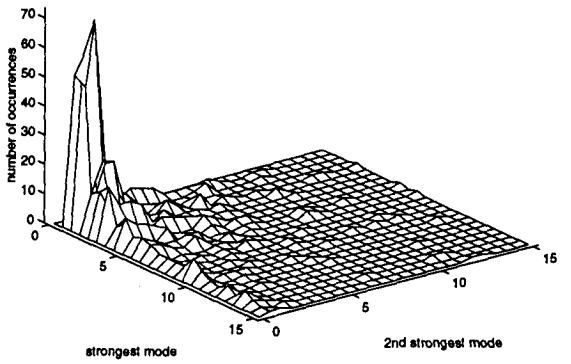


Figure 5.43: Joint distribution of Doppler spread on strongest and second strongest modes, 4.7 MHz, all times of day and year, 1995

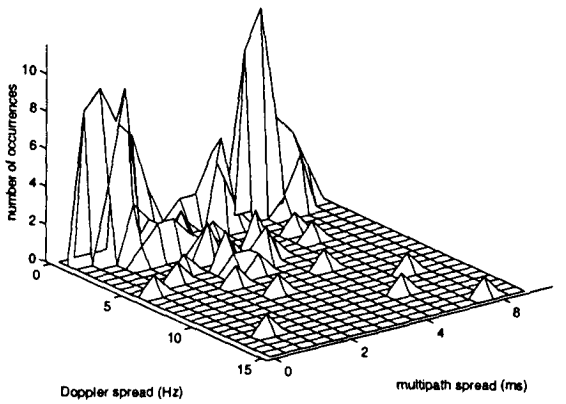


Figure 5.44: Joint distribution of Doppler spread and multipath spread, 4.7 MHz, 08:00 - 14:00, April-May, 1995

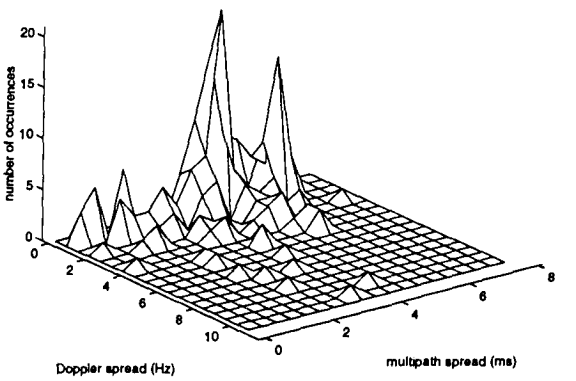


Figure 5.45: Joint distribution of Doppler spread and multipath spread, 4.7 MHz, 08:00 - 14:00, August, 1995

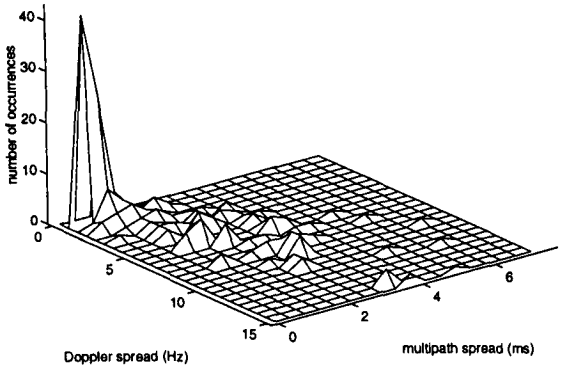


Figure 5.46: Joint distribution of Doppler spread and multipath spread, 4.7 MHz, 20:00 - 02:00, April-May, 1995

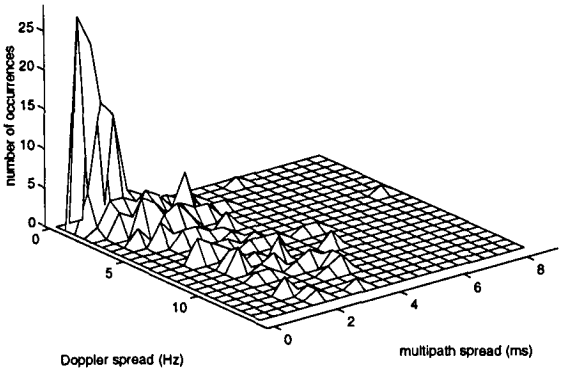


Figure 5.47: Joint distribution of Doppler spread and multipath spread, 4.7 MHz, 20:00 - 02:00, August, 1995

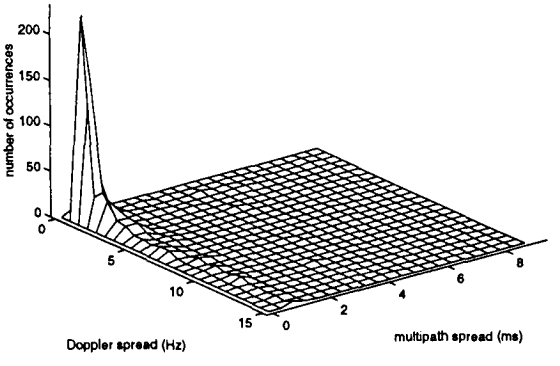


Figure 5.48: Joint distribution of Doppler spread and multipath spread, 14.4 MHz, all times of day and year, 1995

### 5.5.3 Doppler shift and multipath spread interaction

The joint distributions of Doppler shift (i.e. the difference in shift between the first and second strongest modes) during daylight and darkness for frequencies below the MUF are very similar. Figure 5.49 shows the joint distribution at 4.7 MHz over all times of day and year. There is clearly no specific relationship between Doppler shift and multipath spread, as the Doppler shift is minimal. Above the MUF, multiple mode propagation is rare, hence the Doppler shift differential is non-existent.

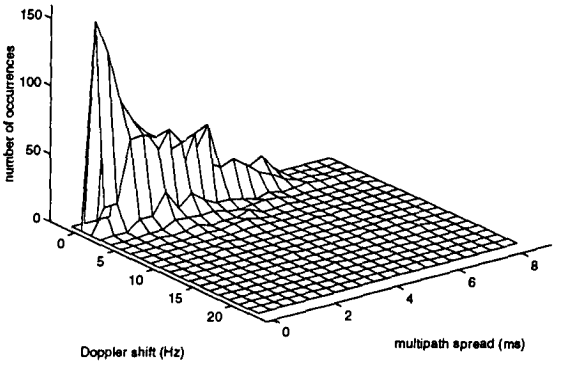


Figure 5.49: Joint distribution of Doppler shift and multipath spread, 4.7 MHz, all times of day and year, 1995

## 5.6 SUMMARY

This north-south link has reflection points that are generally in the auroral oval, which would be expected to lead to fairly large Doppler spreads. The measured SNR showed only small variations across the frequencies, which does not indicate that ICEPAC has accurately estimated the MUF. However, the observed multipath spreads within the predicted LUF/MUF window are compatible with the modal predictions made. When propagation is supported above the predicted MUF, it tends to be quite strong, and has fairly large Doppler spreads.

The Doppler spreads are quite large, especially at higher frequencies where the mean exceeded 10 Hz during the day in April-May. At lower frequencies, particularly in the LUF/MUF window, the nighttime Doppler spreads were larger than the daytime observations. Unlike the other paths analysed, the mean Doppler shift tends to be positive, which is probably due to the reflection point being further north in the auroral zone or polar cap region.

# 6.0 ROBUST DATA COMMUNICATIONS

In this section, the impact of the propagation characteristics on waveform design is considered. On any HF link, when the propagation characteristics are sufficiently benign and good SNR conditions persist, data can be transmitted at a fairly high rate with acceptable performance, see for example [27]. When the propagation conditions worsen, a more robust waveform is required in an attempt to mitigate the channel effects.

From the analysis presented in the previous sections, it is clear that the important parameters for consideration are multipath spread, overall Doppler spread and SNR. The manageable multipath spread depends on several modem properties, such as the width of the synchronisation window, the length of the equaliser training sequences in serial tone modems, and the length of each tone in a parallel tone system. A large Doppler spread requires more frequent updating of the equaliser taps, as well as a more robust synchronisation procedure.

In addition to the propagation path loss, the SNR at the modem input depends on the types of transmit and receive antennas used as well as the transmit power. In many applications, this will be the critical factor, requiring robust data communication waveforms in otherwise benign conditions, for example in aircraft or manpacks at mid-latitudes. The DAMSON system operates with fixed transmitter power and uses readily available antenna equipment. An analysis of the antennas used indicates that the SNR cannot simply be mapped up or down the scale to accommodate different antennas as the scaling factor depends on the angle of arrival [28]. Clearly, the angle of arrival is dependent on the propagating mode, and this cannot be accurately determined for the DAMSON measurements without the parallel operation of a direction-finding system.

An additional problem with considering the SNR is that, in the current DAMSON data analysis procedure, it is measured using the CW signal which is offset by a few seconds from the Doppler and multipath spread measurements. As the channels being measured are fading, there is no guarantee that the recorded SNR accurately reflects the SNR at the time of the Doppler and multipath spread estimation.

With these caveats, the following discussion considers the SNR along with the Doppler and multipath spreads, as it represents the best information available about the channel.

The aim of this section is to determine:

a. what proportion of time a robust waveform would be required on each of the links;

b. which parameters are important in requiring the use of a robust waveform; and

c. the range of propagation parameters that must be handled by a robust waveform.

For the purposes of this analysis, it is assumed that a "robust" waveform is required when one or more of the channel parameters meet the following criteria:

| | |
|---|---|
| SNR | $< 0$ dB |
| multipath spread | $> 6$ ms |
| overall Doppler spread | $> 5$ Hz |

This approach is supported by waveform characterisation experiments performed by the UK Defence Research Agency, and reported in [29]. When none of the above criteria are met, it is assumed that a higher rate data modem can operate at an acceptable performance. When one or more of the criteria are satisfied by the measured propagation parameters, a robust, low rate modem is required.

## 6.1 REQUIREMENT FOR A ROBUST WAVEFORM

Using the criteria specified on page 6-1, the percentage of DAMSON observations which give parameter estimates requiring the use of a robust waveform are shown in table 6.1. Note that only those data points when channel parameters were extracted are considered, i.e. when the received signal was not too weak or too distorted to be classified using the DAMSON system. This corresponds, to a large extent, to those times and frequencies at which an automatic link establishment procedure would identify possible data communications channels. The asterisk denotes fewer than 20 data points in the set. These values are also plotted in figure 6.1, where the legend gives the initials of the transmitter and receiver locations.

| frequency (MHz) | Harstad - Tuentangen | Harstad - Kiruna | Isfjord - Tuentangen | Isfjord - Kiruna |
|---|---|---|---|---|
| 2.8 | 36.9 | 17.8 | 33.3* | 75.2 |
| 4.0 | 41.9 | 17.5 | 64.9 | 43.8 |
| 4.7 | 14.2 | 25.7 | 47.6 | 30.7 |
| 6.8 | 10.2 | 83.9 | 24.4 | 17.2 |
| 9.0 | 10.2 | 90.5 | 18.8 | 30.2 |
| 11.2 | 20.8 | 92.8 | 14.7 | 31.6 |
| 14.4 | 53.7 | 96.4 | 15.2 | 35.2 |
| 17.5 | 61.9 | 98.4 | 37.2 | 48.9 |
| 19.1 | 69.3 | 99.8 | 42.9 | 49.7 |
| 21.9 | 61.7 | 99.4 | 49.2 | 76.6 |

Table 6.1: Percentage of measurements that meet criteria for robust waveform use

It can be seen that above the MUF or below the LUF there is a greater proportion of observations which indicate that a robust waveform would be required. On the Harstad-Kiruna link, which was seen to have very severe propagation, a robust waveform would be required more than 90 % of the time at frequencies at or above 9.0 MHz.

## 6.2 PARAMETER IMPORTANCE

In this section, the relative importance of each parameter in the requirement for a robust waveform is considered. The method is to determine what proportion of the DAMSON measurements in the available data sets meet the parameter criteria specified above.

### 6.2.1 SNR

As discussed earlier, the role played by the SNR in the need to use a robust waveform is highly system dependent. The results presented here apply only to the threshold specified and to the DAMSON system parameters, i.e. transmit and receive antennas, and transmit power. It would be expected that on difficult platforms a robust waveform would be required for a significant proportion of data communication transmissions, whereas on a shore-based system the SNR may be sufficient not to be a relevant parameter in the waveform selection. For the DAMSON system, using a threshold of 0 dB, the percentage of time on each link for which a robust waveform is dictated by the SNR is shown in figure 6.2. On all the links, only 10-20 % of the observations record SNR below 0 dB between the predicted LUF and MUF, although the percentage increases considerably above the MUF, especially on the Harstad-Kiruna link.

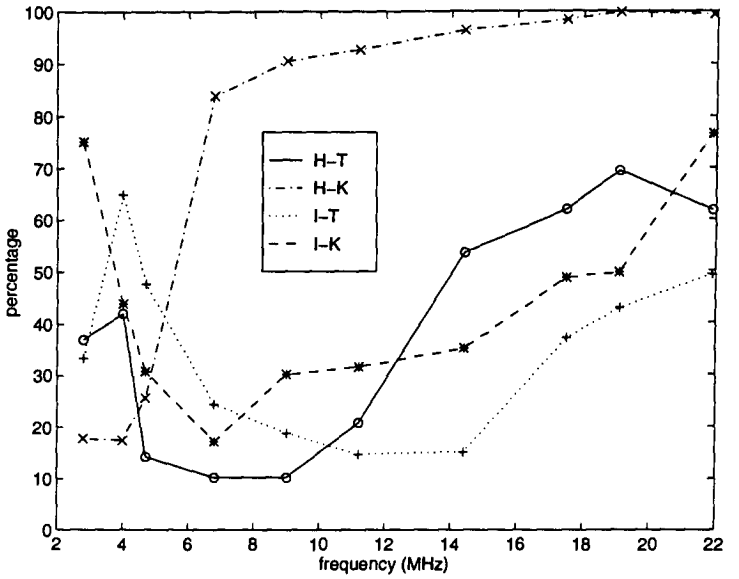


Figure 6.1: Percentage of total observations on each link that require robust waveform

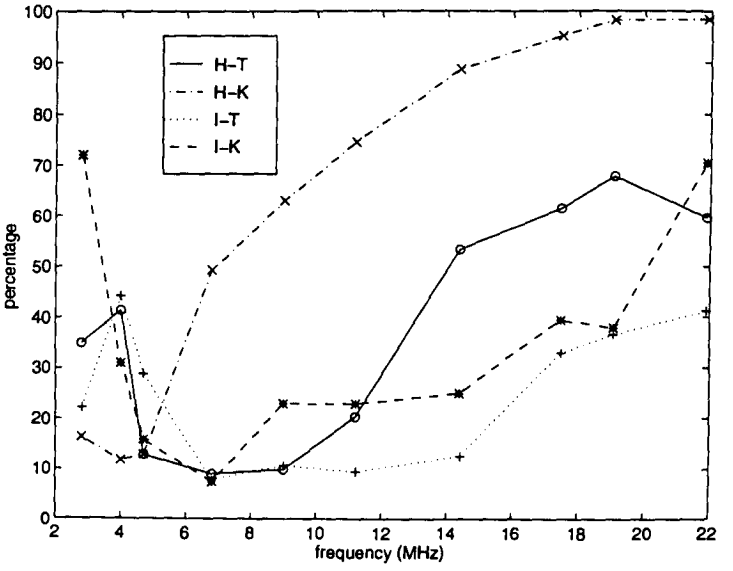


Figure 6.2: Percentage of total observations for which the SNR falls below the threshold

The proportion of measurements which indicate a robust waveform is required, called "robust" observations, in which SNR is one of the deciding factors in waveform choice is shown in figure 6.3. It is seen that SNR is the most significant parameter on the predominantly sub-auroral Harstad-Tuentangen link, where it is wholy or partially responsible for the requirement in over 85 % of observations. On the other links, the proportion increases outside of the predicted LUF/MUF window, but within the predicted usable frequency range the percentage is between 30 % and 60 %. This indicates that, even on platforms with good SNR characteristics, there would be a strong requirement for a robust waveform on these links.

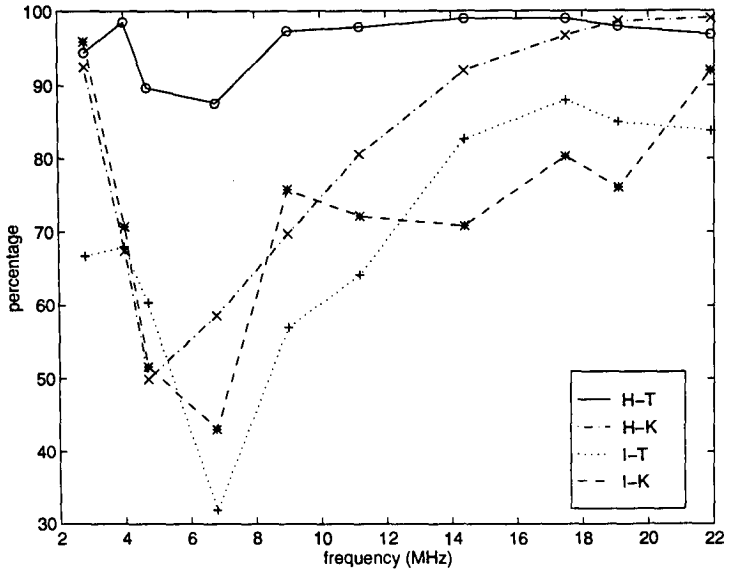


Figure 6.3: Percentage of robust observations for which the SNR falls below the threshold

### 6.2.2 Doppler spread

Figure 6.4 shows the percentage of observations at each frequency that the Doppler spread exceeds the threshold of 5 Hz. On the mainly sub-auroral Harstad-Tuentangen link, less than 5 % of points meet the requirement set for a robust waveform. As would be expected from the analysis presented in section 3.0, a significant proportion of the Doppler spread measurements on the Harstad-Kiruna link exceed the criterion, 25-35 % for frequencies above 6 MHz. On the other two links, the proportion falls between these two extremes.

Another important consideration is the percentage of occurrences in which Doppler spread is one of the factors in determining that a robust waveform is required. Figure 6.5 shows these percentages for each of the four links. There is a clear peak below the MUF on all the paths. On the long Isfjord-Tuentangen path, on which propagation is characterised by multiple hops with some reflection points in the auroral oval or polar cap, the Doppler spread can be a critical factor up to 75 % of the time. Even on the relatively benign Harstad-Tuentangen link, 20 % of the required use of robust waveforms is due, at least in part, to the Doppler spread.

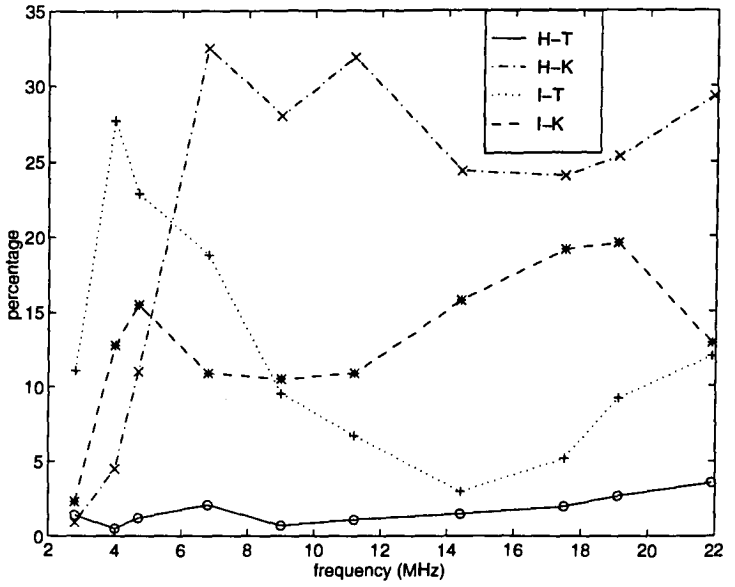


Figure 6.4: Percentage of total observations for which the Doppler spread exceeds the threshold

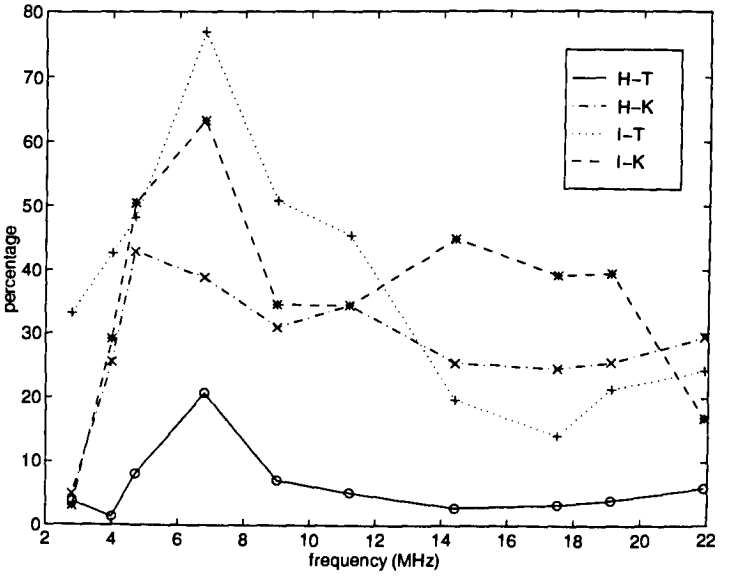


Figure 6.5: Percentage of robust observations for which the Doppler spread exceeds the threshold

### 6.2.3 Multipath spread

In general, the multipath spread is not a major factor in the requirement for robust waveforms. Frequencies close to the MUF on the Harstad-Kiruna link are a significant exception to this, as shown in figure 6.6. Propagation on this link often exhibits off-great-circle scatter, as seen in section 3.0, which results in very large multipath spreads. Fully 50 % of data points at 9.0 MHz on this link have multipath spreads in excess of the 6 ms criterion set for robust waveform use. Even at higher frequencies, approximately 8 % of measurements exceed the threshold. In contrast, on the 2000 km Isfjord-Tuentangen link, no data points were recorded with multipath spreads in excess of 6 ms.

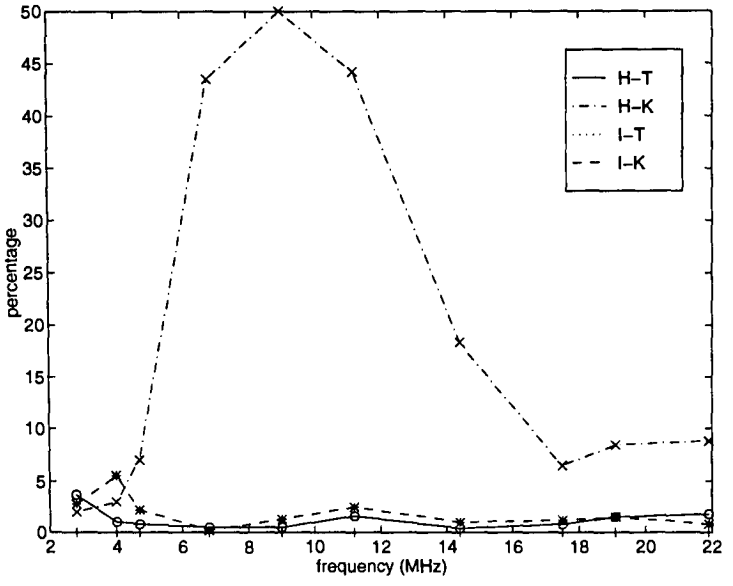


Figure 6.6: Percentage of total observations for which the multipath spread exceeds the threshold

The ratio of data points which have multipath spreads exceeding the criterion to the overall number requiring a robust waveform is shown in figure 6.7. On the Harstad-Kiruna link, over 45 % of the robust waveform requirements for the frequencies 6.8 MHz, 9.0 MHz and 11.2 MHz are caused, at least in part, by the multipath spread. On the two paths of length about 1000 km, Harstad-Tuentangen and Isfjord-Kiruna, generally multipath spread plays a role in the need for a robust waveform in less than 10 % of cases.

## 6.3 SPECIFICATIONS FOR A ROBUST WAVEFORM

In this section, the ranges of conditions which must be handled by a robust waveform are considered.

### 6.3.1 SNR

The DAMSON analysis system has an operational range down to approximately -20 to -25 dB. This range is affected by Doppler spread and shift and certain types of interferers. Discussion of the impact of the range

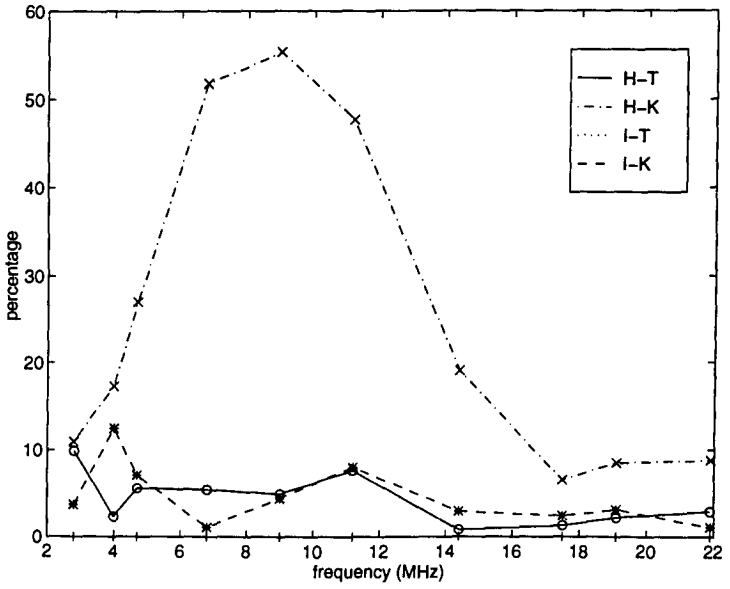


Figure 6.7: Percentage of robust observations for which the multipath spread exceeds the threshold

of SNR observed on the specification of a robust waveform must be applied with care when that waveform is to be used with different signal power and communications equipment.

Figures 6.8 to 6.11 shown the percentage of observations that meet the criteria for robust waveform use with SNRs below -10, -15, -20 and -25 dB. On the Harstad-Tuentangen path, approximately 20 % of robust measurements have SNRs below -10 dB between 4.7 MHz and 11.2 MHz, which corresponds fairly closely to the predicted LUF-MUF window. It was seen previously that the observed propagation on the Harstad-Kiruna link (figure 6.9) does not follow the predicted situation due to off-great-circle scatter. In fact, the percentage of measurements below -10 dB is less than about 30 % up to 19.1 MHz, whereas the predicted MUF is below 6 MHz. The distribution is similar on the Isfjord-Kiruna link, where less than 20 % of points fall below -10 dB across most of the frequency range, figure 6.11. On the Isfjord-Tuentangen link, figure 6.10, the SNR is of more critical consideration, as there is only a small range of frequencies where the proportion of points with SNR $<$ -10 dB is less than 20 %.

The 95th percentiles of the SNR, based on the data points that require a robust waveform, are shown in table 6.2. These very low SNRs indicate the need for an ultra-robust waveform to maintain a high availability. Frequency steering may be able to avoid using the frequencies with the lowest SNRs.

### 6.3.2 Doppler spread

The percentage of robust observations with measured overall Doppler spread exceeding 10, 15, 20 and 25 Hz are shown in figures 6.12 to 6.15. Note that the percentages are based on the total number of points which are identified as requiring a robust waveform. As would be expected from the earlier sections, the most extreme Doppler spread conditions are seen on the short Harstad-Kiruna path, where 10 % of robust measurements exceed 30 Hz at some frequencies. The other trans-auroral links, Isfjord-Tuentangen and Isfjord-Kiruna, also

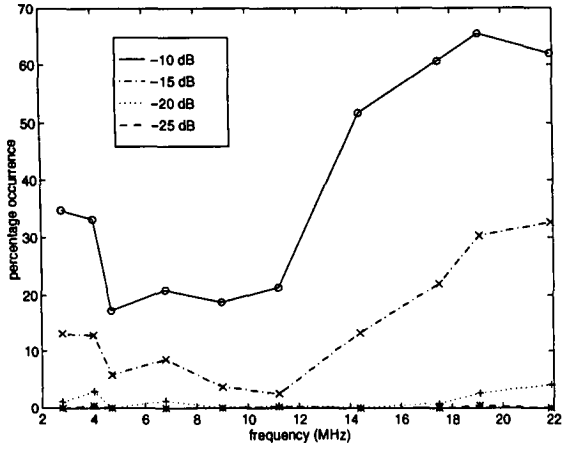


Figure 6.8: Percentage of robust observations falling below specified SNR on Harstad-Tuentangen link

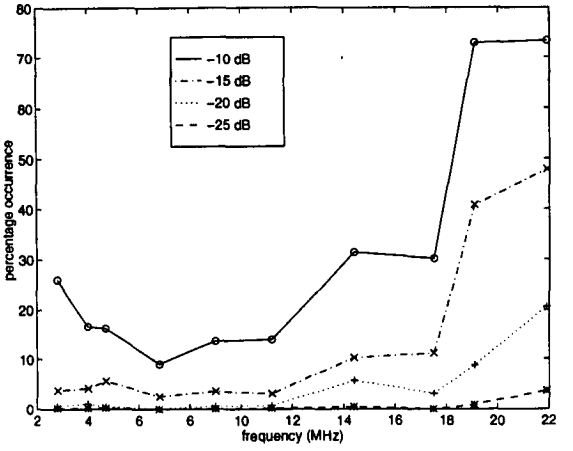


Figure 6.9: Percentage of robust observations falling below specified SNR on Harstad-Kiruna link

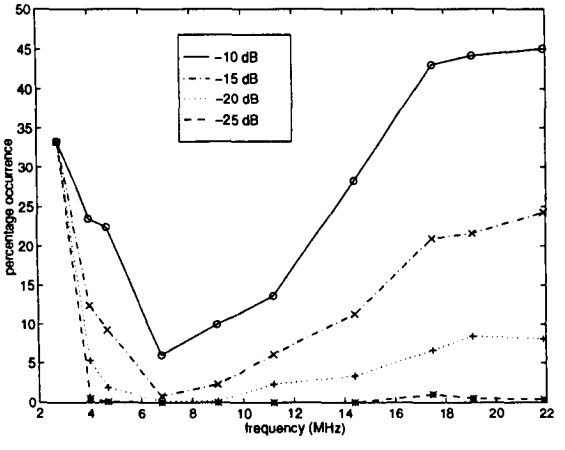


Figure 6.10: Percentage of robust observations falling below specified SNR on Isfjord-Tuentangen link

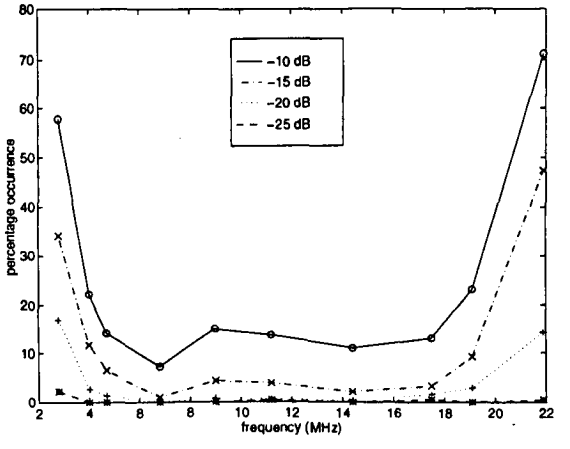


Figure 6.11: Percentage of robust observations falling below specified SNR on Isfjord-Kiruna link

| frequency (MHz) | Harstad - Tuentangen | Harstad - Kiruna | Isfjord - Tuentangen | Isfjord - Kiruna |
|---|---|---|---|---|
| 2.8 | -17 | -14 | -28 | -23 |
| 4.0 | -18 | -14 | -20 | -18 |
| 4.7 | -15 | -15 | -17 | -16 |
| 6.8 | -18 | -12 | -10 | -10 |
| 9.0 | -14 | -13 | -12 | -13 |
| 11.2 | -13 | -13 | -15 | -14 |
| 14.4 | -16 | -21 | -17 | -12 |
| 17.5 | -17 | -17 | -21 | -14 |
| 19.1 | -19 | -21 | -21 | -17 |
| 21.9 | -19 | -24 | -20 | -22 |

Table 6.2: SNR 95th percentile (dB) of measurements that meet criteria for robust waveform use

show some challenging conditions for any waveform. On the Isfjord-Tuentangen link (figure 6.14), 12-30 % of robust observations exceed 10 Hz on frequencies between 4.0 MHz and 11.2 MHz. On the Isfjord-Kiruna link (figure 6.15), over 15 % of robust observations in the range 4.7 MHz to 19.1 MHz exceed 10 Hz. In the same frequency range, 5-10 % of robust observations exceed 20 Hz. Even on the predominantly sub-auroral Harstad-Tuentangen link, figure 6.12, 4-10 % of measurements exceed 10 Hz.

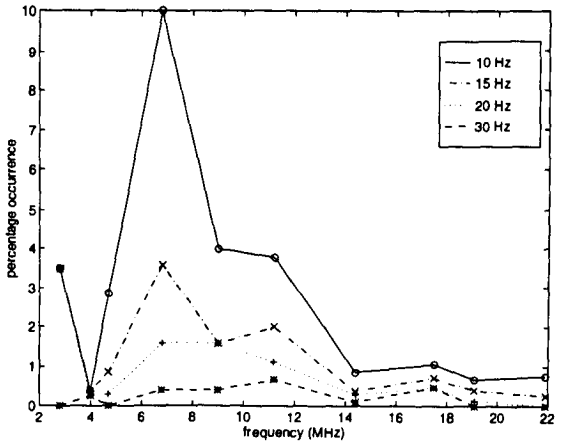


Figure 6.12: Percentage of robust observations exceeding specified Doppler spread on Harstad-Tuentangen link

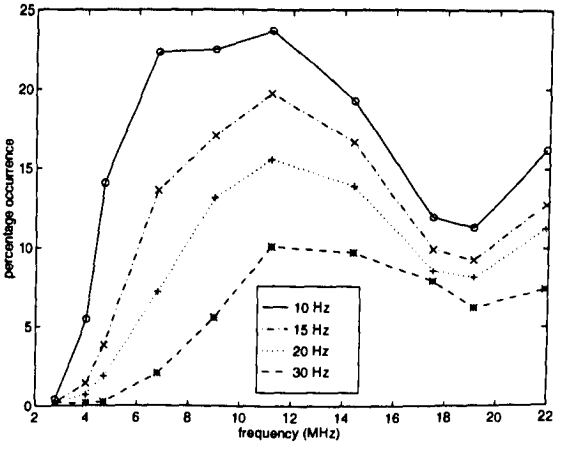


Figure 6.13: Percentage of robust observations exceeding specified Doppler spread on Harstad-Kiruna link

The 95th percentiles of the overall Doppler spread, based on the data points that require a robust waveform, are shown in table 6.3.

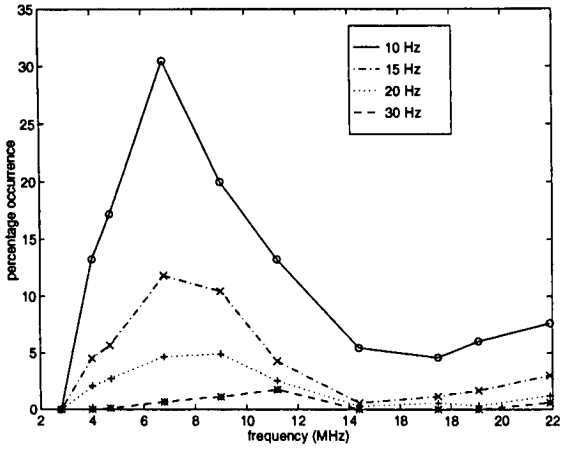


Figure 6.14: Percentage of robust observations exceeding specified Doppler spread on Isfjord-Tuentangen link

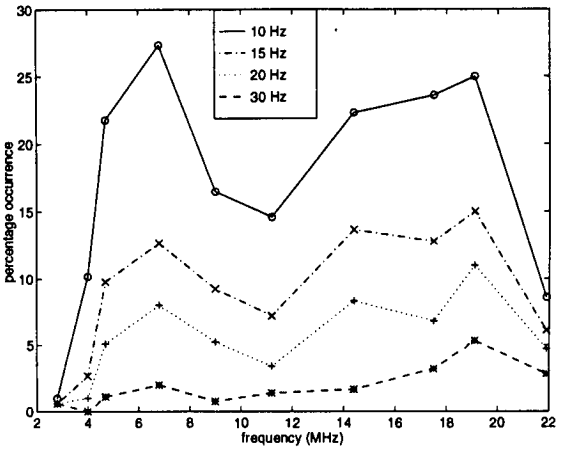


Figure 6.15: Percentage of robust observations exceeding specified Doppler spread on Isfjord-Kiruna link

| frequency (MHz) | Harstad - Tuentangen | Harstad - Kiruna | Isfjord - Tuentangen | Isfjord - Kiruna |
|---|---|---|---|---|
| 2.8 | 5.6 | 5.0 | 5.6 | 3.1 |
| 4.0 | 2.5 | 10.0 | 14.4 | 13.1 |
| 4.7 | 6.3 | 13.8 | 15.6 | 20.0 |
| 6.8 | 13.1 | 22.5 | 18.8 | 25.0 |
| 9.0 | 7.5 | 30.6 | 19.4 | 20.0 |
| 11.2 | 6.3 | 40.6 | 13.8 | 18.1 |
| 14.4 | 4.4 | 47.5 | 10.0 | 23.8 |
| 17.5 | 4.4 | 48.8 | 9.4 | 25.0 |
| 19.1 | 5.0 | 41.3 | 10.6 | 33.8 |
| 21.9 | 5.6 | 41.9 | 11.3 | 18.8 |

Table 6.3: Doppler spread 95th percentile (Hz) of measurements that meet criteria for robust waveform use

### 6.3.3 Multipath spread

As has been seen earlier, the multipath spread tends to be a less critical factor than Doppler spread and SNR, except on the Harstad-Kiruna link. The percentage of points designated as requiring a robust waveform which have multipath spreads exceeding 7, 8, 9 and 10 ms are shown in figures 6.16 to 6.18. Note that on the Isfjord-Tuentangen link, no measurements showed multipath spreads of 6 ms or more. On the Harstad-Tuentangen link, (figure 6.16) only 2 % of robust observations have a multipath spread of 9 ms at frequencies between 6.8 MHz and 11.2 MHz. No measurements of 10 ms were made on this link. On the Harstad-Kiruna link, figure 6.17, almost 30 % of observations at 11.2 MHz indicated multipath spreads of 10 ms or more. Over 35 % of measurements had multipath spreads of at least 7 ms in the frequency range 6.8 MHz to 11.2 MHz. On the Isfjord-Kiruna link, figure 6.18, there are no measurements of 9 ms or more, and the proportion for 7 ms exceeds 10 % only at 11.2 MHz.

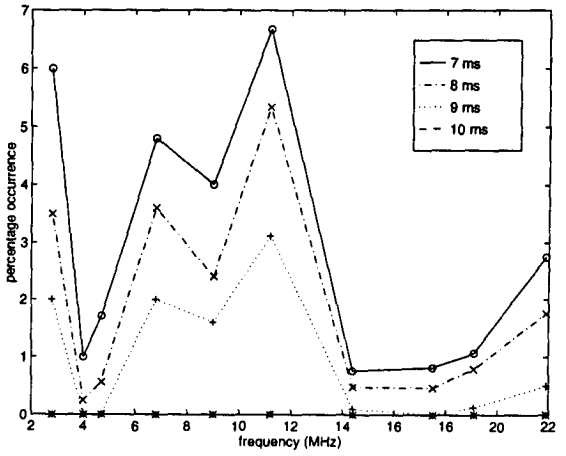


Figure 6.16: Percentage of robust observations exceeding specified multipath spread on Harstad-Tuentangen link

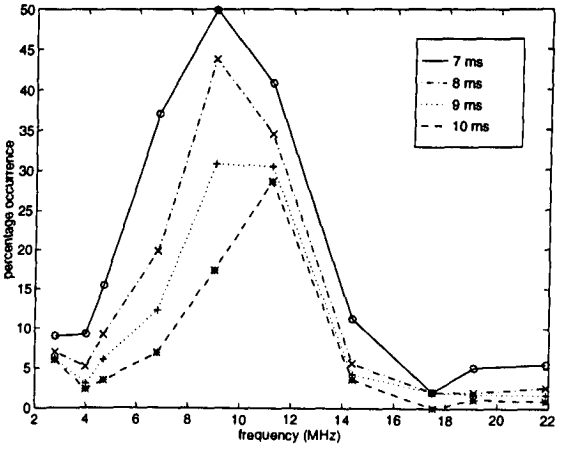


Figure 6.17: Percentage of robust observations exceeding specified multipath spread on Harstad-Kiruna link

The 95th percentiles of the overall multipath spread, based on the data points that require a robust waveform, are shown in table 6.4.

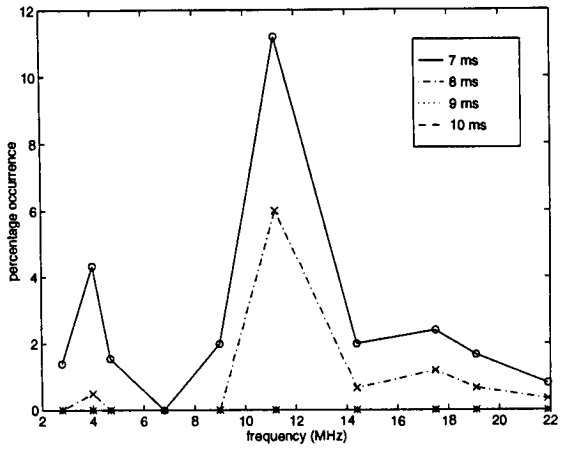


Figure 6.18: Percentage of robust observations exceeding specified multipath spread on Isfjord-Kiruna link

| frequency (MHz) | Harstad - Tuentangen | Harstad - Kiruna | Isfjord - Tuentangen | Isfjord - Kiruna |
|---|---|---|---|---|
| 2.8 | 7.1 | 12.1 | 5.8 | 4.2 |
| 4.0 | 4.2 | 8.4 | 5.0 | 6.7 |
| 4.7 | 5.8 | 9.2 | 5.4 | 6.3 |
| 6.8 | 6.7 | 10.4 | 3.3 | 3.3 |
| 9.0 | 6.3 | 11.3 | 2.5 | 4.6 |
| 11.2 | 8.4 | 12.1 | 1.7 | 8.4 |
| 14.4 | 2.1 | 8.4 | 1.3 | 4.6 |
| 17.5 | 2.1 | 6.3 | 0.8 | 3.3 |
| 19.1 | 1.7 | 7.1 | 0.8 | 4.2 |
| 21.9 | 2.5 | 7.1 | 0.8 | 2.9 |

Table 6.4: Multipath spread 95th percentile (ms) of measurements that meet criteria for robust waveform use

# 7.0 CONCLUSIONS

This report has presented a summary of a comprehensive analysis of data from the DAMSON system in Scandinavia, collected from April to October, 1995. The data sets on each link have been broken into separate times of year, if appropriate, and daylight and nighttime data points have been considered separately at each of the ten DAMSON frequencies. Due to the huge amount of plots generated during the analysis, only selected frequencies have been presented here, from within the predicted LUF/MUF window, and from above the predicted MUF.

The Harstad-Tuentangen link, presented in section 2.0, is considered to be sub-auroral. However, the mean Doppler spread was comparable to that seen on the trans-auroral Isfjord-Tuentangen link. Doppler spread estimates above the MUF were at the upper limit of the system's capabilities fairly often, particularly at night. The reason for this is believed to be scatter off the southerly edge of the auroral oval, which is generally close to the transmitter site. The nighttime multipath spread at these frequencies tended to be somewhat greater than during the daytime, even though propagation at both times of day was substantially single-moded.

The link with the most interesting propagation characteristics is from Harstad to Kiruna. The great-circle path is less than 200 km long, and lies almost parallel to, and sometimes coincident with, the southerly edge of the auroral zone. Below the MUF predicted by ICEPAC, which uses the great-circle path, the multipath spread characteristics are very similar to those predicted. However, above the MUF, considerable propagation is observed, with extreme values of both multipath spread and Doppler spread. It was noted in the section 3.0 that the Doppler spread value is biased low due to the limitations of the measurement system, which have excluded measurements in which the combination of Doppler spread and Doppler shift were very large. These large values of Doppler spread are accompanied by large multipath spreads and negative Doppler shifts. The propagation characteristics above the MUF are thus attributed to off-great-circle scatter from the auroral electrojet.

The two links from the Isfjord transmitter at Svalbard are almost north-south and both have reflection points in the auroral zone or in the polar cap region. It is commonly expected that the location of the reflection points will result in significant Doppler spread observations, although there is very little published in the open literature to quantify these expectations. It has been seen in sections 4.0 and 5.0 that the Doppler spreads are indeed quite large, though not as extreme as on the Harstad-Kiruna link. The mean daytime Doppler spread on the shorter Isfjord-Kiruna link is over 10 Hz on some frequencies above the MUF. On the longer Isfjord-Tuentangen link, the largest Doppler spreads are seen at night in the LUF/MUF window. This difference is believed to be explained by the location of the auroral oval relative to the reflection points. This difference also accounts for the tendency to negative Doppler shifts on the long link, and positive ones on the shorter, more northerly link. Above the MUF on these links, the propagation is predominantly single moded. Below the MUF, three or modes are not uncommon as multiple-hop propagation is supported.

Section 6.0 of this report dealt with the application of the DAMSON data analysis to the design of robust waveforms. SNR is often the driving factor in the need for low data rate, high-reliability waveforms, especially for on airborne platforms or manpacks. This analysis has shown that, on each of the four links considered, a robust waveform would be rquired to deal with the intrinsic properties of the communications channel, i.e. multipath spread and Doppler spread. Some discussion of the conditions which must be handled by such a waveform have been presented.

The data used in this analysis was all obtained during 1995, which was close to the solar sunspot minimum, and hence is expected to be more benign than at a higher level of solar activity. Unfortunately, there is insufficient data available from periods with high values of the geomagnetic index $K_p$ to enable extrapolations to be made for periods with more geomagnetic activity. Future DAMSON campaigns, possibly giving greater measurement capabilities, should provide data during other parts of the solar cycle.

# ACKNOWLEDGEMENTS

The DAMSON project is a collaboration of the Communications Research Centre, the UK Defence Research Agency, the Norwegian Defence Research Establishment and the Swedish Defence Research Establishment. Gerry Venier, a *Friend of CRC*, has provided invaluable ongoing input to the project. Thanks to Bill Moreland, CRC, for useful discussions, particularly on the implications of the DAMSON results on robust data communications. Thanks also to Mike Bova, CRC, for his continuing work on the DAMSON system.

This work has been funded by the Department of National Defence, Canada.

# REFERENCES


[1] K. Davies, *Ionospheric Radio*, Peter Peregrinus Ltd., London, 1990.

[2] R.D. Hunsucker and H.F. Bates, "Survey of polar and auroral region effects on HF propagation", *Radio Sci.*, vol. 4, no. 4, pp. 347–365, April 1969.

[3] R.D. Hunsucker, "Auroral and polar-cap ionospheric effects on radio propagation", *IEEE Trans. Ant. and Prop.*, vol. AP-40, no. 7, pp. 818–828, July 1992.

[4] N.C. Gerson, "High latitude HF communications", *IEEE Trans. Commun. Sys.*, pp. 107-109, March 1964.

[5] R.A. Shepherd and J.B. Lomax, "Frequency spread in ionospheric radio propagation", *IEEE Trans. Commun. Tech.*, vol. COM-15, no. 2, pp. 168–275, April 1967.

[6] P.S. Cannon, N.C. Davies, M.J. Angling, V. Jodalen, K.W. Moreland and B. Lundborg, "Initial results from DAMSON – a system to measure multipath, Doppler spread and Doppler shift on distrubed HF channels", *9th Int. Conf. on Ant. and Prop.*, Eindhoven, Netherlands, 1995.

[7] K.W. Moreland, T.J. Willink, G.O. Venier, P.S. Cannon, N.C. Davies, M.J. Angling, V. Jodalen and B. Lundborg, "Comparison of mid-latitude and high-latitude HF channel measurements of Doppler and multipath effects", *7th Int. Conf. on Wireless Comms.*, Calgary, July 1995.

[8] B. Lundborg, R. Skartlien, V. Jodalen, B. Johansson, M. Bröms, P.S. Cannon, M.J. Angling, N.C. Davies and K.W. Moreland, "Scandinavian DAMSON measurements of multipath and Doppler characteristics over high latitude HF paths", *Proc. Nordic HF Conf., HF 95*, Färo, Sweden, 1995.

[9] M.J. Angling, P.S. Cannon, N.C. Davies, B. Lundborg, V. Jodalen and K.W. Moreland, "Measurements of Doppler spread on high latitude HF paths", *4th AGARD Symp. on Digital Communications Systems*, Athens, Greece, 1995.

[10] E.M. Warrington, "Observations on the structure of ionospherically reflected HF radiowaves by means of super-resolution direction finding", paper 3B-5, *Proc. Ionospheric Effects Symp.*, May 1996, Virginia, USA.

[11] R.H. Holzworth and C.-I. Meng, "Mathematical representation of the auroral oval", *Geophys. Res. Lett*, vol. 2, no. 9, pp. 377–380, Sept. 1975.

[12] Space Environment Center, http://proton.sec.noaa.gov/

[13] B.S. Dandekar, "Determination of the auroral oval Q index from the air weather service K index", *PL-TR-93-2267 Environmental Research Papers, No. 1136* Phillips Laboratory, Air Force Material Command, Hansom Air Force Base, MA, USA, 1993.

[14] V. Jodalen, "A study of observed and predicted HF propagation characteristics at high latitudes", *FFI/PUBL-96/01107*, Forsvarets Forskningsinstitutt, Kjeller, Norway, 1996.

[15] R.H. Barker, "Group synchronizing of binary digital systems", in *Communication Theory*, W. Jackson, Ed., Academic-Butterworth, 1953.

[16] J.G. Proakis, *Digital Communications*, McGraw-Hill, 1983.

[17] B. Lundborg, M. Bröms, V. Jodalen and T. Bergsvik, "Doppler effects on high latitude HF paths during an ionospheric disturbance", *Proc. of HF Radio Systems and Techniques*, Nottingham, UK, July 1997.

[18] T.J. Willink and E.C. Landry, "Analysis of time-varying HF propagation characteristics", *Proc. of HF Radio Systems and Techniques*, Nottingham, UK, July 1997.

[19] G. Guidotti and R. Marchesani, "High speed serial data modem with modified Viterbi decoders", *Proc. HF Radio Systems and Techniques*, York, UK, 1994.

[20] NATO, "Characteristics of 1200/2400/3600 bit per second modulators/demodulators for HF radio links", STANAG 4285, 1990.

[21] M.B. Jorgenson, R.W. Johnson, K.W. Moreland, N. Serinken, S. Chow and T.J. Willink, "Polarization diversity for HF data transmission", *Proc. of HF Radio Systems and Techniques*, Nottingham, UK, July 1997.

[22] T.C. Giles, "A high-speed modem with built in HF noise tolerance", *Proc. HF Radio Systems and Techniques*, York, UK, 1994.

[23] U.S. Military Standard, "Interoperability and performance standards for data modems", Mil-Std-188-110A, 1991.

[24] W.N. Furman, "Robust low bit rate HF data modems", *Proc. of HF Radio Systems and Techniques*, Nottingham, UK, July 1997.

[25] G. Hand, Ionospheric Communications Enhanced Profile Analysis and Circuit prediction program, ICEPAC, Institute of Telecommunications Sciences, Boulder, Colorado USA.

[26] G. Hand, Ionospheric Communications Analysis Prediction program, IONCAP, Institute of Telecommunications Sciences, Boulder, Colorado USA.

[27] R.W. Johnson, M.B. Jorgenson and K.W. Moreland, "Error correction coding for serial-tone HF transmission", *Proc. of HF Radio Systems and Techniques*, Nottingham, UK, July 1997.

[28] M. Bröms, private communication, 1997.

[29] M.J. Angling, P.S. Cannon, N.C. Davies, T. Willink, V. Jodalen and B. Lundborg, "Measurements of Doppler and multipath spread on oblique high-latitude HF paths and their effects on data modems", *submitted to Radio Science*, 1997.

## DOCUMENT CONTROL DATA

(Security classification of title, body of abstract and indexing annotation must be entered when the overall document is classified)

1. ORIGINATOR (the name and address of the organization preparing the document. Organizations for whom the document was prepared, e.g. Establishment sponsoring a contractor's report, or tasking agency, are entered in section 8.)

COMMUNICATIONS RESEARCH CENTRE
3701 Carling Avenue, P.O. Box 11490, Station 'H'
Ottawa, Ontario K2H 8S2

2. SECURITY CLASSIFICATION (overall security classification of the document. including special warning terms if applicable)

UNCLASSIFIED

3. TITLE (the complete document title as indicated on the title page. Its classification should be indicated by the appropriate abbreviation (S,C,R or U) in parentheses after the title.)

ANALYSIS OF HIGH-LATITUDE HF PROPAGATION CHARACTERISTICS AND THEIR IMPACT FOR DATA COMMUNICATIONS (U)

4. AUTHORS (Last name, first name, middle initial)

WILLINK, T.J.

5. DATE OF PUBLICATION (month and year of publication of document)

APRIL 1997

6a. NO. OF PAGES (total containing information. Include Annexes, Appendices, etc.)

105

6b. NO. OF REFS (total cited in document)

2

7. DESCRIPTIVE NOTES (the category of the document, e.g. technical report, technical note or memorandum. If appropriate, enter the type of report, e.g. interim, progress, summary, annual or final. Give the inclusive dates when a specific reporting period is covered.)

CRC REPORT

8. SPONSORING ACTIVITY (the name of the department project office or laboratory sponsoring the research and development. Include the address.)

DEFENCE RESEARCH ESTABLISHMENT OTTAWA
3701 CARLING AVENUE, BLDG. 29
OTTAWA, ONTARIO K1A 0Z4

9a. PROJECT OR GRANT NO. (if appropriate, the applicable research and development project or grant number under which the document was written. Please specify whether project or grant)

5bd14

9b. CONTRACT NO. (if appropriate, the applicable number under which the document was written)

10a. ORIGINATOR'S DOCUMENT NUMBER (the official document number by which the document is identified by the originating activity. This number must be unique to this document.)

CRC REPORT NO.: CRC-RP-97-001

10b. OTHER DOCUMENT NOS. (Any other numbers which may be assigned this document either by the originator or by the sponsor)

11. DOCUMENT AVAILABILITY (any limitations on further dissemination of the document, other than those imposed by security classification)

(X) Unlimited distribution
( ) Distribution limited to defence departments and defence contractors; further distribution only as approved
( ) Distribution limited to defence departments and Canadian defence contractors; further distribution only as approved
( ) Distribution limited to government departments and agencies; further distribution only as approved
( ) Distribution limited to defence departments; further distribution only as approved
( ) Other (please specify):

12. DOCUMENT ANNOUNCEMENT (any limitation to the bibliographic announcement of this document. This will normally correspond to the Document Availability (11). However, where further distribution (beyond the audience specified in 11) is possible, a wider announcement audience may be selected.)

UNLIMITED

13. ABSTRACT ( a brief and factual summary of the document. It may also appear elsewhere in the body of the document itself. It is highly desirable that the abstract of classified documents be unclassified. Each paragraph of the abstract shall begin with an indication of the security classification of the information in the paragraph (unless the document itself is unclassified) represented as (S), (C), (R), or (U). It is not necessary to include here abstracts in both offical languages unless the text is bilingual).

THE PROPAGATION PARAMETERS OBTAINED ON FOUR HF LINKS IN NORTHERN SCANDINAVIA HAVE BEEN OBTAINED USING THE DAMSON MEASUREMENT SYSTEM. SIGNALS WERE TRANSMITTED ON FREQUENCIES FROM 2 TO 22 MHz AND THE SNR, MULTIPATH SPREAD, NUMBER OF MODES, DOPPLER SPREAD AND DOPPLER SHIFT WERE EXTRACTED. A DETAILED ANALYSIS OF THESE PROPAGATION PARAMETERS HAS BEEN UNDERTAKEN IN THIS STUDY, AND THE CHARACTERISTICS OF SOME OF THE DAMSON FREQUENCIES ARE PRESENTED IN DETAIL TO PROVIDE A COMPREHENSIVE OVERVIEW OF THE PROPERTIES OF THESE HIGH LATITUDE HF LINKS. WHERE APPROPRIATE, THE PREDICTIONS OBTAINED FROM A HIGH-LATITUDE MODEL ARE PRESENTED FOR COMPARISON WITH THE OBSERVED DATA. (U)

DATA COMMUNICATION OVER CHANNELS AT THESE LATITUDES CAN BE DIFFICULT, AND LOW DATA RATE ROBUST WAVEFORMS ARE OFTEN REQUIRED. THE DAMSON DATA HAVE BEEN ANALYSED TO DETERMINE THE RANGE OF CONDITIONS THAT MUST BE CONSIDERED WHEN DESIGNING SUCH A WAVEFORM. (U)

14. KEYWORDS, DESCRIPTORS or IDENTIFIERS (technically meaningful terms or short phrases that characterize a document and could be helpful in cataloguing the document. They should be selected so that no security classification is required. Identifiers, such as equipment model designation, trade name, military project code name, geographic location may also be included. If possible keywords should be selected from a published thesaurus. e.g. Thesaurus of Engineering and Scientific Terms (TEST) and that thesaurus-identified. If it is not possible to select indexing terms which are Unclassified, the classification of each should be indicated as with the title.)

HIGH LATITUDE HF PROPAGATION, HF CHANNEL CHARACTERISTICS, HF DATA COMMUNICATIONS